

UNIVERSITA' VITA-SALUTE SAN RAFFAELE

**CORSO DI DOTTORATO DI RICERCA INTERNAZIONALE IN
MEDICINA MOLECOLARE**

CURRICULUM IN EXPERIMENTAL AND CLINICAL MEDICINE

**ROLE OF AUTOPHAGY IN
IMMUNE SYSTEM RESPONSE IN PATIENTS
WITH HEAD AND NECK CANCER AND
NON SMALL CELL LUNG CANCER**

DoS: Prof.ssa Giulia Veronesi

Second Supervisor: Dr. Umberto Malapelle

Tesi di DOTTORATO di RICERCA di Rosa Alessia Battista
matr. 017711
Ciclo di dottorato XXXVI
SSD MED/31, MED/32, MED/21

Anno Accademico 2020/2021

UNIVERSITA' VITA-SALUTE SAN RAFFAELE

**CORSO DI DOTTORATO DI RICERCA INTERNAZIONALE IN
MEDICINA MOLECOLARE**

CURRICULUM IN EXPERIMENTAL AND CLINICAL MEDICINE

**ROLE OF AUTOPHAGY IN
IMMUNE SYSTEM RESPONSE IN PATIENTS
WITH HEAD AND NECK CANCER AND
NON SMALL CELL LUNG CANCER**

DoS: Prof.ssa Giulia Veronesi

Second Supervisor: Dr. Umberto Malapelle

Tesi di DOTTORATO di RICERCA di Rosa Alessia Battista

matr. 017711

Ciclo di dottorato XXXVI

SSD MED/31, MED/32, MED/21

Anno Accademico 2020/2021



CONSULTAZIONE TESI DI DOTTORATO DI RICERCA

La sottoscritta/*I ROSA ALESSIA BATTISTA*
Matricola / *registration number 017711*

Nata a/ *born at SALERNO*
il/on *23/12/1991*

autore della tesi di Dottorato di ricerca dal titolo / *author of the PhD Thesis titled*

**ROLE OF AUTOPHAGY IN IMMUNE SYSTEM RESPONSE IN PATIENTS WITH
HEAD AND NECK CANCER AND NON SMALL CELL LUNG CANCER**

AUTORIZZA la Consultazione della tesi / *AUTHORIZES the public release of the thesis*

NON AUTORIZZA la Consultazione della tesi per mesi /*DOES NOT AUTHORIZE the public release of the thesis for months*
a partire dalla data di conseguimento del titolo e precisamente / *from the PhD thesis date, specifically*

Dal / *from*/...../..... Al / *to*/...../.....

Poiché /*because*:

l'intera ricerca o parti di essa sono potenzialmente soggette a brevettabilità/ *The whole project or part of it might be subject to patentability;*

ci sono parti di tesi che sono già state sottoposte a un editore o sono in attesa di pubblicazione/ *Parts of the thesis have been or are being submitted to a publisher or are in press;*

la tesi è finanziata da enti esterni che vantano dei diritti su di esse e sulla loro pubblicazione/ *the thesis project is financed by external bodies that have rights over it and on its publication.*

E' fatto divieto di riprodurre, in tutto o in parte, quanto in essa contenuto / *Copyright the contents of the thesis in whole or in part is forbidden*

Data /Date 02/02/2024

Firma /Signature 

DECLARATION

This thesis has been:

- composed by myself and has not been used in any previous application for a degree.
Throughout the text I use both 'I' and 'We' interchangeably.
- has been written according to the editing guidelines approved by the University.

Permission to use images and other material covered by copyright has been sought and obtained. For the following image Fig.6, it was not possible to obtain permission and is/are therefore included in thesis under the "fair use" exception (Italian legislative Decree no. 68/2003).

All the results presented here were obtained by myself, except for:

- *Immunohistochemistry analysis, which were conducted in collaboration with the Department of Pathology, San Raffaele Hospital, Milan.*

All sources of information are acknowledged by means of reference.

To my family.
Every time I reach a goal,
my thoughts are always with you,
my constant love, strength
and motivation.

ABSTRACT

Background: Head and Neck (HN)cancer and Non-Small Cell Lung Cancer (NSCLC) are two significant oncological challenges, characterized by intricate biology and a pressing need for innovative therapeutic strategies. The immune system plays a crucial role in cancer progression, and autophagy, a fundamental cellular process, has emerged as a potential mediator of immune responses within the tumor microenvironment.

Aim: This work aims to investigate the interplay between autophagy and the immune system in HN cancers and NSCLC. By unraveling the role of autophagic machinery, exemplified by the p62 marker, in shaping the TME, we seek to identify novel prognostic markers and therapeutic targets within the autophagic pathway.

Methods: Genomic analysis has been conducted in HN cancer and NSCLC, focusing on p53 mutations, autophagy-related genetic alterations, and immune dysregulation at the genetic level. Additionally, we evaluated the TME by analyzing the relationships between Tumor-Infiltrating Lymphocytes (TILs), CD8+ lymphocytes, and the autophagic p62 marker, analyzing clinical correlative data.

Results: Our findings reveal interesting p62 expression patterns, including cytoplasmic, nuclear, and nucleocytoplasmic distribution, which appear to be correlated with advanced stages and higher grades of cancers. In Oral Squamous Cell Carcinoma (OSCC), higher p62 levels and specific cytoplasmic or nucleocytoplasmic patterns are associated with worse overall survival and disease-free survival. Furthermore, Neutrophil-to-Lymphocyte Ratio and Platelet-to-Lymphocyte Ratio demonstrate predictive roles in OSCC and Lung SCC (LUSCC) outcomes, aligning with existing literature. Notably, a higher TILs rate is linked to better prognosis in OSCC and LUSCC.

Conclusion: Preliminary results suggest p62's and TME potential as prognostic factors and therapeutic target in HN cancer and NSCLC. Broader research, including AI applications and multicentric studies, is needed to fully understand these complex interactions. A deeper comprehension of autophagy, the immune microenvironment, and cancer biology offers promise for more effective and personalized treatments.

TABLE OF CONTENTS

TABLE OF CONTENTS	1
ACRONYMS AND ABBREVIATIONS	4
LIST OF FIGURES AND TABLES	8
INTRODUCTION.....	13
Background.....	13
Immune system and cancer.....	17
From Tumor Microenvironment to Tumor Macroenvironment.....	18
Immune system in the tumor niche	18
Systemic immunity and cancer	27
Systemic inflammation biomarkers in cancer	28
The Hallmarks of Cancer: oncogenic addiction	32
The stress phenotypes of cancer: non-oncogenic addiction	33
Autophagy.....	34
The autophagic machinery and its regulation	36
Selective autophagy: the role of p62	39
p62 involvement in multiple pathways	41
Autophagy and cancer: a double-edged sword.....	44
P62 role in cancer biology	47
Autophagy and tumor microenvironment.....	49
The tumor suppressor p53 and autophagy	50
Autophagy and Immune system response	52

Tumor antigen presentation: MHC class I	53
CD8+ cytotoxic lymphocytes.....	55
CD4+ lymphocytes	55
Tumor associated Macrophages polarization.....	56
AIM OF THE WORK	58
RESULTS.....	59
Role of immune dysregulation and autophagic genetic mutations in HN cancer and NSCLC	59
Prognostic value of the tumor characteristics and host response in OSCC and Squamous NSCLC	64
OSCC patients' clinical characteristics.....	65
Evaluation of the disease-free survival and overall survival in OSCC.....	68
LUSCC patients' clinical characteristics	73
Evaluation of the disease-free survival and overall survival in LUSCC	76
Evaluation of the systemic Immune response: Tumor Macroenvironment.....	78
Tumor-autonomous factors.....	82
P53 positivity express worst prognosis in OSCC	82
PDL1	85
P62/SQSTM1	86
Role of tumor microenvironment in Lung SCC and Oral SCC.....	93
Prognostic assessment of tumor burden and host response	98
DISCUSSION	102
Unraveling the Enigmatic World of p62 Patterns: Insights from Tumor Microenvironments.....	102
Future Perspectives and Therapeutic Potential.....	104
Deciphering the Host Immune system in oncological patients: A Prognostic Paradigm	105

Study limitations	108
Conclusion	108
MATERIALS AND METHODS	111
Genomic analysis.....	111
Neutrophils to lymphocytes ratio, Platelets to lymphocytes ratio, Monocytes to lymphocytes ratio.....	112
Tumor Infiltrating Lymphocytes	112
Immunohistochemistry staining and evaluation of the samples	112
p62/SQSTM1 Immunohistochemistry	113
PDL-1 Immunohistochemistry.....	114
Ethic declaration	114
Statistical and data analysis	114
REFERENCES	115
ACKNOWLEDGMENTS.....	130

ACRONYMS AND ABBREVIATIONS

ABBREVIATIONS

AB	Antibody
ACRs	Autophagy cargo receptors
AG	Antigen
AI	Artificial Intelligence
AJCC/UICC	American Joint Committee on Cancer/Union Internationale Contre le Cancer
AMBRA1	Activating molecule in Beclin-1-regulated autophagy 1
AMP	Adenosine monophosphate
AMPK	AMP-activated protein kinase
APCs	Antigen presenting cells
APKCs	Atypical protein kinase Cs
ATG	Autophagy related (gene/protein)
ATP	Adenosine triphosphate
BECLIN-1	B-cell lymphoma 2 (Bcl-2)-interacting protein
BMI	Body mass index
BRCA1	BRCA1 Cancer gene 1
CA²⁺	Calcium ion
CAFs	Cancer associated fibroblasts
CCL2	Chemokine (C-C motif) ligand 2 or monocyte chemoattractant protein 1
CCL5	Chemokine (C-C motif) ligand 5
CD3	Cluster of differentiation 3, T cell Ag
CD4	Cluster of differentiation 4, T helper cell Ag
CD45RO	Memory T cell Ag
CD8	Cluster of differentiation 8, T cytotoxic cell Ag
CI	Confidence Interval
CRC	Colorectal cancer
CRP	C-reactive protein
CSS	Cancer-specific survival
CT	Center of the tumor / tumor core
CTLA-4	Cytotoxic T-lymphocyte associated protein 4
CTLs	CD8 ⁺ T lymphocytes
DCs	Dendritic Cells
DFS	Disease-free survival
DOI	Depth of invasion
DSS	Disease specific survival
ECM	Extracellular matrix
ECOG PS	Eastern Cooperative Oncology Group Performance status
ECS	Extracapsular spread

EMT	Epithelial-mesenchymal transition
ENE	Extra nodal extension
ER	Endoplasmic Reticulum
ERK	Extracellular signal-regulated kinases
EXPORTIN1/CRM1	Exportin1/Chromosomal Maintenance 1
FOXP3+	Forkhead box P3+
GABARAP	γ -aminobutyric acid receptor-associated protein
GMPs	Granulocyte-monocyte progenitors
H&E	Hematoxylin and eosin staining
HCC	Hepatocellular carcinoma
HN	Head and Neck
HNSCC	Head and Neck squamous cell carcinoma
HP	Helicobacter Pylori
HPV	Human Papilloma Virus
HR	Hazard ratio
HSC70	Heat shock cognate 70
IBD	Inflammatory bowel disease
ICIS	Immune check point inhibitors
IFN-γ	Interferon gamma
IHC	Immunohistochemistry
IKK	Ik-B Kinase
IL-10	Interleukin 10
IL-13	Interleukin 13
IL-2	Interleukin 2
IL-4	Interleukin 4
IM	Invasive margin of the tumor
KEAP1	Kelch-like ECH-associated protein 1
KIR	Keap1 interacting region
KRAS	Kirsten rat sarcoma
LAMP-2A	Lysosomal-associated membrane protein 2
LC3	Light chain 3
LDH	Lactate dehydrogenase
LIR	LC3-interacting region
LMR	Lymphocyte-to-monocyte ratio
LPS	Lipopolysaccharide
LUAD	Lung Adenocarcinoma
LUSCC	Lung squamous cell carcinoma
M-CSF	Macrophage colony-stimulating factor or CSF1
M1	Macrophage proinflammatory type 1
M2	Macrophage anti-inflammatory type 2

MAPK	Mitogen-activated protein kinase
MHC-I	Major histocompatibility complex class I
MHC-II	Major histocompatibility complex class II
MLR	Monocyte-to-lymphocyte ratio
MTORC1	Mammalian target of rapamycin complex 1
NBR1	Neighbour of BRCA1 gene 1
NCCN	National Comprehensive Cancer Network
NCRs	Natural cytotoxicity receptors
NEAA	Non essential amino acids
NES	Nuclear export signal
NETS	Neutrophil extracellular traps
NF-KB	Nuclear factor- kappa B
NK	Natural killer
NLR	Neutrophil-to-lymphocyte ratio
NLS	Nuclear localization signal
NRF2	Nuclear factor erythroid 2-related factor 2
NSCLC	Non small cell lung cancer
OPSCC	Oropharyngeal squamous cell carcinoma
OPTN	Optineurin
OR	Odds Ratio
OS	Overall survival
OSCC	Oral Squamous Cell Carcinoma
OTSCC	Oral tongue squamous cell carcinoma
p62/SQSTM1	p62/sequestosome 1
PB1	Phox/Bem1p domain
PD-1	Programmed cell death protein 1
PD-L1	Programmed death-ligand 1
PDAC	Pancreatic ductal adenocarcinoma
PE	Phosphatidylethanolamine
PFS	Progression-free survival
PI3K	Phosphoinositide-3-kinase
PI3K C3	Phosphoinositide-3-kinase class 3 complex
PLR	Platelets-to-lymphocyte ratio
PNI	Perineural invasion
PS	Performance status
PVI	Perivascular invasion
RIP	Receptor-interacting protein
ROS	Reactive oxygen species
RT-PCR	Reverse transcriptase-polymerase chain reaction.
SARS	Selective autophagy receptors
SCC	Squamous cell carcinoma

SCLC	Small Cell Lung Cancer
SIRS	Systemic inflammatory response syndrome
SLNB	Sentinel lymph node biopsy
TAAS	Tumor-associated antigens
TAMs	Tumor-associated Macrophages
TAN1	Neutrophil antitumoral phenotype 1
TAN2	Neutrophil protumoral phenotype 2
TANs	Tumor-associated neutrophils
TB	Tumor necrosis factor receptor-associated factor 6 (TRAF6)-binding domain
TCGA	The Cancer Genome Atlas
TCR	T cell receptor
TH1	CD4+ T helper 1
TH2	CD4+ T helper 2
TILS	Tumor infiltrating Lymphocytes
TIME	Tumor immunemicroenvironment
TLE	Transoral local excision
TME	Tumor microenvironment
TNF	Tumor necrosis factor
TNM	Tumor Node Metastasis classification
TNM-I	TNM-Immunoscore
TRAF6	Tumor necrosis factor receptor-associated factor 6
TREG	CD4+ regulatory T cells
UB	Ubiquitin
UBA	Ubiquitin-binding activity
ULK1	UNC-51-like kinase 1
UPS	Ubiquitin-proteasome system
VEGF	Vascular endothelial growth factor
WHO	World Health Organization
WPOI	Worst pattern of invasion
ZZ	Zinc finger domain

LIST OF FIGURES AND TABLES

Figure 1: Evolution of 5-years relative survival over the past decades for different types of tumors. Data were collected from the Surveillance, Epidemiology, and End Results (SEER) Program of the National Cancer Institute.

Figure 2: Graphic representation of the cells involved in the host immune response towards tumor cells. The imbalance towards the pro-inflammatory anti-tumoral response or the anti-inflammatory pro-tumoral environment may determine tumor regression or progression. [see table of acronyms and abbreviation] Courtesy of Hendry et al. 2017

Figure 3: Neutrophil to Lymphocyte Ratio (NLR)-meter [SIRS, Systemic inflammatory response syndrome], modified from Kourilovitch et al., 2023

Figure 4: The hallmarks and the stress phenotypes of cancer [courtesy of Luo et al., 2009].

Figure 5: Different types of autophagy: macroautophagy, microautophagy and chaperone-mediated autophagy [courtesy of Mizushima et al., 2011].

Figure 6: Autophagic machinery and regulation (modified from Choi, A.M.K. Et al, Autophagy in Human Health and Disease, NEJM) [see table of abbreviations]

Figure 7: p62 functional domains and interactions in different pathway [see table for abbreviations]

Figure 8: Impairment in non-selective and selective autophagy: role in human disease [courtesy of Mizushima et al]

Figure 9: Tumor microenvironment's autophagy and its influence on tumor cells [courtesy of Debnath et al. 2023]

Figure 10: Autophagic pathway, its regulations, and its effects [modified from Debnath et al. 2023]

Figure 11: Autophagy Enhances DC-Mediated Cross-Presentation by Facilitating Autophagosome Formation with Tumor Antigens, while NBRI-Mediated MHC Class I Degradation Impairs CTL Recognition in Cancer Cells. [Courtesy of Xia et al., 2021]

Figure 12: NSCLC OS in unaltered group and subgroups of patients with alterations in the p53 pathway (top), autophagic pattern (middle), or in the immune dysregulation (bottom). [data extracted from C-Bioportal]

Figure 13: Head and Neck cancers OS in unaltered group and subgroups of patients with alterations in the p53 pathway (top), autophagic pattern (middle), or in the immune dysregulation (bottom). [data extracted from C-Bioportal]

Figure 14: Pie charts representing the distribution of the oncological stage and pathological grade in our OSCC population.

Table 1: Clinical characteristics of OSCC population

Figure 15: Top left: Kaplan-Meier curve illustrating DFS in Oral Squamous Cell Carcinoma (OSCC) patients according to the known pathological prognostic marker T, classified according to the 8th edition of TNM. The difference in DFS between the groups is statistically significant ($p = 0.045$). Top right: Kaplan-Meier curve depicting OS in OSCC patients according to the T stage. The difference in OS between the groups is statistically significant ($p = 0.002$). Bottom left: Kaplan-Meier curve demonstrating DFS in OSCC patients stratified according to the stage. The difference in DFS between the groups is not statistically significant ($p = 0.092$). Bottom right: Kaplan-Meier curve illustrating OS in OSCC patients stratified according to the stage. The difference in OS between the groups is statistically significant ($p = 0.005$).

Figure 16: Kaplan-Meier curve illustrating OS in Oral Squamous Cell Carcinoma (OSCC) patients stratified by age (cutoff 67 years old). The difference in OS between the groups is statistically significant ($p = 0.048$)

Table 2: Data on DFS and OS according to the ECOG Performance status of the patients (median [IQR])

Figure 17: Top left: Kaplan-Meier curve illustrating Overall Survival (OS) in Oral Squamous Cell Carcinoma (OSCC) patients according to the known pathological prognostic marker “Depth of invasion” (DOI) < 10mm or >10 mm. The difference in OS between the groups is statistically significant ($p = 0.007$). Top right: Kaplan-Meier curve depicting DFS in OSCC patients with R0 (clear) and R1 (positive) surgical margins. The difference in DFS between the groups is statistically significant ($p = 0.044$). Bottom left: Kaplan-Meier curve demonstrating DFS in OSCC patients stratified by the absence (ECS 0) or presence (ECS 1) of extracapsular spread. The difference in DFS between the two groups is statistically significant ($p = 0.034$). Bottom right: Kaplan-Meier curve illustrating OS in OSCC patients based on the presence or absence of extracapsular spread. The difference in OS between the two groups is statistically significant ($p = 0.014$).

Figure 18: Pie charts representing the distribution of the oncological stage and pathological grade in our Lung SCC population.

Table 3: Clinical characteristics of Lung Squamous Cell Carcinoma population.

Figure 19: Left: Kaplan-Meier curve demonstrating DFS in Lung SCC patients stratified according to the stage. The difference in DFS between the groups is statistically significant ($p < 0.001$). Right: Kaplan-Meier curve illustrating OS in LUSCC patients stratified according to the stage. The difference in OS between the groups is statistically significant ($p < 0.001$).

Figure 20: Spearman's correlation between Systemic Inflammatory Markers Neutrophil-to-Lymphocyte Ratio (NLR), Monocyte-to-Lymphocyte Ratio (MLR), and Platelet-to-Lymphocyte Ratio (PLR) in Oral Squamous Cell Carcinoma (OSCC) and Lung Squamous Cell Carcinoma (LUSCC).

Figure 21: At the top: Boxplots illustrating the distribution of NLR, MLR, and PLR values between early and advanced stages of Oral Squamous Cell Carcinoma (OSCC) patients. At the bottom: Kaplan-Meier survival curves depicting Disease-Free Survival (DFS) and Overall Survival (OS) in OSCC based on NLR levels (< 2.44 and > 2.44), with corresponding p-values (DFS: $p = 0.005$, OS: $p = 0.008$).

Figure 22: At the top: Boxplots illustrating the distribution of NLR, MLR, and PLR values between early and advanced stages of Lung Squamous Cell Carcinoma (LUSCC) patients. At the bottom: Kaplan-Meier survival curves depicting Disease-Free Survival (DFS) and Overall Survival (OS) in LUSCC based on PLR levels (cut-off 167.5), with corresponding p-values (DFS: $p = 0.012$, OS: $p = 0.026$).

Figure 23: Violin plots for the distribution of p53 positivity (%) according to the stage of disease in Oral SCC and Lung SCC (ns).

Figure 24 On the left Kaplan-Meier curves depicting Disease-Free Survival (DFS) in Oral Squamous Cell Carcinoma (OSCC) patients stratified by p53 expression levels ($< 10\%$ and $> 10\%$). Statistical significance ($p = 0.029$) is observed. On the right, an illustrative case displays p53 immunostaining in OSCC.

Figure 25: Representative histological sections for p53 IHC evaluation in the tumor cells, Lung SCC: a) 10x and b) 20x, p53+ immunohistochemistry (IHC) showing complete absence of P53 staining (0%); c) 10x and d) 20x, p53+ immunohistochemistry (IHC) with a high presence of P53 staining (100%).

Figure 26: On the left: Violin plots for the distribution of p62 positivity (%) in Oral SCC and Lung SCC (ns); the great majority of samples have high expression of p62. In the middle, a graphical representation using box plots depicting the differential expression of p62 positivity in tumor cells and dysplastic/reactive epithelium (%). On the right, an illustrative case of p62 IHC staining in dysplastic/reactive epithelium adjacent to tumoral tissue.

Figure 27: Representative histological sections for p62+ evaluation, cytoplasmic pattern in LUSCC: p62+ immunohistochemistry (IHC) a) 20x, b) 40x of the same section. Notably, p62 staining is diffuse in the cytoplasm, but nuclei are unstained (arrowheads).

Figure 28: Representative histological sections for p62+ evaluation, nuclear pattern in LUSCC: p62+ immunohistochemistry (IHC) a) 10x, b) 20x of the same section. Notably, p62 staining is concentrated in the nuclei (arrowheads).

Figure 29: Representative histological sections for p62+ evaluation, nucleo-cytosolic pattern in LUSCC: p62+ immunohistochemistry (IHC) a) 10x, b) 20x of the same section. Notably, p62 staining is present in both the nuclei and cytoplasm, and this pattern is consistent at the tumor invasive margin and the core.

Figure 30: On the left, pie charts depict the distribution of the three patterns (cytoplasmic, nuclear, and nucleo-cytoplasmic) in the tumor core and at the invasive tumor margin. In the middle, the same three patterns are presented based on the tumor cell differentiation grade, both in the tumoral core and at the tumor invasive margin. On the right, two representative histological sections illustrate p62+ evaluation in OSCC. The image above displays the nuclear pattern in a well-differentiated tumor area, while the image below shows a combined nuclear and cytoplasmic pattern in a less differentiated tumor area at the invasive front of the tumor.

Figure 31: Representative histological sections for p62+ evaluation in the tumor core and at the invasive margin, in LUSCC: p62+ immunohistochemistry (IHC) a) 20x, b) 40x of the same section. Arrows highlight the tumor infiltrative margin where a nucleo-cytoplasmic pattern is identified. Of note, in the tumor core, a prevalent nuclear pattern is depicted (arrowheads).

Figure 32: Kaplan-Meier curves illustrating DFS (left) and OS (right) in the OSCC population. The curves represent the subgroups of patients categorized based on p62 levels >80% and cytoplasmic or nucleo-cytoplasmic staining at IHC.

Figure 33: Top: Representative histological sections for TILs evaluation in LUSCC: a) High presence of TILs (60%) compared to b) Low presence of TILs (5%), Hematoxylin and eosin staining, 10x. Bottom: Kaplan-Meier curves illustrating Overall Survival (OS) in the combined

Oral Squamous Cell Carcinoma (OSCC) and Lung Squamous Cell Carcinoma (LUSCC) cohort. The curves represent the subgroups of patients categorized based on Tumor-Infiltrating Lymphocytes (TILs) levels within the tumor stroma, specifically TILs <15% and TILs >15%.

Figure 34: Representative histological sections for CD8+ lymphocytes evaluation at the invasive tumoral margin (dotted line) in OSCC (a) and LUSCC (b), CD8+ immunohistochemistry (IHC), 20x

Figure 35: Representative histological sections for CD8+ lymphocytes evaluation at the invasive tumoral margin in LUSCC: CD8+ immunohistochemistry (IHC) a) Grade 2 CD8 positivity, 10x; b) same section, 20x, very few CD8+ lymphocytes at the tumor margin; c) Grade 3 CD8 positivity at the invasive tumor margin (dotted line); arrow highlights nests of lung squamous cell carcinoma. Notably, mononuclear cells at the invasive tumoral margin consist mostly of CD8+ lymphocytes; b) Grade 4 CD8+ cells at the tumor margin (dotted line), with an area of necrosis in the left superior corner (arrowheads).

Figure 36: Representative histological sections for CD8+ lymphocytes evaluation at the invasive tumoral margin in LUSCC: a) Hematoxylin and eosin staining, 20x, b) CD8+ immunohistochemistry (IHC), 20x. Arrows highlight nests of lung squamous cell carcinoma, while circles indicate one of the regions of the infiltrative tumoral margin rich in lymphocytes. Notably, consecutive sections of the same sample stained with CD8 Ab reveal that these mononucleate cells are only in part CD8+ lymphocytes (arrowhead).

Table 4: Summary of Univariate Analysis for Overall Survival (OS) and Disease-Free Survival (DFS) in Oral Squamous Cell Carcinoma (OSCC) Patients, showcasing variables demonstrating significance as predictors of oncological outcomes.

Table 5: Summary of Multivariate Analysis for Overall Survival (OS) and Disease-Free Survival (DFS) in the Combined Cohort of Oral Squamous Cell Carcinoma (OSCC) and Lung Squamous Cell Carcinoma (LUSCC) Patients, including only variables with potential significance as predictors of oncological outcomes.

Table 6: Antibodies used in Immunohistochemistry for p62, CD8 and p53 staining.

INTRODUCTION

Background

Tumor diagnosis represents one of the most challenging scenarios, impacting both patients and medical professionals. Recognized relatively recently as the “*disease of the century*”, cancer can be profoundly debilitating and significantly affect life expectancy. In fact, among all other diseases, cancer stands as a prominent contributor to mortality and a significant obstacle to improving life expectancy across the globe.¹ Fortunately, substantial progress has been made in recent decades, enhancing our capabilities in prevention, early diagnosis, and treatment options. This progress has contributed to improved survival rates and increased chances of complete remission for patients.

Despite these advancements, the ultimate victory over cancer remains elusive. The complexity of the disease necessitates the consideration of numerous variables. Ongoing research in this field delves into an extensive landscape, focusing on different tasks: identifying and mitigating risk factors, developing minimally invasive screening tests, exploring potential prognostic tools for guiding aggressive therapies, and expanding the array of available treatment options.

Among all the cancer subtypes Lung cancer and Head and neck (HN) cancers represents respectively the second and the seventh most prevalent oncological diagnosis worldwide.^{2,3}

Various histological subtypes are encompassed within each category, but squamous cell carcinoma (SCC) stands out as the most prevalent in HN cancer. In the classification of lung cancer, tumors are primarily divided into Non-Small-Cell Lung Cancer (NSCLC, nearly 85%), which commonly includes SCC, along with large cell carcinoma, adenocarcinoma, and other minority subtypes. The other distinct category is Small Cell Lung Cancer (SCLC, about 15%), originating from neuroendocrine cells.

Lung cancer counts about 2,200,000 new cases worldwide (11,4% of all cancer cases) with a total of nearly 1,800,000 estimated deaths (18% of global cancer deaths) being the

leading cause of cancer death. Both incidence and mortality has a higher incidence in male than female.²

Head and neck SCC (HNSCC) contribute to approximately 890,000 new cases worldwide, constituting roughly 4.5% of all cancer diagnoses, and result in around 450,000 deaths annually, representing approximately 4.6% of global cancer-related deaths.³ The ratio of males to females, as indicated by extensive epidemiological studies and national cancer registries, ranges from 2:1 to 15:1, contingent on the specific site of the disease. Incidence rates for head and neck cancers rise with advancing age.⁴ The oral cavity is the most frequently affected organ in HNSCC, followed by the larynx, nasopharynx, oropharynx, hypopharynx, and ultimately, the salivary glands.³

Extensive research has substantiated a strong correlation with tobacco for both Lung and Head and Neck cancers. Alcohol consumption represents a risk factor for HN cancers while exposure to some agents (asbestos, arsenic, chromium, beryllium, nickel...) or radiation are associated with both type of tumors. Recent investigations have revealed a noteworthy increase in cases of HNSCC linked to the Human Papilloma Virus (HPV). In fact, HPV is implicated in 30–65% of all HNSCC cases and up to 80% of oropharyngeal cancers.⁵

Conventional treatment strategies for lung cancer and head and neck cancer typically encompass a combination of surgery, radiotherapy, and systemic therapy, adapted to the particular stage of the tumor. Immunotherapy has become a crucial aspect of lung cancer treatment, particularly for cases expressing effective immunomodulatory targets. In the context of head and neck cancer, immunotherapy currently holds a more limited role, primarily reserved for advanced stages.^{6,7}

Despite these interventions, treatment outcomes remain far from being completely effective. Reflecting on the survival rates documented in the USA since 1975 (Fig.1), the medical field has experienced a significant improvement in life expectancy for certain cancer subtypes, such as urinary tract malignancies (prostate, urinary bladder, kidney, and renal pelvis). Notable advancements have also been observed in the treatment of hematological tumors. However, despite improvements over the last three decades, lung cancer continues to exhibit one of the poorest outcomes among various organ malignancies, being the second most common cause of death among cancer patients.

Considering its high incidence among the general population, lung cancer necessitates in-depth research to alleviate its tumor burden.

Moreover, HN cancer patients have not seen a substantial breakthrough in treatment success. They are unfortunately recognized for the heightened risk of suicide linked to the diagnosis and tumor burden, second in frequency among all the Oncological patients,^{8,9} which is attributed to the highly visible region typically affected, the extensive surgeries required, and the subsequent functional difficulties related to speaking and swallowing capacity. More effective and less invasive treatments are always desirable in these cases, aiming to strike a balance between curative treatment goals and the quality of life. However, among HN cancers, laryngeal cancer has witnessed a paradoxically unchanged trend over years in the survival rate. Within HN cancers, laryngeal cancer has experienced a paradoxically unchanged trend in survival rates over the years. This trend was initially observed by Hoffmann and colleagues in 2006, who noted a decrease in survival among patients with laryngeal cancer from the mid-1980s to mid-1990s in the United States. Further analysis of this finding, along with contributing factors, revealed a correlation with the increased use of non-surgical treatment for laryngeal cancer.¹⁰ The excessive adoption of laryngeal function-sparing treatment, particularly combined chemo-radiotherapy, over various surgical options, ranging from aggressive open surgery to less invasive transoral laser surgery introduced in the 1970s, has resulted in a worse prognosis. Many patients undergoing chemo-radiotherapy did not achieve the anticipated results, facing issues such as tumor persistence, local recurrence, or post-treatment complications.

Regarding oral cavity cancers, the trend in recent decades has shown an improvement in overall survival, although it remains below 70% for 5-year survival rates across all stages. Oral squamous cell carcinomas (OSCC) are classified using a dimensional TNM system, incorporating two specific variables—depth of invasion (DOI) and extra nodal extension (ENE)—which have proven effective in determining prognosis.¹¹ However, an emerging body of literature highlights a small subset of T1-T2N0 OSCC that, despite proper resection based on margins, exhibits higher-than-expected rates of loco-regional/distant failure and disease-specific mortality. Consequently, some authors emphasize the need for histopathological risk stratification based on factors such as worst pattern of invasion (WPOI), perineural invasion, and lymphocytes at the tumor/host interface.¹² This

stratification has been shown to be a strong predictor of local disease-free and overall survival.

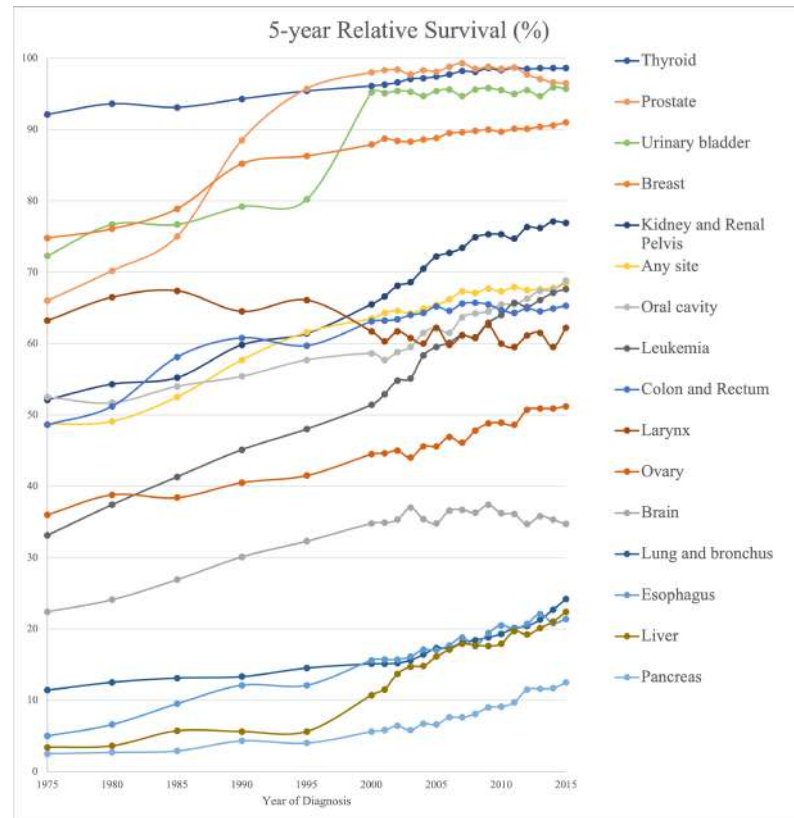


Figure 1: Evolution of 5-years relative survival over the past decades for different types of tumors. Data were collected from the Surveillance, Epidemiology, and End Results (SEER) Program of the National Cancer Institute.^{13,14}

In the field of oncology, the pursuit of improved outcomes revolves around three key objectives:

1. **Eliminating Risk Factors or aiming Early detection:** Emphasizing the importance of eliminating known risk factors for oncological diseases and, when not feasible, implementing screening strategies for individuals at high risk. This approach aims to facilitate early diagnoses.
2. **Identification of Prognostic Markers:** Investigating prognostic markers to enhance the classification of patients into high-risk and low-risk subpopulations. This allows for the tailored allocation of patients to treatments with lower aggressiveness yet higher efficacy.

3. Development of New Therapeutic Targets: Ultimately, focusing on the continuous development of new therapeutic targets to augment our capacity for curing various cancers.

In this perspective, new insights are evolving concerning the relationship between tumor cells and the host system. Specifically, within this context, the exploration of the immune system's potential emerges as a promising avenue for managing both lung cancer and head and neck cancer.

Immune system and cancer

Tumor patients should be viewed as individuals affected by a systemic disease that profoundly alters the biology not only at the primary site but throughout the entire body. One hallmark of cancer is the *inflammatory state*, which can act as both a “victim and author” of tumorigenesis or tumor progression in a context-dependent manner. Indeed, chronic inflammation has been established to play a role in tumorigenesis in almost 25% of cancers. This association varies and can be linked to chronic exposure to irritant substances (as tobacco, alcohol or other toxic inhalants), microbial infections, such as in HPV or Helicobacter pylori (HP)-related cancers, autoimmunity, as seen in tumors associated with inflammatory bowel disease (IBD), and immune deregulation, demonstrated by the heightened cancer susceptibility observed in immunocompromised patients.¹⁵

Ultimately, the immune system response across the body is molded as the cancer advances. Indeed, the body's defenses against cancer are intricately regulated by interactions among various cell types. The Tumor Microenvironment (TME) has been a subject of extensive research for years, and its interactive role in tumor initiation and progression has been well-established, though far from being completely understood. Within the TME, malignant cells interact with other resident or infiltrating cells such as fibroblasts, immune cells, and stroma. This dynamic milieu fosters intense connections among these diverse cellular components, and their reciprocal influences (through cytokines and receptor with stimulatory or inhibitory activities) play a crucial role in either restricting or promoting tumor growth. Furthermore, to better understand how tumors interact with the immune system, we need to examine the bigger picture of

immunity beyond just the local TME. In particular, the peripheral immune system is necessary to generate effective natural and treatment-induced immune responses against tumors.¹⁶

Over the last decade, the utilization of immunotherapy to leverage the immune system in combating tumoral cells has determined a remarkable transformation in cancer therapy.¹⁶

Immune checkpoint inhibitors (ICIs), like anti-Cytotoxic T-lymphocyte associated protein 4 (CTLA4), anti-Programmed cell death protein 1 (PD1), and anti-Programmed death-ligand 1 (PD-L1) used in modulation of the patient's immune system, have resulted in enduring remissions across a diverse range of tumor types. Additionally, expanded autologous tumor-specific T cells or chimeric antigen receptor T cells' infusion has demonstrated efficacy in leukemia patients.¹⁶ Despite these notable successes, immunotherapy remains ineffectual for the majority of cancer patients.¹⁷

From Tumor Microenvironment to Tumor MAcroenvironment

As underlined by Hiam-Galvez et al. in a recent review article, the field of tumor immunology has primarily concentrated on local immune responses within the *tumor microenvironment* (TME). However, it's crucial to recognize that immunity is orchestrated across various tissues in the so-called *Tumor Macroenvironment* that comprehends not only the local TME but also blood and secondary lymphoid organs (bone marrow, lymph nodes and spleen). In this perspective both peripheral and tumor-infiltrating immune cells are considered essential subjects for in-depth study to gain a better understanding of their roles in combating tumors.¹⁶

In fact, the various methods by which the immune system is prompted to undergo alterations due to the tumor burden include both systemic and local changes.

Immune system in the tumor niche

The innate and adaptive immune systems are pivotal for maintaining tissue homeostasis by eliminating abnormal cells, including those that have undergone malignant transformation. However, during tumorigenesis, the immune system initially confronts highly immunogenic tumor cells. Eventually, it tends to favor the less immunogenic

clones that can evade immune responses and possess the potential to proliferate and shape the tumor microenvironment (Fig.2). Specifically:

- *Tumor-associated Macrophages (TAMs)*. They are involved in every step of tumor progression. In particular there are 2 distinctive subpopulations of activated macrophages: the M1-proinflammatory (anti tumoral) type, which are driven by LPS and IFN γ , and M2-anti-inflammatory (pro-tumoral) type, which respond to IL-4 or IL-13.¹⁸ At the initial stages of tumorigenesis, the polarization toward M1-type of TAMs is consequently associated with a better control of tumoral immunogenic cells. However, once tumor is established, its proliferation is facilitated by a shift to M2 anti-inflammatory subtype, which eventually exert a pro-tumoral role. In particular, TAMs contribute to the advancement of tumors through various mechanisms. These include promoting angiogenesis and lymphangiogenesis, fostering cancer cell proliferation and epithelial–mesenchymal transition (EMT), reducing the effectiveness of treatments, restructuring the extracellular matrix (ECM), facilitating metastasis, and instigating immunosuppression to hinder the anti-tumor activity of immune cells.¹⁹ Chemokines as VEGF, CCL2, CCL5 and M-CSF promotes TAMs recruitment and may be potential therapeutic targets.¹⁵
- *Tumor-associated Neutrophils (TANs)*. It is largely known that neutrophils play an important role in tissue inflammation secondary to pathogens, by their immediate response at the damage tissue consisting in eliminating pathogens acting through phagocytosis, antibacterial proteins' secretion, exocytosis of protease-containing granules and deposition of neutrophil extracellular traps (NETs). However, in oncological patient evidence of Neutrophilia, with an increased Neutrophil-to-lymphocytes ratio (NLR), and high levels of TANs are associated with poor prognosis.²⁰ The latter appears to play a complex role in the TME and can be polarized between the anti-tumoral phenotype TANs (TAN1) and the pro-tumoral phenotype TANs (TAN2).²¹
- Natural Killer cells (NK), renowned for their documented anti-tumoral function, play a crucial role in tumor control. Specifically, they induce programmed cell death in cells that lack expression of Major Histocompatibility Complex class I (MHC-I). Conversely, the recognition of MHC-I by NK cells' receptors in healthy

cells leads to a significant inhibition of their function.²² Presence of NK cells in the TME is correlated with favorable outcomes.¹⁵

- Dendritic Cells (DCs), serving as specialized Antigen Presenting Cells (APCs) for both endogenous and exogenous antigens, function at the crossroads of innate and adaptive immunity. They play a pivotal role in either inducing tolerance or initiating an effector T cell response, a decision influenced by their interaction with MHC molecules and the presence of co-stimulatory signals. Certain clinical trials have explored the use of the so-called DC vaccine, which involves using autologous DCs loaded with tumor antigens to provoke a T-cell response against cancer. While the results have shown promise, they are not yet conclusive. Recent studies propose the combination of the DC vaccine with immune checkpoint inhibitors.²³
- T cells, which control and carry out the adaptive immune response, are the second most frequent cell type which found in the TME after TAMs. In fact, during early stages of tumorigenesis naïve T cells are primed in the lymph nodes and eventually moved to the TME to address immunogenic tumor cells. A high level of tumor infiltrating lymphocytes (TILs) are associated with a better prognosis and predictable better response to immunotherapy in different cancer types including breast,²⁴ colorectal cancer,²⁵ melanoma.²⁶ Furthermore, the so-called TILs therapy holds a promising role. This process entails the extraction of T cells residing in the patient's specific tumor, expanding these T cells outside the body, and subsequently reintroducing them into the same patient post a preparative regimen that depletes lymphocytes. The procedure is supplemented with the administration of IL-2 for support.²⁷ Within this population of lymphocytes, specific subtypes have been studied for their role in cancer. Particularly, CD8⁺ T cells play a crucial role in the anti-tumoral response. Usually, these cells are activated by APCs to transform into cytotoxic T cells (CTLs), resulting in the elimination of tumor cells by releasing granules containing perforin and granzyme through exocytosis.¹⁵ Another role in the antitumoral response is done by CD4⁺ T helper 1 (Th1), which, secreting proinflammatory cytokines (IL-2, TNF- α , and IFN- γ), promote priming and activation of CTLs, antigen presentation and antitumoral activity of NK cells and macrophages. High rate of CD8⁺ T cells and

Th1 lymphocyte are found to be correlated with better OS and DFS in different cancers.²⁸

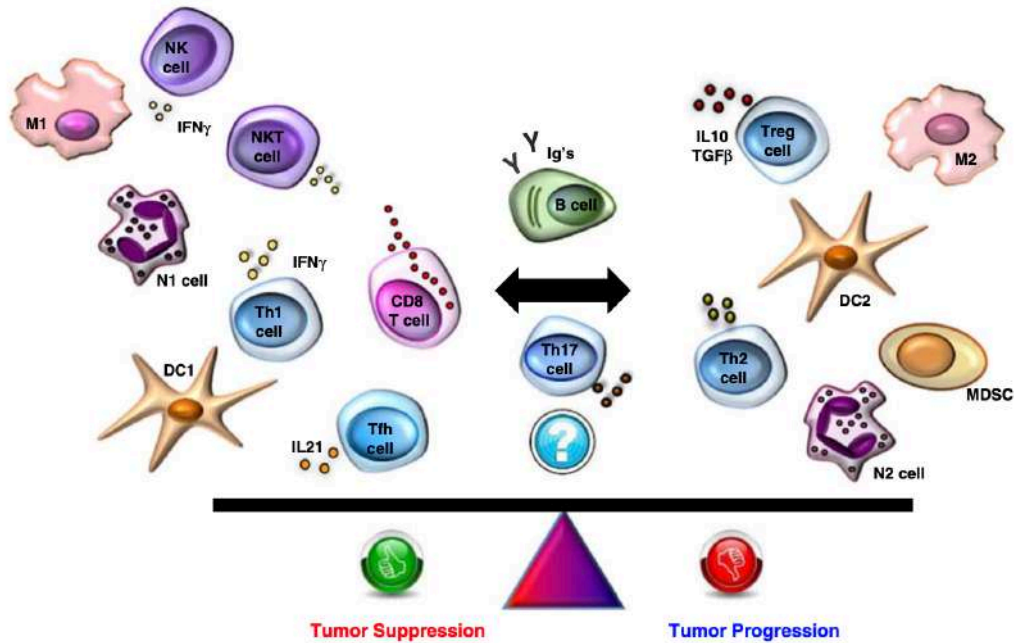


Figure 2: Graphic representation of the cells involved in the host immune response towards tumor cells. The imbalance towards the pro-inflammatory anti-tumoral response or the anti-inflammatory pro-tumoral environment may determine tumor regression or progression. [see table of acronyms and abbreviation] Courtesy of Hendry et al. 2017.²⁹

Tumor Infiltrating Lymphocytes in the TME as prognostic oncological factor

While various studies have identified the prognostic significance of Tumor-Infiltrating Lymphocytes in oncological patients, the integration of TILs as a prognostic factor with therapeutic implications remains absent from clinical settings and global oncological treatment guidelines. Notably, the eighth edition of the American Joint Committee on Cancer/Union Internationale Contre le Cancer (AJCC/UICC) TNM classification of malignant tumors does not include TILs or other histological representatives of the immune system as a considered variable.

Indeed, the TNM classification currently provides a staging system that is focused on the size and invasiveness of tumors (in terms of local infiltration, lymphatic-, vascular-, perineural- invasion, extranodal extension), offering an estimation of disease progression.

The primary aim is to offer prognostic insights into the aggressiveness of the disease, encompassing the potential of tumor cells to metastasize to lymph nodes or distant organs. As a result, the objective of the TNM classification is to establish a globally recognized stratification of the risk of recurrence and survival among oncological population. This standardization aids in determining the appropriate therapeutic options for patients, guiding decisions related to curative or palliative treatments.

However, recent literature suggests a growing interest in integrating the prognostic significance of TNM classification with the immunological pathological features of various cancer types to enhance oncological risk stratification. The TNM classification traditionally operates under the assumption that tumor progression results from *tumor-cell autonomous processes*. The incorporation of the host immune response into this classification may provide a more comprehensive understanding of tumor biology within the systemic context of the tumor-host relationship.³⁰

Evaluation of TILs is possible and low-cost in hematoxylin and eosin (H&E)-stained sections. However, to further distinguish immune cells subtypes with their different functional characterization (CD4+ Th1, Th2, Treg, CD8+, NK, B cells), is quite more difficult, requiring different Ab-labeled immunohistochemistry (IHC).

In colorectal cancer (CRC), Galon et al. have firstly proposed in 2012 the adoption of a novel histological score, known as the *Immunoscore*.³¹ They underlined the prognostic significance of TILs (CD3+ total T cells, CD8+ effector T cells and CD45RO+ memory T cells) depending on their infiltration in the tumor core (CT) or at the tumor invasive margin (IM), as previously reported.^{30,32} In fact, CD3+ counts in CT and IM revealed to possess an independent prognostic value for DFS and OS in multivariate analysis, surpassing TNM classification in CRC. As a solution for difficult reproducibility in the immunohistochemistry for CD45RO+ memory T cells, the international group led by Galon proposed introducing the *Immunoscore* into clinical practice using an automated cell counter and excluding CD45RO+ cells.

Immunoscore in CRC has been finally defined by the quantification of two specific lymphocyte populations, total CD3+ T cells and CD8+ effector T cells, through IHC analysis in two distinct tumor regions—the tumor core and the invasive tumor margin. The score ranges from 0 (low infiltration of both populations found in both regions) to 4

(high infiltration of both populations in both regions). Furthermore, it has demonstrated prognostic significance, emphasizing the necessity for a more precise definition of prognostic stages in conjunction with the TNM classification.^{30,33}

Likewise, the International Immuno-Oncology Biomarker Working Group proposed in 2015 the standardization of TILs evaluation as a prognostic biomarker in breast cancer.³⁴ However, in this case, the TILs evaluation was recommended on simple H&E staining, exclusively in the stromal compartment, without the use of lymphocytic markers in IHC. To date, TILs evaluation still remains out of consideration in Breast cancer National Comprehensive Cancer Network (NCCN) guidelines,³⁵ although their demonstrated prognostic significance.³⁶

In 2017, a comprehensive review was conducted to assess the role of TILs in various types of cancer.^{29,37} For melanoma, the inclusion of TILs information in pathological reports has become a routine practice, highlighting its prognostic significance and potential as a predictive marker for immunotherapy response. However, it has not yet been officially recognized in the 8th edition of the AJCC/UICC TNM staging system or the NCCN guidelines for melanoma treatment.³⁸

In the context of gastric cancer, Zhang et al. introduced a scoring system in 2019 inspired by Galon's studies. This system was applied to TILs assessed on H&E slices, considering both the intensity and percentage of TILs in the CT and IM. Their findings revealed noteworthy prognostic implications, showing a significant association between TILs levels (high or low) and various clinicopathological factors such as dimension of the tumor, histological grading, involvement of regional lymph nodes, perineural invasion, tumor thrombus, pathological TNM (pTNM) stage, and World Health Organization (WHO) subtypes ($p < 0.001$, respectively). Furthermore, a high level of TILs demonstrated a positive predictive impact on overall survival (OS) in both Kaplan-Meier and multivariate analyses.³⁹

Role of TILs in Head and Neck Cancer and Lung cancer

Focusing on HN and Lung cancers, there is still limited understanding of the role played by immune system cells within the TME as prognostic factors.

Specifically, while some studies have shown the prognostic significance of TILs in various solid tumors, there has not been a substantial clinical translation of these findings.

In 2015, the Donnem group introduced the promising prognostic role of CD8+ TILs in NSCLC, akin to Galon's Immunoscore for CRC. They validated this scoring system in a cohort of 797 patients diagnosed with resectable stage I–IIIA NSCLC. CD8+ TILs emerged as an independent prognostic factor for all endpoints (OS, Disease-Free survival DFS, Disease-specific survival DSS with $p < 0.001$). In multivariate analysis, this variable demonstrated prognostic significance independent of pStage.⁴⁰ Additionally, they introduced the TNM-Immunoscore (TNM-I) for NSCLC, drawing on prior experience in colorectal cancer and guidelines proposed for gastric cancers. To simplify the evaluation, TILs were assessed in a unified compartment, considering the total expression in both the intraepithelial and stromal compartments. This approach holds the potential for easier use, especially in automated analyses, while maintaining the same prognostic impact.⁴¹

The ease of analyzing TILs may further facilitate the advancement of automated pathological examination. In fact, Pan et al. recently published the validation of an artificial intelligence-driven pathological scoring system for evaluating TILs on H&E-stained whole-slide images of Lung Adenocarcinoma (LUAD). This system calculates a risk score based on TIL counts in both the cancer epithelium and stroma (WELL score) which demonstrated an independent prognostic value on OS and DFS.⁴²

In 2017, de Ruiter et al. conducted a meta-analysis on HNSCC, emphasizing the prognostic importance of CD3+ TILs in OS with a HR of 0.63 and DFS with an HR of 0.64. Additionally, CD8+ TILs were found to be prognostically significant in OS with an HR of 0.67 and in DFS with an HR of 0.50. This analysis encompassed various types of Head and Neck Squamous Cell Carcinoma (HNSCC), including those affecting the oral cavity, oropharynx, hypopharynx, and larynx.⁴³

In 2021 Almagush et al. outlined the fact that patients diagnosed with early-stage oral tongue squamous cell carcinoma (OTSCC) generally experience more favorable outcomes compared to those with advanced disease. However, even among early-stage cases, a subset may still face challenges such as recurrence, cancer-related mortality, and overall survival disparities. They proposed a modified TNM-Immune staging system for early-stage OTSCC, incorporating TILs as a variable in the TNM framework, categorized

into low and high TILs. In their study involving 290 early-stage OTSCC cases, no statistically significant difference OS was found between T1 and T2 classifications based on the 8th edition TNM classification. However, significant discrimination in OS was achieved by introducing the two classes of T1N0M0-Immune vs. T2N0M0-Immune. This classification defined:

- T1 as a tumor with size ≤ 2 cm, depth of invasion (DOI) ≤ 5 mm, and TILs $> 20\%$,
- T2 as a tumor with size ≤ 2 cm, DOI > 5 mm and ≤ 10 mm, or tumor > 2 cm but ≤ 4 cm, and DOI ≤ 10 mm. TILs should be $\leq 20\%$, otherwise downstaging is necessary.

This proposed staging system allows the classification of T2-Immune tumors as high risk for worse OS, DFS, and DSS. In this staging system the presence of high TILs infiltrate ($>20\%$) suggested the benefit of the proinflammatory anti-tumoral environment even in tumor larger than the classical T1 with consequent downstaging of T2 to T1-Immune classification.⁴⁴

Lately in the 2022 the same group analyzed the prognostic significance of TILs in oropharyngeal squamous cell carcinoma (OPSCC). They reaffirmed the use of the 20% division point to differentiate between low and high TILs in the tumor stroma. In the multivariate analysis, TILs showed an association with OS and DSS with Hazard Ratios (HR) of 1.87 and 2.13, respectively. Notably, significant prognostic value was observed even within specific subgroups based on the presence or absence of HPV.⁴⁵ Data were confirmed in a meta-analysis conducted in 2023 on 11 published studies on OPSCC.⁴⁶ The Pokrývková's group has additionally shown that HPV+ OPSCC, known for their favorable outcomes, exhibit a higher infiltration of lymphocytic subpopulations, including CD3+CD4+, CD3+CD8+, PD1+CD4+, PD1+CD8+ T cells, and Treg cells, in comparison to HPV- OPSCC.⁴⁷

In 2021, Borsetto et al. conducted a systematic review and meta-analysis among all anatomical sites of HNSCC, analyzing 28 selected studies. A high level of CD4+ and CD8+ TILs was associated with a reduced risk of death when considering various HN sites combined. However, while OPSCC and hypopharyngeal SCC demonstrated better OS in patients with high CD4+TILs, no significance was observed in laryngeal or oral

cavity SCC.⁴⁸ This may suggest that further studies are needed in these anatomical sites to assess the prognostic role of TILs.

The recent trajectory of research in this domain has notably shifted its focus toward assessing the potential impact of Artificial Intelligence (AI) in the analysis of TILs within pathological sections. A noteworthy instance of this paradigm shift occurred in 2018 when the research group led by Saltz et al. embarked on a groundbreaking exploration of the vast reservoir of data housed in The Cancer Genome Atlas (TCGA) archives.⁴⁹ In a groundbreaking initiative, they harnessed digitized H&E-stained images of TCGA samples spanning 13 types of tumors. This research endeavor involved leveraging the power of neural networks to discern distinct patterns of TILs within the digitized images. Through the meticulous analysis of 5,455 images across 13 cancer types, the research team successfully generated four distinct TIL maps using deep learning techniques. Furthermore, their approach aimed to establish correlations between these TIL maps and clinical data, seeking to unravel potential associations with patient outcomes.

A key aspect of Saltz et al.'s work involved the identification of cutoff values derived from their AI-driven analysis, which demonstrated a prognostic role in OS. The exploration of these cutoff values provided valuable insights into the predictive capacity of TIL patterns, offering a potential avenue for refining prognostic assessments in cancer patients. It's imperative to recognize the pioneering nature of this research, as it not only delves into the potential of AI in TIL analysis but also underscores the transformative impact of deep learning methodologies in deciphering complex patterns within pathology images. This research contributes significantly to the ongoing discourse surrounding the integration of AI in oncological research and highlights the potential for enhancing prognostic assessments through advanced computational approaches.

In conclusion, examining the immune profile of tumors could offer essential and innovative prognostic insights. The results of a worldwide validation of the Immunoscore for various cancer types may result in its incorporation as a novel element in cancer classification, leading to the establishment of TNM-I (TNM-Immune).³¹

Systemic immunity and cancer

Different changes affect not only the local tumor environment but also the systemic changes of the immune system in response to tumor burden:

- Hematopoietic disruption with the proliferation of hematopoietic stem cells, multipotent progenitors, and granulocyte-monocyte progenitors (GMPs) within the bone marrow, ultimately leading to the presence of immature immunosuppressive monocytes, macrophages, and neutrophils in both the bloodstream and the TME, as demonstrated in various types of cancer.^{16,50} Hence, peripheral blood cells can be viewed both as a potential therapeutic target and as a plausible prognostic factor, as elaborated further.
- Reduced levels of peripheral blood DCs, a distinct type of APCs, which play a crucial role in CD8⁺ and CD4⁺T cell priming, differentiation and proliferation.⁵¹⁻
56
- Alteration on the T cells circulating subpopulation, ranging from a reduced diversity of the T cell receptors (TCRs), while greater diversity is associated with better tumor control in melanoma,⁵⁷ perturbation of their functions as the secretion of specific cytokines (IL-2, IFN- γ)⁵⁸, to the expansion of peripheral and intratumoral suppressive CD4⁺ FoxP3⁺ regulatory T cells (Treg) which contribute to tumor immune evasion inhibiting the anticancer immunity.⁵⁹ As they have been identified in both the peripheral and intratumoral environments with the same TCR specificity against autologous tumors and mutated neoantigens, Tregs appear to originate from naturally occurring thymic Tregs rather than being induced through local differentiation at the tumor-stroma interface.⁶⁰ Tregs secrete immunosuppressive cytokines like IL-10 and TGF- β , and deplete IL-2, thus fostering immune escape. Moreover, they dampen T cells' activity through the expression of negative co-stimulatory immune checkpoint inhibitors as PD-1 and CTLA-4.
- Although the total number of B-cells remain stable, oncological patients shows an increase of the suppressive subpopulation of regulatory B cells which, by the secretion of the anti-inflammatory cytokine IL-10, play an important role in tumor progression, as demonstrated in lung and gastric cancers.^{61,62}

- Natural Killer cells play a dual role in both direct killing and influencing other immune cells to combat tumors. However, certain studies focused on breast⁶³ and NSCL⁶⁴ cancers have indicated a reduced presence of activating receptors (such as NCR1, NCR2, and NCR3) in peripheral NK cells. This diminished presence correlates with impaired anti-tumoral capacity in vitro and serves as a negative prognostic factor for OS.

Considering the modifications induced by the tumor burden on the systemic immune response and recognizing the cross-relationships that ultimately influence the fate of cancer cells through pro-tumoral or antitumoral immune system activities, blood cells may play a role in both prognostic and therapeutic aspects.

Systemic inflammation biomarkers in cancer

In recent decades, several blood biomarkers have been suggested as surrogates for systemic inflammation in oncological patients. Their significance has been investigated in terms of prognosis and response to therapy. Notably, C-reactive protein (CRP), the Neutrophil-to-Lymphocyte Ratio (NLR), Platelet-to-Lymphocyte Ratio (PLR), and Monocyte-to-Lymphocyte Ratio (MLR) have been among the most extensively studied. The reason is their easy assessment in all patients through simple blood sample and routine hematological analysis.⁶⁵

A systematic review updated to 2014, encompassing various solid tumors such as pancreatic cancer, renal cell carcinoma, carcinoma of the colon and the rectum, gastroesophageal cancer, NSCLC, mesothelioma, cholangiocarcinoma, and hepatocellular carcinoma, underscored the adverse prognostic significance of the NLR in a cohort exceeding 40,000 oncological patients. In all oncologic categories according to tumor sites, stage and histology, NLR greater than a median cutoff of 4 had a significant hazard ratio for OS, Disease-specific survival (DSS), progression-free survival (PFS) and DFS (1.81, 1.61, 1.63, and 2.27, all $p < .001$, respectively).⁶⁶

The prognostic significance of NLR remains inadequately comprehended and has not yet been widely implemented in clinical settings. In the latest 8th edition of the TNM classification, it is acknowledged solely as a promising prognostic risk factor in pancreatic cancer and hepatocellular carcinoma (HCC) among all cancers. However, it is

still excluded from risk stratification and does not play a role in both the staging system or therapeutic direction.⁶⁷⁻⁶⁹

The potential basis for NLR role in prognosis and therapeutic decision may lie in the link between a high NLR and a general inflammatory state.⁶⁶

Neutrophils are integral components of the innate immune response, whereas lymphocytes play a central role in the adaptive immune response. The equilibrium between these two cell types serves as a marker for the fundamental aspects of the immune response: acute and chronic inflammation (neutrophils) vs adaptive response (lymphocytes). Consequently, the Neutrophil-to-Lymphocyte Ratio has been investigated in diseases where the interplay between these cell types is crucial, including cancer, trauma, sepsis, and autoimmune diseases.⁷⁰ Beyond their first-line high efficient phagocytic activity in controlling inflammatory and infectious processes, neutrophils have an important role in moulding the adaptive immune response through cytokines.⁷⁰ Elevated neutrophil levels (neutrophilia) relative to lymphocyte counts contribute to an immunosuppressive role, impacting the cytolytic activity of immune cells (lymphocytes, T-cells, NKs).⁶⁶

Its characteristic of easy availability and good reliability is prompted NLR as a largely diffuse biological marker in different clinical settings, across all the medical specialities.⁷¹ However, its value is still influenced by different conditions as age, therapy, chronic or acute illness (heart disease, diabetes, anemia, stress, obesity).⁷¹ To note, in 2021 Zahorec proposed a NLR scale explaining how different ranges of this marker may uncover different pathological conditions (Fig.3).^{71,72}

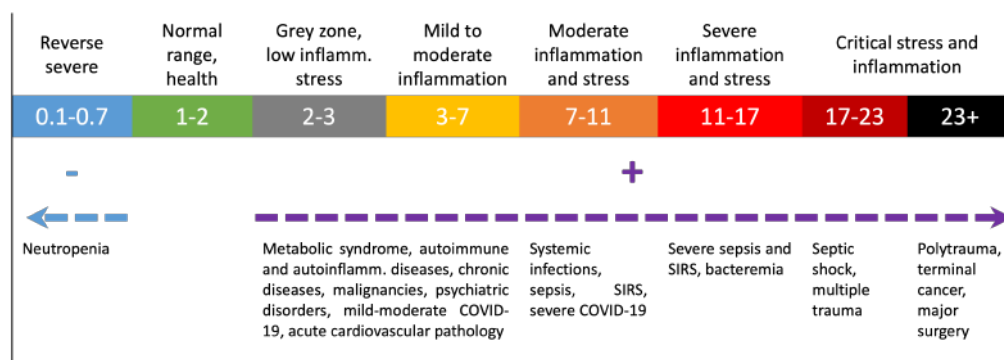


Figure 3: Neutrophil to Lymphocyte Ratio (NLR)-meter [SIRS, Systemic inflammatory response syndrome], modified from Kourilovitch et al., 2023⁷²

A recent meta-analysis on HNSCC was conducted by Mariani et al. in 2021, focusing on surgical patients who underwent or did not undergo adjuvant therapy. The study excluded cases of HPV+ cancers. Ultimately, they analyzed 17 and 10 studies meeting the inclusion criteria for quantitative analysis, involving a total of 4597 and 2020 patients for OS and DFS, respectively. The findings confirmed in HNSCC the well-established trend of a worse prognosis in terms of OS (HR 1.56, $p < 0.001$) and DFS (HR 1.64, $p < 0.0001$) in patients with higher preoperative NLR values.⁷³

Additionally, in 2022, the group led by Takenaka investigated the role of NLR in predicting response to therapy and subsequent OS and PFS in patients affected by recurrent or metastatic HNSCC treated with immune checkpoint inhibitors. Conducting a meta-analysis of 14 studies involving a total of 929 patients, Takenaka et al. discovered that higher NLR was significantly associated with all endpoints (OS, HR 2.03; PFS, HR 2.15; response to therapy, OR 0.49; and disease control, OR 0.3).⁷⁴ These findings were corroborated by Kang's group in a comprehensive meta-analysis on prognostic biomarkers predicting response to ICIs treatment in HNSCC. In this analysis, low NLR was associated with better OS, aligning with other biomarkers, whether already included or not in clinical practice. These additional biomarkers encompassed HPV positivity, PD-L1 positivity, as well as factors such as a low Glasgow prognostic score (derived from albumin and CRP values), low performance status, high BMI, low PLR, high albumin, and low lactate dehydrogenase (LDH).⁷⁵

Indeed, there are other biomarkers considered as surrogates for the immune system's response to tumor burden, with promising role in risk stratification. Specifically, the Platelet-to-Lymphocyte Ratio, which typically indicates an elevated platelet count (thrombophilia) and low lymphocyte count in blood samples (lymphopenia), may reflect an imbalance in the immune system response, impacting the adequate control of tumor cells. In 2018 Li et al. demonstrated a significant association of high PLR with poor OS and PFS in patients with advanced cancers, including NSCLC, nasopharyngeal cancer, renal cell carcinoma, pancreatic cancer, biliary tract cancer, liver cancer, gastric cancer and CRC.⁷⁶

Similar studies conducted in NSCLC have affirmed the prognostic significance of NLR and PLR even in these types of tumors. In 2015, a meta-analysis made by Yin et al. on 14

previous studies demonstrated the significance of NLR in predicting prognosis for Lung cancer. The analysis encompassed both NSCLC and SCLC across both early and advanced stages.⁷⁷ In 2022, a meta-analysis published by Platini et al. examined 12 studies involving a total of 1719 patient affected by advanced NSCLC and treated with ICIs. The results consistently validated the prognostic value of high NLR and PLR in predicting poor outcomes in terms of OS and PFS.⁷⁸

Accordingly, the Monocyte-to-Lymphocyte Ratio (MLR), serving as a simple biomarker representing the host immune system, has been proposed to have implications for prognosis in various cancers.

In fact, the MLR, calculated by dividing the absolute monocyte count by the absolute lymphocyte count, has a significance that lies in its potential role as a novel indicator in the context of cancer-related processes. Monocytes have the capability to suppress the activation of lymphocytes, which are crucial components of the immune system. This suppression, in turn, can contribute to the enhancement of tumor progression. Moreover, an elevated monocyte count has been associated with promoting tumorigenesis and angiogenesis through localized immune suppression and the stimulation of tumor neovasculogenesis. On the flip side a low lymphocyte count may result in a weakened and insufficient immunologic reaction to a tumor, potentially compromising the body's ability to mount an effective anti-cancer response.

In HN cancer, a meta-analysis conducted by Tham et al in 2018, involving 4260 patients across seven cohorts, demonstrated significant findings. The pooled data indicated that an elevated Lymphocyte-to-Monocyte Ratio (LMR, as the terms are inverted in this study) was associated with significantly improved OS (HR 0.5; 95% Confidence Interval (CI) 0.44-0.57) and DFS (HR 0.70; 95% CI 0.62-0.80).⁷⁹

Similar findings were reported in a recent meta-analysis conducted by Jin et al. in 2021, that focused on the prognostic role of pretreatment LMR in lung cancer. The comprehensive analysis incorporated data from 23 studies, comprising a sizable cohort of 8361 lung cancer patients. The consolidated findings from this meta-analysis highlighted a significant correlation between decreased pretreatment LMR and adverse clinical outcomes in lung cancer patients. Specifically, a reduced pretreatment LMR was notably associated with diminished PFS and OS. The HR for these associations were

considerable, with a HR of 1.49 (95% CI: 1.34-1.67, $p < 0.01$) for PFS and a HR of 1.61 (95% CI: 1.45-1.79, $p < 0.01$) for OS, indicating a substantial impact on these critical outcome measures. Moreover, the subgroup analyses, particularly focusing on SCLC, revealed intriguing insights. Importantly, the results suggested that a lower pretreatment LMR was not significantly associated with poorer OS among SCLC patients.⁸⁰ The nuanced exploration, including subgroup analyses based on histologic subtypes, enhances our understanding of the potential variations in the prognostic impact of LMR across different types of lung cancer.

Similar prognostic implications have been underscored across various cancer types, encompassing ovarian,⁸¹ prostatic,⁸² pancreatic,⁸³ colorectal,⁸⁴ bladder,⁸⁵ and gastric cancers.⁸⁶ This recurring trend emphasizes the potential universality of the identified prognostic role in diverse malignancies, showcasing the relevance of this parameter across a spectrum of cancer types. The consistency of these findings across different organ systems further strengthens the argument for the broader applicability of the identified prognostic marker in understanding and predicting clinical outcomes in cancer patients.

The Hallmarks of Cancer: oncogenic addiction

In recent decades, biomedical research has laid the groundwork for a deeper understanding of cancer pathogenesis. Scientific progress has elucidated that the malignant transformation of cancer cells follows a series of acquired 'hallmarks,' which stem from mutations in two distinct groups of genes known as oncogenes or tumor suppressor genes. These mutations drive malignant cells to acquire six essential functions that contribute to their survival, proliferation, and dissemination: independence from growth signals, insensitivity to growth-inhibitory (antigrowth) signals, evasion of programmed cell death (apoptosis), limitless replicative potential, sustained angiogenesis, and tissue invasion and metastasis.⁸⁷ Additional studies have outlined two 'emerging hallmarks,' namely the reprogramming of energy metabolism and, most notably, the ability to evade the immune system. Moreover, an important role has been given to normal cells recruited by transformed ones which create the TME, contributing to the survival and tumor progression.⁸⁸

These hallmarks are attained in various types of tumors through unique pathways and at different stages throughout the process of multistep tumorigenesis. The underlying mechanism has been identified as genomic mutations occurring in widely diffuse oncogenes (gain of function mutation, amplification, genetic overexpression) and oncosuppressor genes (loss of function mutation, deletion, epigenetic silencing). However, there is a large number of low-frequency genetic changes that contribute to oncogenesis, delineating a great complexity in cancer pathogenesis. This heterogeneous and variable scenario represents a daunting problem in targeting cancer treatment.

Of note, in order to achieve malignant phenotype, cancer cells are used to reactivate and modify existing pathway, normally used during development. The identification of these key-players and modulation of their function in an anti-tumoral direction may constitute the success of oncological therapy. Moreover, targeting these nodes by therapy will result in a large therapeutic window useful to kill tumor cells while sparing normal cells.⁸⁹

The stress phenotypes of cancer: non-oncogenic addiction

A large body of evidence in the past ~20 years has established the concept that cancer cells rely more than normal cells on cytoprotective pathways also active in normal cells and not involved in tumorigenesis. In 2009, the growing awareness of the scientific community culminated in a seminal review by Luo et al. that proposed some additional hallmarks of tumor cells, named the “*stress phenotypes of cancer*”. Although not responsible for initiating tumorigenesis these stress phenotypes are common patterns of transformed cells, which therefore show heightened dependence not only on oncogenes, but also on genes with fundamental stress-adaptive functions, offering previously unimaginable therapeutic opportunities. Such *non-oncogene addiction* defines a framework for effective targeted therapies. They include DNA damage/replication stress, proteotoxic stress, mitotic stress, metabolic stress, and oxidative stress (*Fig. 4*).⁸⁹

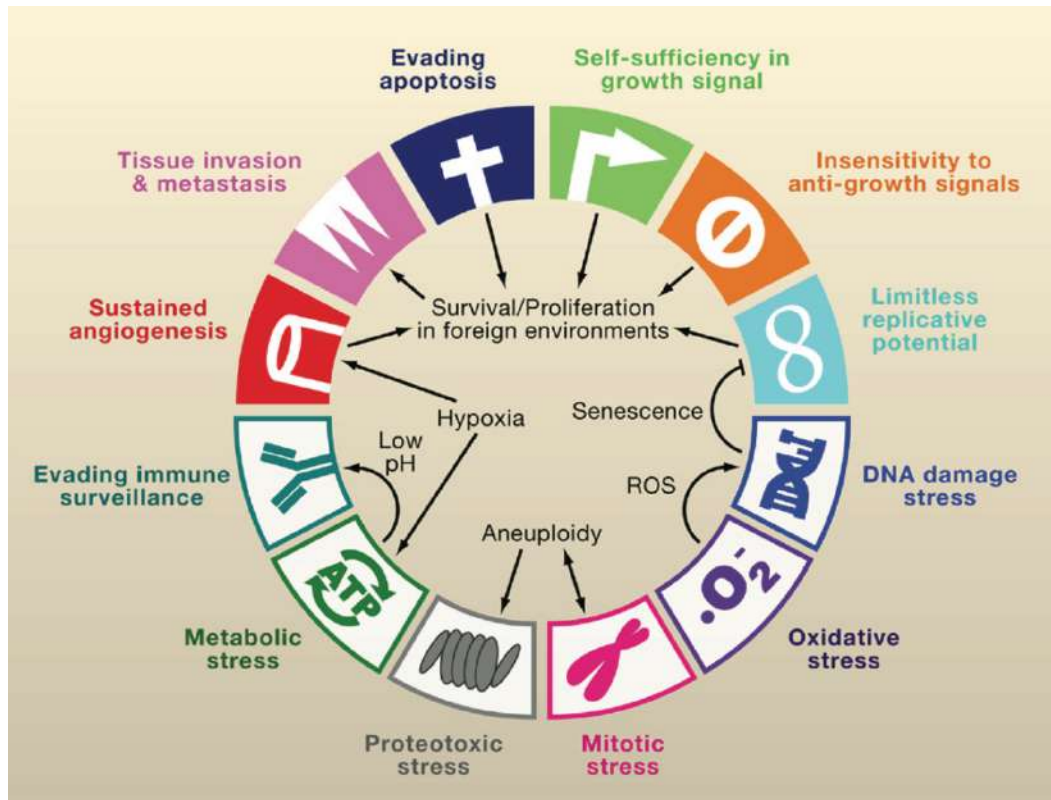


Figure 4: The hallmarks and the stress phenotypes of cancer [courtesy of Luo et al., 2009].⁸⁹

In this complex scenario of malignant cell transformation and survival, one cellular pathway that appears to be implicated in both oncogenic and non-oncogenic addiction is the autophagic pathway. In fact, basal autophagy takes place in cells under regular circumstances, but this activity significantly intensifies in response to specific cellular stresses. We have chosen to delve deeper into this cellular mechanism to elucidate how it can modulate tumor progression and survival, explore the intricate relationship between cancer cells and host immunity, understand its role in predicting the prognosis of oncological patients, and ultimately shape the response to therapy.

Autophagy

Autophagy is an intracellular catabolic process that consists in the sequestration of cytoplasmic components or organelles in autophagosomal vesicles that eventually fuse with the lysosome, leading to their degradation.

In contrast to the apparently more selective Ub-dependent, but more limited proteasomal degradative pathway, this lysosomal strategy has a nearly unlimited recycling capacity. It is able to degrade large protein aggregates and entire organelles, and it can break down lipids, DNA and RNA, providing new substrate pools for anabolic processes.

Many different pathways can deliver substrates to lysosomes through the autophagic machinery: chaperone-mediated autophagy, microautophagy and macroautophagy (Fig.5).

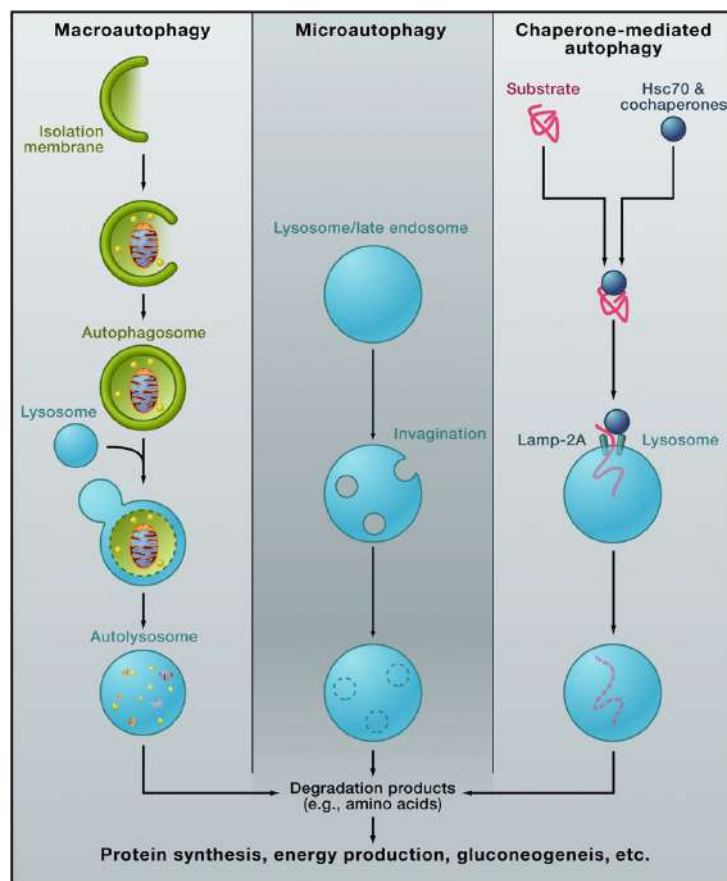


Figure 5: Different types of autophagy: macroautophagy, microautophagy and chaperone-mediated autophagy [courtesy of Mizushima et al.,2011].⁹⁰

Chaperone-mediated autophagy consists in the capturing of proteins engifted by the KFERQ-like motif by the mediation of heat shock cognate 70 (Hsc70) and its co-chaperones. Once sequestered, proteins are directed towards the lysosomal enzymatic degradation through a receptor mediated-internalization, lysosomal-associated membrane protein 2 (LAMP-2A).

Instead, microautophagy occurs through a self-invagination of the lysosomal membrane engulfing portions of the cytoplasm, which are eventually degraded.

The difference between the two processes above and Macroautophagy lies in the engagement of specialized vacuoles for cargo transportation, known as autophagosomes, and the reliance of macroautophagy on Autophagy-related gene (ATG) proteins. Autophagosomes derived from *de novo* synthesis of double-membrane vesicles (phagophores), which, finally fuse with lysosomes. For its importance and for the deep studies of its mechanisms, macroautophagy is usually referred to simply as autophagy.⁹⁰

The autophagic machinery and its regulation

Autophagy has multiple roles, but it is considered above all a homeostatic process. Its function is related to development, differentiation, immune homeostasis, defense against pathogens, ageing, and cell death.

Its induction is strictly regulated by a complex machinery that leads to the activation of autophagy-related genes and their products, responding to different intracellular and environmental conditions. There are many signals that function as activators of autophagy: nutrients and energetic levels of the cell (as per adenosine triphosphate (ATP) levels), growth factors and hormones, intracellular Ca^{2+} -concentrations, sensors of hypoxia or Reactive oxygen species (ROS), accumulation of misfolded proteins, and many more. These triggers converge at the level of the mammalian target of rapamycin complex 1 (mTORC1), a central integrator that in turn regulates different cellular responses as growth, synthesis of protein and proliferation of cells, together with autophagy (Fig.6).⁹¹

In the presence of amino acids and growth factors mTORC1 is activated and suppresses autophagic signaling by the ULK complex (made up of UNC-51-like kinase 1 (ULK1) and ULK2, FIP200, ATG13 and ATG101). Conversely, nutrient deprivation inhibits mTORC1 and activate autophagy. Rapamycin, a macrolide compound clinically employed as anti-fungal, immunosuppressant, with potential applications in anti-viral and anti-cancer activities, serves as an autophagic activator by inhibiting of mTORC1. Recycling of disposable constituents of the cell under starvation in order to provide simple elements for cell viability was the first role hypothesized for autophagy.⁹²

Another important regulation of the ULK1 complex is exerted by the AMP-activated protein kinase (AMPK). This kinase is activated by a high AMP/ATP ratio, thereby sensing the cellular energetic status. In response to energy depletion, AMPK triggers autophagy activating ULK1 through direct phosphorylation.⁹³ The precise function of the ULK complex has been unclear for a significant period. Nevertheless, recent evidence indicates its participation in ensuring the correct positioning of another essential complex that triggers autophagy, the phosphoinositide-3-kinase (PI3K) class 3 complex.⁹⁰

Usually, PI3K C3 complex connects to the cytoskeleton. However, when an autophagic trigger activates ULK1, it releases the PI3K C3 complex from the microtubules allowing its relocalization to the ER, the major contributor to autophagosome formation.

Autophagosome biosynthesis can be described as a progressive phenomenon of vesicle nucleation, elongation and maturation. In the initial step of autophagy induction, the phosphatidylinositol-3-kinase class-III (PI3KC3) forms a complex with key regulatory proteins, including activating molecule in Beclin-1-regulated autophagy 1 (Ambra1), Bcl-2-interacting protein (Beclin-1), and other associated proteins, on the endoplasmic reticulum (ER) membrane. The Beclin-1 platform facilitates the binding of various interactors, leading to the recruitment of additional autophagy-related (Atg) proteins for autophagosome nucleation.

The process of autophagosome membrane expansion, shaping, and sealing involves two ubiquitin-like conjugation systems.⁹⁴ Firstly, an Atg12-Atg5 conjugate interacts with Atg16L1 to form a trimer, which homodimerizes into a large multimeric complex. This Atg16L1 complex transiently associates with the outer autophagosomal membrane, contributing to its curvature.⁹⁵ Additionally, the Atg16L1 complex acts as an E3 ligase, facilitating the completion of the second ubiquitin-like conjugation pathway involving Light chain 3 (LC3) lipidation. Through the concerted action of Atg7, Atg3, and the Atg16L1 complex, LC3 is conjugated to phosphatidylethanolamine (PE) to produce LC3-PE (LC3-II), a specific marker for autophagic membranes.

The quantification of autophagic flux in a cell can be reliably measured by evaluating the net increase in LC3-II or LC3 punctate structures following lysosomal inhibition.⁹⁶ After vesicle completion, Atg4 deconjugates LC3-II from the outer autophagosomal

membrane, while LC3-II remains associated with the inner autophagosomal membrane and undergoes partial degradation upon fusion with the lysosome.(Fig.6).⁹¹

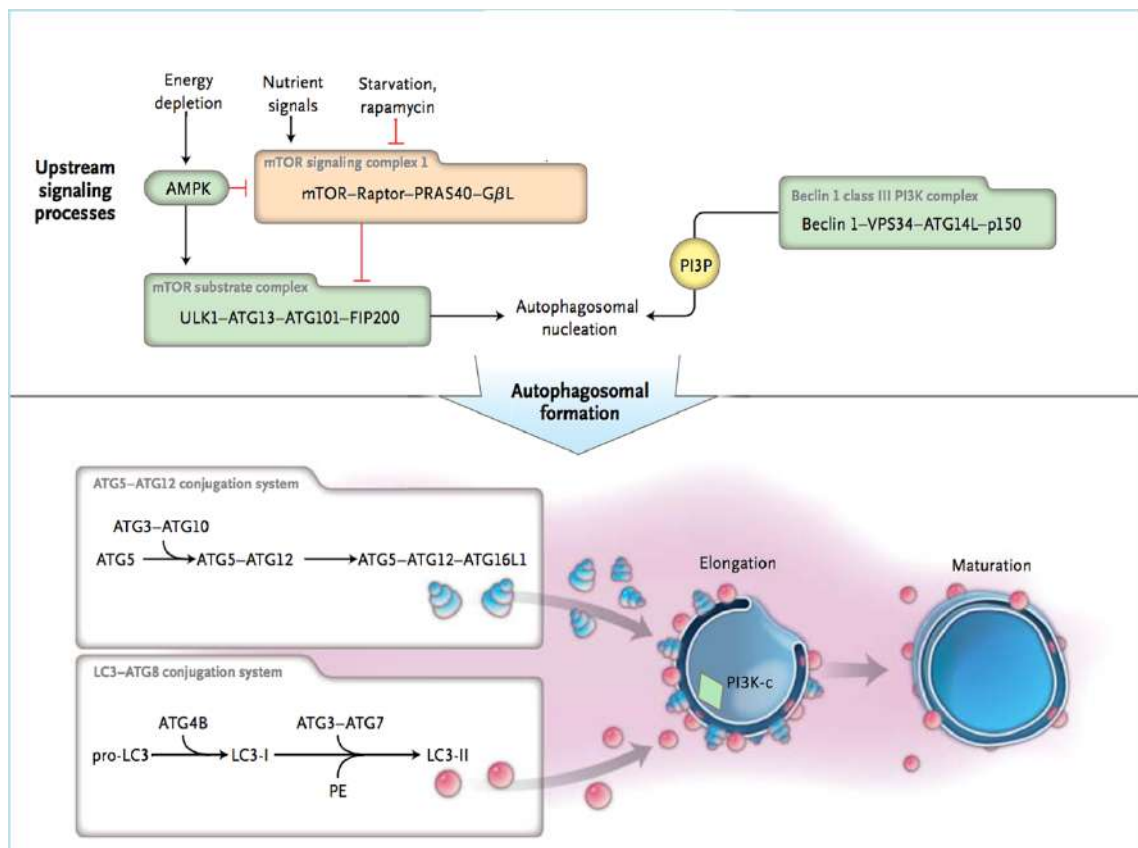


Figure 6: Autophagic machinery and regulation (modified from Choi, A.M.K. Et al, *Autophagy in Human Health and Disease, NEJM*) [see table of abbreviations]⁹¹

Following the completion of autophagosome formation, these structures can undergo fusion with early or late endosomes, resulting in the formation of amphisomes. The fusion process involves the outer autophagosomal membrane merging with lysosomes, leading to the release of the inner autophagosomal membrane and its contents into the lysosomal lumen. Once the autophagic body is internalized by the lysosome, it undergoes disintegration, and its cargo is subjected to degradation by lysosomal hydrolases and lipases.

Subsequently, lysosomal efflux transporters facilitate the release of the resultant amino acids, fatty acids, and nucleosides back into the cytosol. This intricate process ensures the recycling and utilization of cellular components for maintaining cellular homeostasis and meeting metabolic demands. (Fig. 5, Macroautophagy)

Selective autophagy: the role of p62

Autophagy has conventionally been viewed as a non-selective degradation process responsible for breaking down long-lived proteins and organelles, particularly during periods of nutrient scarcity, to recycle building blocks and contribute to restoring the cell's energy balance. In contrast, it is closely linked to, but distinct from, the Ubiquitin-proteasome system (UPS), which handles the degradation of short-lived proteins and misfolded monomers.

Recent studies, however, have revealed its activity even at basal levels in a nutrient-rich environment, shedding light on its role in quality control. Indeed, autophagy can selectively target and degrade only damaged macromolecules and organelles, indicating an unexpected level of selectivity in its function.

Autophagy plays a crucial role in the selective degradation of various endogenous supramolecular structures within cells. This targeted degradation includes peroxisomes (pexophagy), protein aggregates (aggrephagy), ribosomes (ribophagy), mitochondria (mitophagy), lipid droplets (lipophagy), secretory granules (zymophagy), and endoplasmic reticulum (ER-phagy).

The selectivity in autophagic degradation relies on the presence of specific signals on the autophagic substrates. These signals are recognized by dedicated autophagic receptors or adapters, which facilitate the sequestration of cargo into autophagosomes. This process bears similarities to proteasomal degradation, where proteins marked with covalently linked polyubiquitin chains are selected for degradation by the proteasome. Notable examples of autophagic cargo receptors include NBR1, optineurin (OPTN), p62, NDP52, TAX1BP1, and BNIP3.⁹⁷

The initial selective cargo receptor discovered was p62/SQSTM1. In two studies, Terje Johansen's research group demonstrated that p62 was present in ubiquitinated protein aggregates, including those containing mutant proteins and ALIS (transient protein aggregates induced by puromycin or stress conditions).⁹⁸ Moreover, these aggregates positive for p62 were subjected to degradation through the autophagic process. Importantly, when p62 was depleted in cells, there was no accumulation of ubiquitin-

positive aggregates, suggesting that p62 plays a crucial role in the constitutive autophagy of misfolded proteins.⁹⁹

The p62 protein, also called sequestosome 1 (identified as a 62 kDa protein), is a multifunctional adaptor protein implicated in cell signaling and differentiation by interactions with several proteins through conserved domains. Human p62 is 441 aminoacid long and presents from N- to C-terminus the following recognised domains: Phox/Bem1p (*PB1*) domain, ZZ-type zinc finger domain, a tumor necrosis factor receptor-associated factor 6 (TRAF6)-binding (TB) domain, two nuclear localization signal (NLS1 and NLS2), a nuclear export signal (NES), a LIR (LC3-interacting region), a KIR (Keap1 interacting region) domains, and a C-terminal domain responsible for its ubiquitin-binding activity (UBA).¹⁰⁰ (Fig.7)

The p62 domains involved in autophagy are PB1, LIR and UBA.

The initial stages of autophagy commence with the phosphorylation of p62 dimers by the Atg1/ULK1 kinase. This phosphorylation leads to the destabilization of p62 dimers, followed by additional phosphorylation by other kinases. Ultimately, this renders p62 more susceptible to binding to ubiquitin chains on specific cargos through the *UBA domain*.¹⁰¹ These ubiquitinated protein aggregates are led to the autophagosome through the *LIR domain*, which mediates direct interaction with the autophagy-specific protein LC3, but also other autophagic effector proteins like Beclin-1, γ -aminobutyric acid receptor-associated protein (GABARAP), and GABARAP-like molecules.^{99,102} Of note, p62 itself is a substrate for autophagic degradation, and pharmacological inhibition or decreased levels of autophagy leads to the accumulation and aggregation of p62 through *PB1 domain*, necessary for p62 self-oligomerization. Elevated p62 may compete with other Ub-binding proteins involved in proteasomal degradation and may prevent ubiquitinated proteins from passing through the narrow central pore of the proteasome.

In addition to its function as a cargo receptor, p62 plays an interesting, recently defined, role in the amino acid-mediated mTORC1 activation pathway.

In detail, p62 may promote mTOR translocation to the lysosome and its subsequent activation in two ways. The first one consists in directly stabilizing Raptor and Rags proteins, responsible for the amino acid-mediated activation of mTORC1, due to the

interaction with a newly recognized p62 region between ZZ and TB domains.¹⁰³ On the other hand p62 can activate K63 polyubiquitination of mTOR through p62-TRAF6 complex.¹⁰⁴

Active mTORC1 downregulates autophagy. As p62 is also a substrate for autophagy, this creates a feed-forward loop in which p62 activation of mTORC1 increases p62 levels, by blocking autophagy and thus p62 degradation, further promoting mTORC1 activity.

Under nutrient deprivation, the p62–mTORC1–autophagy loop might provide a safeguard mechanism to ensure the irreversibility of cell death when nutrients are not available.

p62 involvement in multiple pathways

Thanks to the high complexity of its structure, p62 has the capability of interaction with many proteins, regulating other various signaling pathways, including metabolic process, oxidative stress response and bone remodeling. There are different domains involved in various interactions (Fig.7).

The PB1 domain is responsible for homo- or heterodimerization. It enables p62 to self-dimerize and further oligomerize, a process crucial for the accumulation of p62 into aggregates with ubiquitin proteins. Notably, the polymerization of p62 has been shown to enhance the affinity of the UBA domain for ubiquitinated proteins.¹⁰⁵ The PB1 domain plays a vital role in the autophagic degradation of p62 itself.¹⁰⁶ Additionally, it serves as a heterodimerization site with other proteins that express PB1 motifs, including atypical protein kinase C (aPKC) and members of mitogen-activated protein kinase (MAPK) modules, such as MEK5, which are implicated in both proliferative and stress-induced signaling through the activation of the nuclear factor- kappa B (NF-κB) pathway.¹⁰⁷

The ZZ-type zinc finger domain confers on p62 the ability to interact with key components such as RIP (receptor-interacting protein), which modulates NF-κB pathway in conjunction with atypical PKCs.

p62 interacts with both TRAF6 and caspase 8 and has been proposed to act as a signaling hub capable of triggering both pro-survival (via TRAF6) and pro-apoptotic (via caspase 8) signaling cascades. Oligomerization of p62 and TRAF6 (an E3 Ub ligase), mediated

by TRAF6 Binding domain (TB), leads to the K63-auto-ubiquitination of TRAF6. This auto-ubiquitination activates TRAF6 supporting the activation of IKK (I κ -B Kinase) and the nuclear translocation of NF- κ B, transcription factor involved in multiple cellular pathways including neuronal development, survival, inflammation, immunity, and cellular differentiation.¹⁰⁸

In contrast, p62 promotes the aggregation of caspase 8 and cullin-3, leading to the full activation of poly-ubiquitinated caspase 8, and committing cells to mitochondria-independent apoptosis.¹⁰⁹

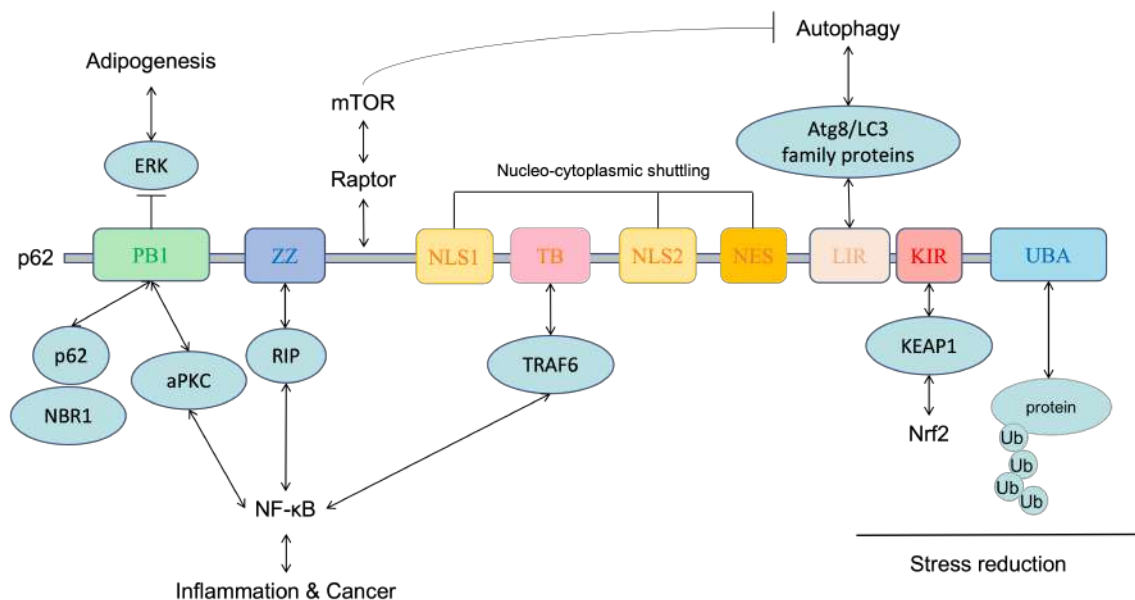


Figure 7: p62 functional domains and interactions in different pathway [see table for abbreviations]

Lack of p62 in mouse models lead to the development of mature-onset insulin resistance and obesity, possibly via suppression of p62-dependent negative regulation of ERK1 signaling during adipogenesis.¹¹⁰

Of interest, humans with germline mutations in p62 develop Paget’s disease, an age-onset chronic bone disorder characterized by focal increases in bone turnover. In Paget’s disease of bone, mutations of p62 generally map to the UBA domain and have been shown to impede Ub binding. UBA mutations hinder p62 interactions with TRAF6 and the DUB enzyme CYLD, and may result in the alteration of RANKL/NF- κ B mediated activation of osteoclastogenesis.¹¹¹

p62 is also a key determinant in the Nrf2-dependent oxidative stress response, being a link between proteotoxic and oxidative stress. As described in 2007 by Luesch and colleagues, p62 mediates the activation of the transcriptional factor Nrf2 with its subsequent nuclear translocation and activation of ARE-driven genes.¹¹² This interaction has been demonstrated to be mediated by the association between p62 and Keap1,¹¹³ through the Keap1-interacting region (KIR) domain of p62. This region accounts for the direct interaction between the two proteins and allows p62 to sequester Keap1 into the autophagosomes. It disrupts the proper conformation of the Keap1–Nrf2 complex, hindering the ubiquitylation of the transcription factor. This disruption results in the activation of the non-canonical Nrf2 signaling pathway, ultimately triggering a comprehensive anti-oxidative stress and detoxification response.^{114,115} p62 not only leads to Keap1 sequestration into aggregates or autophagosomes but also regulates its turnover through autophagy-mediated degradation. In fact, overexpression of p62 significantly decreased the half-life of Keap1 whereas siRNA-mediated knockdown of p62 increased the half-life of Keap1 twofold, increased the levels of Keap1, lowered the level of Nrf2, and reduced the expression of Nrf2 target genes (Fig.8).¹¹⁶

Finally, p62, initially recognized as a cytosolic protein, has been shown to also localize within the nucleus.¹¹⁷ In fact, Pankiv et al. revealed that p62 possesses two nuclear localization signals (NLS1 and NLS2), consisting of short peptide sequences with several basic amino acids that bind to importin- α for nuclear entry through the nuclear pore complex. Additionally, a nuclear export signal (NES) characterized by four regularly spaced hydrophobic amino acids binds to exportin-1/CRM1, facilitating the exit from the nucleus.¹¹⁸ In HeLa cells, the researchers observed diverse p62-staining patterns, including predominantly cytosolic with low nuclear expression, exclusively cytosolic, and, in a small number of cells, solely nuclear expression. When exportin-1, a mediator of protein exit from the nucleus, was inhibited, p62 rapidly redistributed in the nucleus with a half-life ($t_{1/2}$) of approximately 10–15 minutes. This indicates that p62 shuttles quickly between the nucleus and cytoplasm.¹¹⁸ These researchers also demonstrated that the nuclear import of p62 depends on the degree of phosphorylation of NLS1 and NLS2, with the latter being more crucial in determining the translocation.¹¹⁸

Autophagy and cancer: a double-edged sword

Due to its numerous crucial functions, it is unsurprising that autophagy has been implicated in a wide range of pathological states, including malignancies, neurodegenerative disorders, cardiomyopathy, Crohn's disease, diabetes, and fatty liver disease.^{114,119,120}

Ensuring cell homeostasis in response to metabolic stress, autophagy is a housekeeping mechanism that prevents cell damage, aging and malignant transformation. A defect in this pathway can contribute to diseases in different ways.

Impairment of non-selective autophagy, generally activated during cell nutrient deprivation, causes amino acid insufficiency, which reduces protein synthesis and energy production for cell survival.

Furthermore, a defect of autophagy is accompanied by *accumulation of p62*, both actor and substrate of this degradative process. It implies a failure in degradation of dysfunctional mitochondria and misfolded or damaged proteins. This leads to the formation of large p62 and Ub containing aggregates.¹²¹ Similar inclusion bodies are characteristic of different diseases, from neurodegenerative ones, as Alzheimer, Huntington, Parkinson disease, and amyotrophic lateral sclerosis. They were also found in liver disorders like alcoholic hepatitis and steatohepatitis; and some cancers, including malignant glioma and hepatocellular carcinoma. p62 is therefore deemed implicated in the formation of disease-related inclusion bodies.⁹⁰

Moreover, not-degraded p62 is able to interact with its multiple substrates activating all the downstream pathways; this results, among other things, in hyperactivation of the Nrf2 signaling axis, with its pro-cancer survival role, and altered regulation of NF- κ B pathway and apoptosis, favoring tumorigenesis (Fig.8).

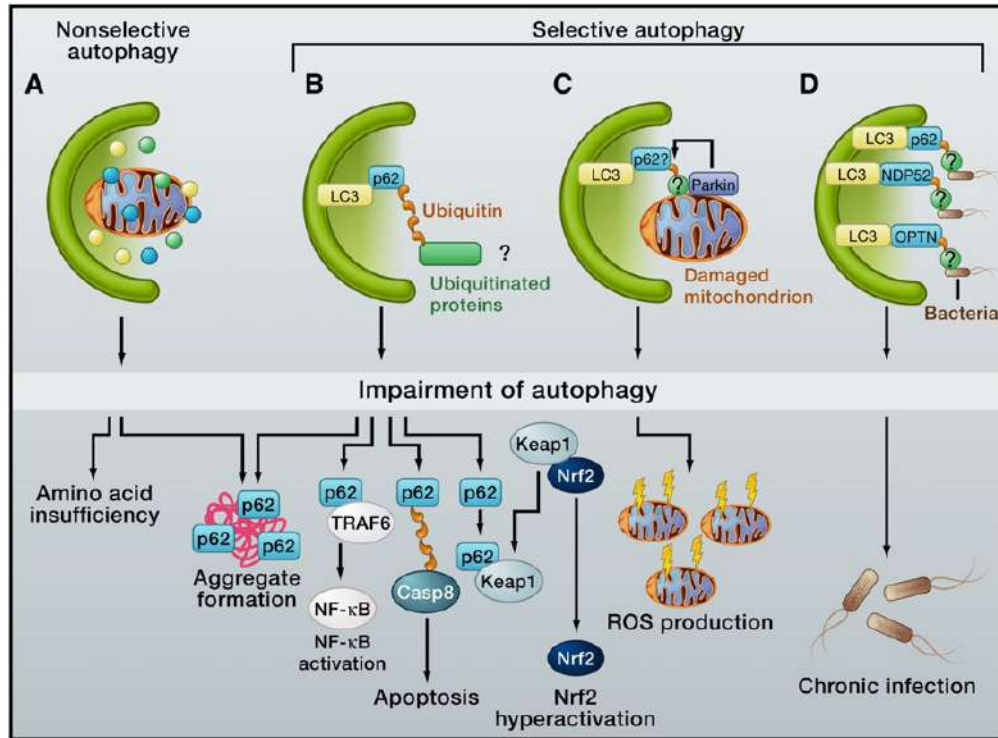


Figure 8: Impairment in non-selective and selective autophagy: role in human disease [courtesy of Mizushima et al]⁹⁰

In cancer, it has become evident that autophagy plays a *context-dependent and time-dependent role*. In fact, autophagy has demonstrated a dual role in cancer with its capacity to both inhibit and promote cancer cell proliferation or tumorigenesis.¹²⁰

Autophagy was initially considered a tumor-suppression mechanism. In fact, it constitutively works preventing oxidative and proteotoxic stress, suppressing tissue damage, chronic inflammation, DNA damage response, and genome instability, which are known to create an environment for cancer initiation. Moreover, early reports have shown that the essential autophagy gene *ATG6/BECN1* was monoallelically lost in 40% to 75% of human prostate, breast, and ovarian cancers.^{120, 122} In mouse model, *BECN1* heterozygosis make mutant mice at risk for lymphomas, liver and lung tumors. Mosaic loss of *ATG5* or *ATG7* produces chronic liver damage, inflammation, and the development of benign liver tumors that fail to progress to carcinoma.¹²³ Similar findings are seen in pancreas.¹²⁴ These data suggest the possible role of *BECN1* as an oncosuppressor gene; however, this statement carries the bias of its strict proximity to the well-known tumor suppressor breast cancer 1 (*BRCA1*) on human chromosome 17q21,

whose mutations are known drivers in diverse human tumors. Further studies failed to identify statistically significant recurrent missense mutations in BECN1 related to a tumorigenic role, but many tumors have not yet been sufficiently characterized.

However, the observation that autophagy-deficient mice develop benign hepatomas that ultimately do not progress to malignant transformation suggests the role of autophagy not only in the initiation of liver tumors but also in the subsequent development of transformed cells.¹²⁰

Of note, multiple studies oriented towards a tissue-specificity and autophagic gene-specificity in the effects of autophagy perturbation. In fact, in different tissues, the significance of autophagy becomes apparent only in conjunction with other genetic abnormalities.¹²⁵ It has been demonstrated that the oncogene Ras, which promotes tumor progression and survival in specific cancers, relies on autophagy for the further progression of the malignant disease. In Ras-driven cancers, the suppression of autophagy may promote tumor progression in the initial stages but ultimately hinder the subsequent tumor growth. This is likely due to the failure to adapt to the typical stress conditions experienced by tumor cells, which normally rely on intact autophagy under normal circumstances.¹²⁶

It's worth noting that autophagy may exert a role even in the tumorigenesis generated by loss-of-function mutation in oncosuppressor genes, as p53 (described below). This prompts the inquiry into whether autophagy actively functions as a tumor-suppressive process or if its complete absence merely leads to a microenvironment that fosters tumor promotion.¹²⁵ Apparently, the impact of autophagy in cancer may vary depending on the specific oncogenic mutation responsible for driving cellular transformation.

Adapting to stress conditions, autophagy serves as a crucial strategy for cancer survival. Studies have showcased the dynamic regulation of autophagy in tumor cells facing various metabolic stresses, such as nutrient, factor, and oxygen deprivation. These stressors arise from an insufficient blood supply, a consequence of deregulated growth and deficient angiogenesis. In hypoxic regions of tumors situated farthest from blood vessels, autophagy is significantly activated, enabling cancer cells to manage the heightened metabolic stress in these areas.¹²⁷ Additionally, autophagy is enhanced in response to radiation and various anti-cancer drugs, potentially playing a role in cancer

resistance, recurrence, and progression.^{120,128} Genetic and pharmacological inhibition of autophagy induces apoptotic cell death in different types of cancer and potentiates the cytotoxic effects of metabolic stressors.¹²⁹ The genetic context that creates autophagy dependency in cancer is still poorly understood and warrants further investigation.

This emerging dual role of autophagy in cancer has been defined as a “double-edged sword”.¹²⁹ In this complex scenario, a better understanding of the variable role of autophagy is crucial. This could lead to the identification of the correct therapeutic window to target this process. It will depend on multiple variables such as the right phase of cancer cell life, the inhibiting or activating signals involved, the right cell type to target, and the impact that this could have on other signaling pathways.

The prevailing consensus acknowledges the inhibitory role of autophagy in tumor initiation. However, accumulating evidence indicates that autophagy processes become essential in established tumors to facilitate uncontrolled cell growth and heightened metabolic activities, establishing a dependence on autophagy for tumor maintenance. Furthermore, autophagy plays crucial roles both within the tumor cells themselves (intrinsic) and in the surrounding stroma (extrinsic), with significant implications for tumor growth and resistance to drugs. In summary, the impact of autophagy seems contingent on the tumor stage, specific oncogenic mutations, and the cellular context.¹²⁵

P62 role in cancer biology

p62 is both a key player and substrate in the autophagic catabolic pathway. It stands out as one of the most well-known and characterized autophagy cargo receptors (ACRs) or selective autophagy receptors (SARs), functioning as a selector for ubiquitylated cargo particles targeted and addressed to the autophagic pathway.

Due to this, the accumulation of p62 may play diverse roles in cancer biology. Specifically, it could signify an impaired turnover of p62 resulting from decreased levels of autophagy. Such accumulation might induce proteotoxicity in cellular metabolism, as evidenced in neurodegenerative diseases. Conversely, elevated levels of p62 may contribute to the promotion of parallel pathways. One example is the oxidative stress response obtained by the activation of the NRF2 pathway. Moreover, p62 is also a signaling scaffold of the NF-κB pro-tumorigenic cascade (Fig.8).

A diffuse intense cytosolic staining for p62 has been demonstrated in IHC of prostatic adenocarcinoma and high-grade prostatic intraepithelial neoplasia with only little nuclear expression. In normal and benign hyperplastic prostatic cells, p62 resulted negative or with only weak nuclear expression.¹³⁰ p62 is also overexpressed in breast cancer,¹³¹ and in patients-derived breast cancer specimen, higher p62 expression was correlated with tumor grade and presence of distant metastasis.¹³²

Of note, in our previous preclinical experience we pursue the understanding of the involvement of adaptive pathways in the development of acquired drug resistance in carcinoma cells, establishing an in vitro conditioning model using three commonly used chemotherapeutic agents: cisplatin, 5-fluorouracil, and docetaxel. This model employed the HEP-2 epithelial cancer cell line, and our investigation aimed to elucidate the underlying mechanisms responsible for reduced drug sensitivity. Our findings revealed that the triple-resistant cells experienced elevated levels of oxidative stress and displayed heightened responses to counteract this stress. These responses included the activation of the antioxidant Nrf2 pathway and an increase in autophagy, marked by the adapter protein p62/SQSTM1. Consequently, re-administration of chemotherapeutic agents failed to induce further accumulation of reactive oxygen species and p62. Furthermore, we observed that autophagy played a pivotal role in mediating chemoresistance by preventing the accumulation of p62 into toxic protein aggregates. Remarkably, the removal of p62 alone was sufficient to confer resistance in the parental cells, and both genetic and pharmacological inhibition of autophagy restored drug sensitivity in resistant cells, dependent on p62. In addition, our experiments involved the introduction of mutant p62 lacking the ubiquitin- and LC3-binding domains, which are essential for autophagic engulfment. This manipulation resulted in increased chemosensitivity in TDR HEP-2 cells. In summary, our findings establish a cellular model that can be used to explore the underlying mechanisms of acquired chemoresistance in epithelial cancers. Furthermore, they highlight the potential prognostic and anti-neoplastic therapeutic implications of p62 toxicity, encouraging further investigation in this promising area of research.¹³³

Autophagy and tumor microenvironment

As mentioned previously, the roles of autophagy in cancer exhibit seemingly contradictory functions—acting to prevent early tumor development while also supporting the maintenance and metabolic adaptation of established and metastasizing tumors. Recent research has delved into not only the intrinsic functions of autophagy within tumor cells but also its impact on the tumor microenvironment and the immune cells associated with it.¹²⁵

Studies conducted on *systemic autophagy inhibition* in cancer models have demonstrated a more significant impact on inhibiting tumor proliferation compared to exclusively modulation of autophagy within cancer cells. For example, in a lung cancer mouse model of kRAS-driven tumors, systemic inhibition of autophagy through Atg7 deletion has been demonstrated to promote tumor regression within a reasonably safe therapeutic window. However, it should be noted that autophagy inhibition can eventually lead to lethal metabolic alterations and, in particular, neurodegenerative diseases.¹³⁴ From this perspective, there has been a renewed interest in *host autophagy*, as it can exert influence on tumor growth itself. Moreover, a deeper understanding of the autophagic machinery has revealed not only its degradative role but also its involvement in trafficking and secretive functions.¹²⁵

In particular, tumor microenvironment demonstrated to exert a role in different ways on tumor cells' biology (Fig.9)

- Tumor cells usually suffer from an anabolic condition that imply their high dependency on generation and secretion of nutrients, particularly amino acids, from host cells, including Cancer Associated Fibroblasts (CAFs). Experiments with various combination of autophagy inhibition in tumor cells and host cells demonstrated that both populations contribute to tumor growth depending on autophagy, in a strict metabolic relationship based on essential and non-essential amino acids (NEAA) release from CAFs to tumor cells.¹²⁵
- CAFs' autophagy is also involved in the secretion into the TME of pro-inflammatory cytokines as IL-6, IL-8 and IL1 β , which eventually contribute to create a tumor-permissive environment thanks to their modulation of Immune

cells. In fact, CAFs have demonstrated a higher basal level of autophagy compared to normal fibroblast in patient-derived HNSCC cells. Chloroquine-mediated inhibition of autophagy in this model resulted in decreased tumor cells proliferation, migration and invasion.¹³⁵

- Autophagy in stromal fibroblasts exerts also a role in the generation of “desmoplasia” referred to the inflamed and fibrotic microenvironment, secondary to fibroblasts activation and deposition of type I collagen, which has been demonstrated to be associated with poor prognosis in solid tumors.¹²⁵

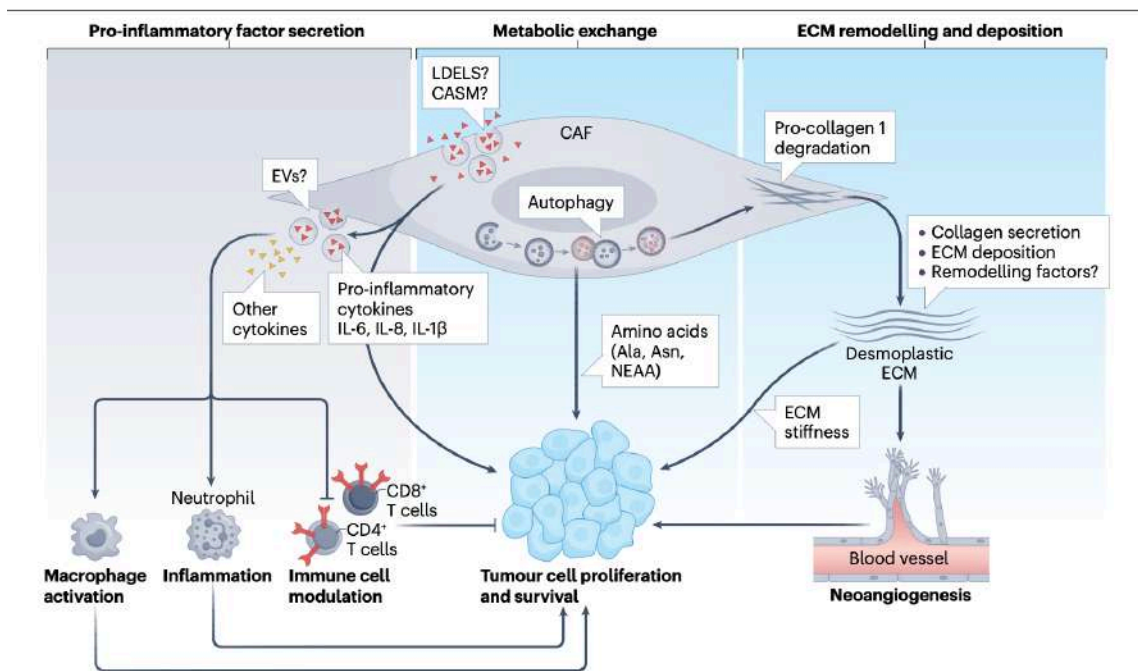


Figure 9: Tumor microenvironment's autophagy and its influence on tumor cells [courtesy of Debnath et al. 2023]¹²⁵

The tumor suppressor p53 and autophagy

p53 functions as a transcription factor, overseeing the regulation of genes crucial for tumor suppression. In approximately half of human cancers, tumorigenesis is mediated by p53 mutations and for this reason p53 is one of the major recognized oncosuppressor gene. The extensive regulatory role of p53 involves the control of hundreds of target genes, influencing diverse cell outcomes, including apoptosis, cell cycle arrest, and DNA damage repair. Additionally, p53 plays a pivotal role in anti-tumor immunity by

modulating various factors such as TRAIL, DR5, TLRs, Fas, PKR, ULBP1/2, and CCL2; T-cell inhibitory ligand PD-L1; pro-inflammatory cytokines; immune cell activation status, and antigen presentation.

The genetic alterations in p53 can impact immune evasion mechanisms by influencing immune cell recruitment to the tumor, cytokine secretion within the TME, and inflammatory signaling pathways. Interestingly, in certain scenarios, p53 mutations can elevate neoantigen load, thereby enhancing the response to immune checkpoint inhibition. Therapeutically restoring mutated p53 has shown promise in reinstating anti-cancer immune cell infiltration and mitigating pro-tumor signaling, leading to tumor regression. Clinical evidence suggests that reinstating p53 can elicit an anti-cancer immune response, particularly in immunologically cold tumors.

Clinical trials exploring the combination of compounds restoring p53 or p53-based vaccines with immunotherapy have exhibited immune activation against tumors and tumor regression, with variations observed across different cancer types.¹³⁶

Over the last few decades, several studies have also focused on the role of the well-known tumor suppressor p53 in modulating autophagy. The results revealed complex interplays between these two factors, particularly in the context of cancer biology.

As per the investigations conducted by Amaravadi et al., the activation of p53 in B-cell lymphoma results in the induction of autophagy.¹³⁷ However, further studies demonstrated how the control of autophagy by p53 is quite more intricate, depending on the cellular stress and transformed condition. In fact, under normal, unstimulated conditions, the tumor suppressor p53 is documented to inhibit autophagy. Accordingly, in 2008 Tasdemir et al. showed their surprising results on how p53 depletion can trigger autophagy too. Elimination of p53 through knockout, knockdown, or drug inhibition in human, mouse, and nematode cells, in fact, leads to the hyperactivation of the autophagic flux, ultimately resulting in increased cell survival.¹³⁸ Nevertheless, when heightened and triggered by cellular stress, p53 stimulates a set of target genes, including those responsible for damage-regulated autophagy modulator 1 (DRAM1) and AMPK through its subunit PRKAB1, thereby fostering autophagy (Fig.10).¹²⁵

Autophagy and p53 exhibit somewhat bidirectional connections, with ATG7 inhibiting the activation of p53, while chaperone-mediated autophagy promotes the degradation of mutant p53.

It's worth noting that the mutational status of p53, owing to its crucial role in tumor biology, has also been explored through the pattern and intensity of p53 presence in pathological samples assessed by immunohistochemistry (IHC). Sung et al. demonstrated that the absence of p53+ in IHC corresponds to disrupted mutations of the TP53 gene (truncations, frameshifts, splice site mutations, and deep deletions). On the other hand, a high presence of p53 positivity in tumoral cells depicts an in-frame mutation, specifically in the DNA-binding domain. This type of mutation eventually leads to higher expression of the protein and its accumulation.¹³⁹

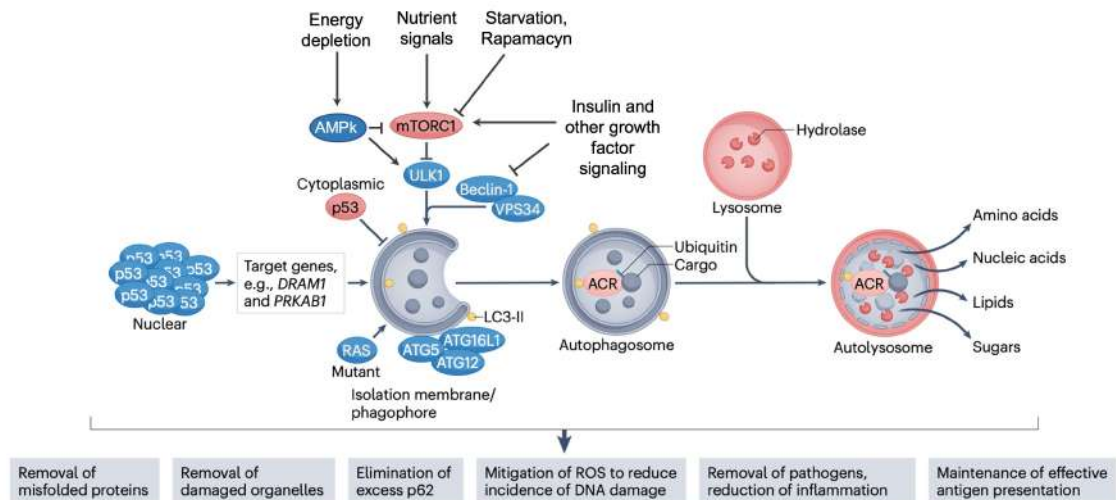


Figure 10: Autophagic pathway, its regulations and its effects [modified from Debnath et al. 2023]¹²⁵

Autophagy and Immune system response

The interplay between the immune system and cancer is intricate and multifaceted, involving various mechanisms of interaction. Central to this dynamic is the immunosurveillance role of immune cells, which perpetually monitors abnormal cells, including those with the potential for malignant transformation. Specifically, deceased tumor cells typically release tumor-associated antigens (TAAs), which are then processed

by APCs. Ultimately, this process activates a cytotoxic response mediated by CD8⁺ T lymphocytes (CTLs).

In this biological functional process, autophagy has been shown to play a crucial role in both tumor cells and immune cells.

Tumor cells exhibit varying levels of autophagy activation at different stages. Nevertheless, in specific cell lines, it has been shown that the baseline hyperactivation of autophagy in tumor cells contributes to a pro-tumor role (e.g., pancreatic ductal adenocarcinoma (PDAC) cell lines¹⁴⁰). A crucial observation is that the inhibition of autophagy leads to an anti-tumoral effect exclusively in immunocompetent mice,¹⁴¹ not in those with immunodeficiency.¹⁴² This observation underscores the critical role of the immune system in cancer survival. Macroautophagy is consistently operational in leukocytes and has the capability to facilitate both adaptive and innate immune responses. We will delve deeper into the specific processes involved in the interplay between the immune system and tumor cells, highlighting instances where autophagy has been shown to play a role.

Tumor antigen presentation: MHC class I

Molecules belonging to the major histocompatibility complex (MHC) play a crucial role in presenting antigens to T cells. MHC class I is expressed by all nucleated cells, while MHC class II is exclusive to professional APCs. MHC class I typically presents antigens on the cell surface derived from endogenously synthesized cell-specific proteins. These antigens are processed by the ubiquitin-proteasome system and loaded for recognition by the immune system on the cell membrane.

The presence of heterologous antigens presented by MHC-I on nucleated cells serves as a distinctive signal of abnormal cells, which need to be targeted by cytotoxic CD8⁺ T lymphocytes. Tumor cells often employ a strategy of downregulating the expression of MHC-I on their cell membrane as a common mechanism to evade immunosurveillance. Simultaneously, within the innate immune system, DCs, a subtype of APCs, employ phagocytosis to internalize and process external antigens, presenting them subsequently to CTLs on MHC-I (Fig.11).

Loi et al. showed that autophagy plays a role in the internalization of MHC-I in dendritic cells (DCs). The absence of Atg8 lipidation led to the stabilization of MHC-I on DCs, resulting in an enhanced CD8⁺ T cell response to viral infections.¹⁴³

It is suggested that MHC-I internalization is mediated by autophagic degradation in tumor cells too. Yamamoto et al. demonstrated the lysosomal rerouting and degradation of MHC-I in different pancreatic tumor cells and NSCLC lines via a selective autophagy mediated by the ubiquitin-binding receptor NBR1 (neighbor of BRCA1 gene 1 protein). From his studies is evident that PDAC, which frequently manifest a downregulated expression of surface MHC-I, with consequent resistance to immune check point inhibitors (ICIs) therapy, achieve this immunosurveillance escape not through genetic loss of MHC-I but through its degradation dependent from canonical autophagy. In line with this, the genetic inhibition of autophagy in PDAC using a (Dox)-inducible dominant-negative mutant of ATG4B, a potent inhibitor of autophagy, resulted in increased Ag presentation through MHC-I. This led to the activation of a robust cytotoxic CD8⁺ lymphocyte response and a reduction in viability, as observed in co-culture experiments.¹⁴⁴

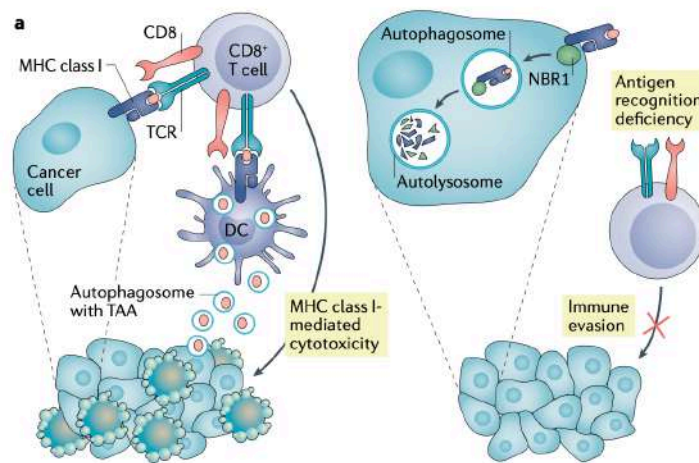


Figure 11: Autophagy Enhances DC-Mediated Cross-Presentation by Facilitating Autophagosome Formation with Tumor Antigens, while NBR1-Mediated MHC Class I Degradation Impairs CTL Recognition in Cancer Cells. [Courtesy of Xia et al., 2021]¹⁴⁵

CD8+ cytotoxic lymphocytes

As mentioned earlier, the cytotoxic CD8+ cell response is enhanced, with increased proliferation and expression of IFN- γ and TNF, when co-cultured in vitro with autophagy-inhibited pancreatic tumor cells. This is associated with a higher presence of MHC-I on tumor cells, attributed to reduced degradation through selective autophagy. Moreover, in vivo studies have shown a significant infiltration of CD8+ T cells in orthotopically transplanted PDAC mouse models when autophagy is inhibited, with an overall reduction in the size of the tumor tissue. Significantly, the growth of autophagy-inhibited tumors was restored upon antibody-mediated depletion of CD8+ T cells. This underscores the confirmed role of CD8+ T cells in tumor control. ¹⁴⁴

Furthermore, in Wang et al.'s study, they made several significant observations regarding the interplay between autophagy and PD-L1 expression in gastric cancer cells and xenograft models. Their findings indicated that when autophagy was suppressed using pharmacological inhibitors or small interfering RNAs, the levels of PD-L1 increased both in cultured gastric cancer cells and in xenograft tumors. Additionally, interferon (IFN)- γ played a role in enhancing PD-L1 gene transcription, particularly when autophagy was inhibited. As a result, these findings have therapeutic implications, suggesting that the concurrent use of immune checkpoint inhibitors (ICIs) and autophagy inhibition could be a valuable approach in the treatment of gastric cancer. ¹⁴⁶

CD4+ lymphocytes

The suppression of antitumor immunity by CD4+ Treg cells stands as a prominent mechanism employed by tumors to evade the immune system and resist immunotherapy. Notably, the autophagy pathway has been identified as playing a crucial role in determining the lineage commitment of Treg cells, thereby influencing the overall antitumor immune response. This is exemplified by the specific deletion of genes responsible for key autophagy components, such as ATG5, ATG7, and AMBRA1, within Treg cells. Such genetic alterations result in apoptosis and functional impairment of Treg cells in murine models. ¹⁴⁵

In essence, these findings underscore the significance of autophagy in shaping the behavior of Treg cells, which in turn has a substantial impact on antitumor immune responses and the potential efficacy of immunotherapeutic interventions.

Tumor associated Macrophages polarization

As we have previously emphasized, TAMs have a crucial role in the tumor microenvironment, according to the distinction between the tumoricidal M1 and tumor-promoting M2 macrophage subtypes.

Guo et al. (2019) and Li et al. (2018) conducted separate studies focusing on the role of lysosome-associated agents Hydroxychloroquine (HCQ) and Chloroquine (CQ), known inhibitors of autophagy, in cancer treatment, particularly their impact on tumor-associated macrophages (TAMs) and their potential as chemo-sensitizers and immune regulators.

In Guo et al.'s study, the use of CQ was studied to repolarize M2 macrophages into the antitumor M1 phenotype. Their findings demonstrated that CQ treatment effectively reprogrammed M2 macrophages, enhancing their phagocytic activity against Hep2 cells and making these cells more responsive to cisplatin (CDDP) treatment in vitro. Additionally, CQ reduced laryngeal tumor growth and improved CDDP treatment outcomes in vivo. The results suggested that the repolarization of M2-to-M1 macrophages induced by CQ played a crucial role in inhibiting tumor growth, implying potential clinical applications for laryngeal cancer treatment with a CQ/CDDP combination therapy.¹⁴⁷

On the other hand, Li et al.'s research focused on HCQ and its potential in lung cancer treatment. They explored the impact of HCQ on lysosomal pH, drug sequestration, and its effects on the tumor immune microenvironment. Their study revealed that HCQ elevated lysosomal pH, leading to the inactivation of P-glycoprotein and increased drug release from lysosomes into the nucleus. Furthermore, HCQ therapy alone was found to inhibit lung cancer growth by modulating macrophages, thereby enhancing the anti-tumor CD8⁺ T cell immune response. HCQ also promoted the transition of M2 TAMs into M1-like macrophages, resulting in the infiltration of CD8⁺ T cells into the tumor microenvironment.¹⁴⁸

To summarize, it is highly advantageous to acquire a more comprehensive understanding of the intricate biological processes involved in autophagy within tumor cells and the dynamic interactions within the tumor immune microenvironment. This enhanced knowledge can provide valuable insights into these complex biological phenomena.

AIM OF THE WORK

The aim of this work is to investigate the role of autophagy and immune system actors in Head and Neck cancers and Non-Small Cell Lung Cancers. Understanding tumor autophagic machinery and the TME could lead to novel prognostic markers and potential therapeutic targets in the autophagic pathway for cancer treatment.

The primary objectives of this study are as follows:

1. Characterize autophagic machinery's role in cancer biology, through the well-known marker, p62. Describe the autophagic tumoral signature and its role in moulding the nearby tumor microenvironment. Investigate the prognostic value of this cellular pathway.
2. Explore Systemic Immune response and correlate markers of inflammation with clinicopathological variables: We will examine how immune system markers correlate with clinicopathological variables, such as tumor stage, grade, and patient demographics. We elucidate the prognostic role in predicting oncological outcomes.
3. Investigate the role of Immune Microenvironment: In addition to p62, we will investigate the immune microenvironment within these tumors, focusing on Tumor-Infiltrating Lymphocytes (TILs) and CD8+ lymphocytes. We aim to determine whether the immune composition of the TME correlates with p62 expression patterns and patient survival.

In summary, this research aims to provide a comprehensive understanding of p62 expression patterns in HN cancer and NSCLC, their prognostic significance, and their potential implications for therapeutic strategies. By investigating the intricate interplay between p62, the immune microenvironment, and autophagy, we aspire to contribute valuable insights to the field of cancer biology and treatment.

RESULTS

Role of immune dysregulation and autophagic genetic mutations in HN cancer and NSCLC

In our study, we started exploring the genomic complexities of Head and Neck Cancers and Non-small cell lung Cancers, aiming to understand whether mutations in the autophagic pathway or genetically induced immune dysregulation play a role in the clinical context. To address this inquiry, we conducted a thorough genomic analysis, utilizing existing genomic libraries accessible on C-Bioportal.^{149–151}

We focused our attention on specific genes associated with crucial cellular pathways, including the P53 pathway, autophagic pathway and genes involved in cancer immune dysregulation.

We analyze genomic data available on both Head and neck cancers (2983 samples / 2977 patients in 15 studies) and NSCLC (13603 samples / 11168 patients in 27 studies).

Our genes of interest were:

- **P53 pathway:** TP53 MDM2 MDM4 CDKN2A CDKN2B TP53BP1
- **Autophagic pathway:** SQSTM1 MAP1LC3A ATG5 ATG3 ATG7 ATG12 ATG13 ATG14 ULK1 ULK2 ATG101 ATG10 RB1CC1 AMBRA1 BECN1 ATG4A ATG4B
- **Genes associated with Immune dysregulation in cancer:** FAS CTLA4 LRBA JAK3 JAK1 JAK2 TYK2 STAT1 STAT3 STAT5B IKZF1 GATA2 CYLD NFKB1 NFKB2 REL RELA RELB

As expected, we found a very high mutational rate for p53 gene in both HN cancer (39%) and NSCLC dataset (52%). Those mutations in p53 gene occurred as somatic mutation in all the HN mutated samples and in the 50.7% of Lung cancer samples. They were considered driver mutation for the malignant transformation in the vast majority of cases.

On the contrary, mutations depicted in the autophagic pathway are very low in frequency in both HN cancer and NSCLC. We found only 3 classified driver mutations determined in p62 gene in NSCLC while only copy number mutations were detected in HN cancer.

Regarding immune dysregulation, our analysis revealed a remarkably low frequency of mutations in genes associated with the immune response. This observation suggests that the genomic landscape of the studied population exhibited limited alterations in the genetic components related to immune system function.

The scarcity of mutations in immune response genes may imply that other factors, such as epigenetic modifications or non-genetic influences, could play a more prominent role in the regulation of the immune system in this particular context. Moreover, as previously described, the interplay between p53 downstream factors, which may be dysregulated in mutated cancers, may lead to a modulation of autophagy and immune system response in malignant disease.

It's essential to interpret these findings cautiously, considering that immune dysregulation is a complex phenomenon influenced by various genetic and environmental factors. Further investigations into the specific pathways and mechanisms involved in immune dysregulation, beyond the scope of gene mutations alone, may provide a more comprehensive understanding of the underlying processes in this population.

According to their mutational status we have to wisely interpret overall survival data on those patients' groups.

The data extracted from cBioPortal concerning the mutation status of p53 in NSCLC and HN cancer reveal a clear and statistically significant association between p53 mutations and a poorer prognosis for patients diagnosed with NSCLC and HN cancer.

In the context of NSCLC, the presence of p53 mutations emerges as a robust prognostic factor, indicating a more unfavorable outcome for affected individuals. Patients with NSCLC harboring p53 mutations exhibit a statistically significant reduction in Overall Survival compared to those without these mutations. This association underscores the clinical relevance of assessing the p53 mutational status in NSCLC patients, providing valuable information for clinicians to gauge the likely trajectory of the disease and make informed decisions regarding treatment strategies (Figure 12).

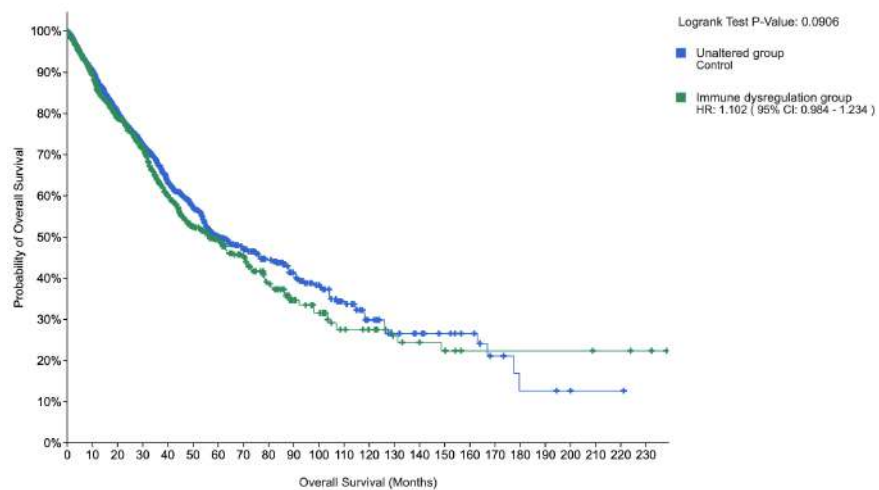
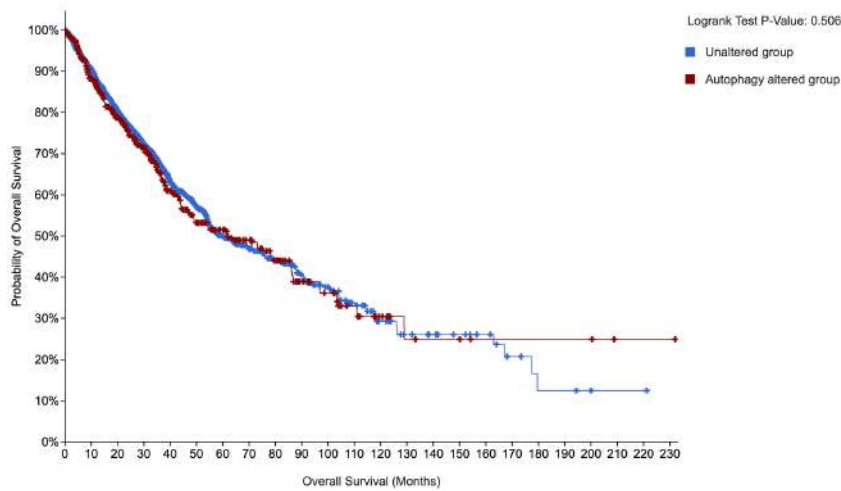
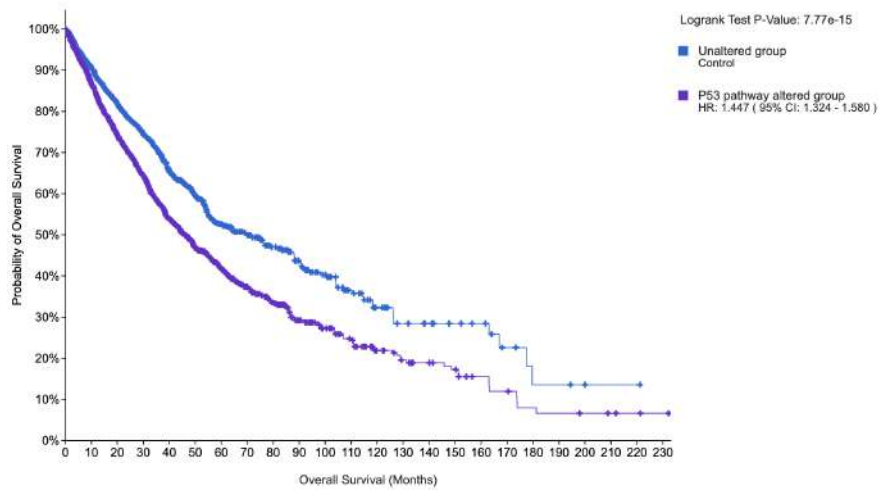


Figure 12: NSCLC OS in unaltered group and subgroups of patients with alterations in the p53 pathway (top), autophagic pattern (middle), or in the immune dysregulation (bottom). [data extracted from C-Bioportal]¹⁴⁹⁻¹⁵¹

Similarly, the data extracted for HN cancer underscores the prognostic significance of p53 mutations. Individuals with p53 mutations in HN cancer demonstrate a clear association with a poorer prognosis in terms of Overall Survival, and this association reaches statistical significance. Again, the mutational landscape of p53 in HN cancer may serve as a critical indicator of patient outcomes, guiding clinicians in their efforts to tailor treatment approaches based on the molecular characteristics of the tumor (Fig.13).

The statistical significance observed in both NSCLC and HN cancer reinforces the notion that p53 mutations are not merely molecular aberrations but have tangible clinical implications. This information is crucial for clinicians and researchers alike, providing insights into the prognostic landscape of these cancers and offering a basis for further investigations into targeted therapeutic strategies that may address the challenges posed by p53-mutated tumors.

The investigation extended to explore the impact of the mutational status of autophagy-related pathways and genetic immune dysregulation on Overall Survival (OS) using data obtained from cBioPortal. The focus was particularly on understanding how alterations in these pathways might influence the prognosis of patients with Head and Neck (HN) cancer and Non-Small Cell Lung Cancer (NSCLC).

For HN cancer patients, the analysis revealed a significant and noteworthy decrease in Overall Survival associated with mutations in both autophagy-related pathways and genetic immune dysregulation. This implies that individuals with mutations in these specific pathways within the HN cancer context experienced a more unfavorable prognosis, leading to reduced overall survival rates. The statistical significance of this finding underscores the potential clinical relevance of these mutational events in shaping the disease trajectory and outcomes for HN cancer patients (Fig.13).

Contrastingly, the same trend was not observed in the case of NSCLC patients. This suggests that the impact of these mutations on patient survival might vary across different cancer types, emphasizing the importance of cancer-specific considerations in understanding the clinical implications of molecular alterations.

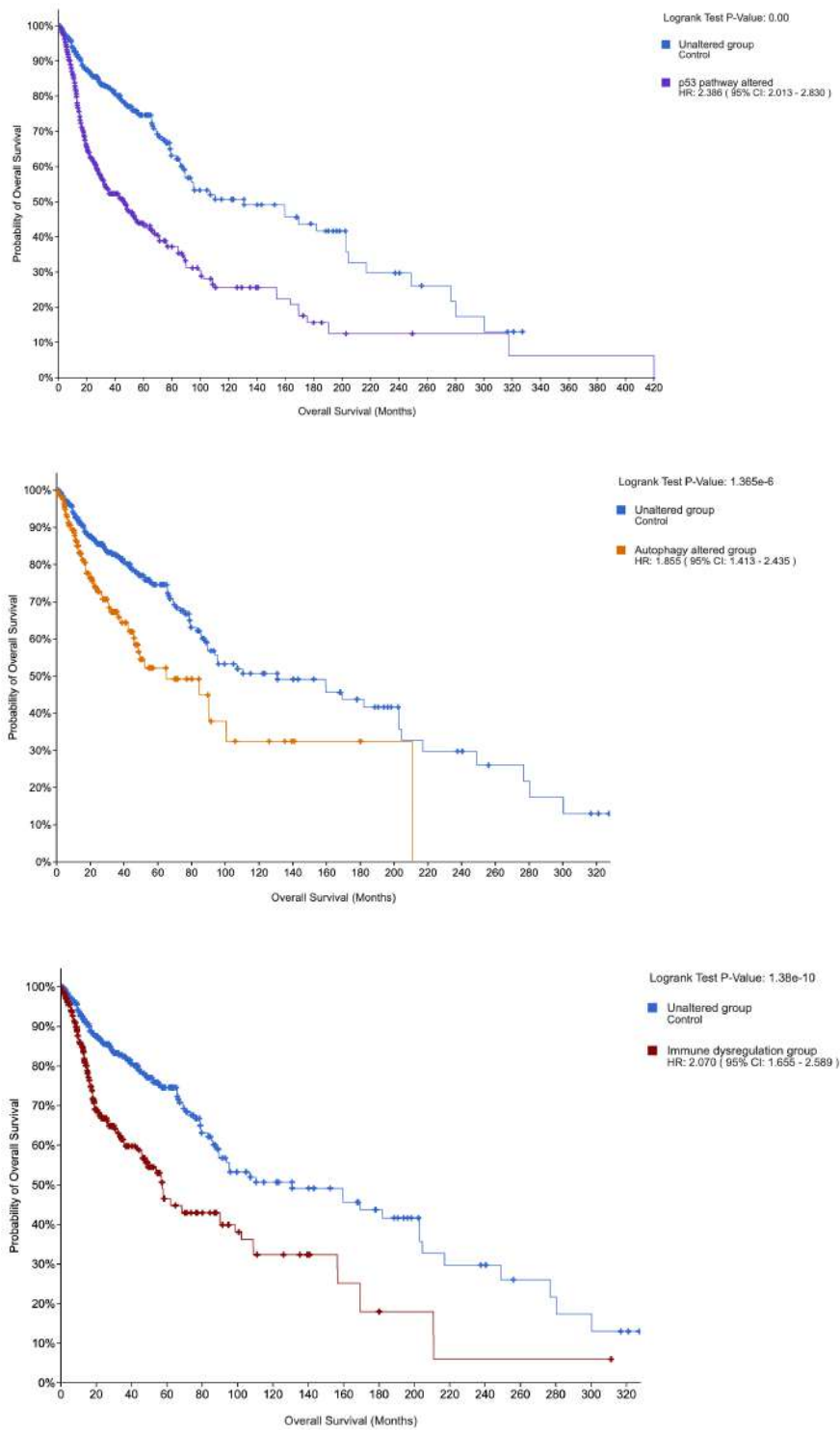


Figure 13: Head and Neck cancers OS in unaltered group and subgroups of patients with alterations in the p53 pathway (top), autophagic pattern (middle), or in the immune dysregulation (bottom). [data extracted from C-Bioportal] ¹⁴⁹⁻¹⁵¹

Prognostic value of the tumor characteristics and host response in OSCC and Squamous NSCLC

We narrow our focus to the most prevalent Head and Neck cancer, Oral Squamous Cell Carcinoma (OSCC), and Squamous Non-small Cell Lung Cancer.

We have chosen to explore the prognostic significance of autophagy within tumor cells, along with examining the immunological antitumor response in both the tumor macroenvironment and the tumor immune microenvironment (TIME) in a retrospective population.

Data from 104 consecutive patients who underwent surgery for OSCC at the Head and Neck Department of San Raffaele Hospital between 2008 and 2020 were gathered. The median follow-up period was 90.1 months (95% confidence interval: 62.5-119.4).

A comprehensive analysis was conducted on a total of 138 consecutive patients in the Squamous Non-Small Cell Lung Cancer (NSCLC) group. These patients underwent either diagnostic or therapeutic surgery at the Thoracic Surgery Department at San Raffaele Hospital between 2017 and 2023. The median follow up period was 23.7 months (95% confidence interval: 19.4 - 27.9).

Data encompassed clinical and pathological stages, patients' comorbidities, risk factors, performance status, details of surgical treatment, assessment of surgical margins, and the administration of neoadjuvant or adjuvant chemotherapy, radiotherapy, or immunotherapy. Information on persistent disease, recurrent disease, or mortality was also compiled.

In addition, our focus extended to specific histopathological variables that, while considered significant in recent literature, have yet to be incorporated into national or international oncological guidelines for these particular patient subgroups. These variables include p53, worst pattern of invasion (WPOI), perineural invasion (PNI), and vascular invasion (PVI).

To address our research questions, we delved into the assessment of systemic inflammation through pre-surgical values of neutrophils, lymphocytes, monocytes, and platelets. Furthermore, in a subgroup of patients (42 patients for OSCC and 32 patients

for Squamous NSCLC) the tumor microenvironment was histopathologically evaluated by quantifying CD8-positive cells. The assessment of autophagic flux was conducted through the quantification of p62 expression.

OSCC patients' clinical characteristics

Herein we present an in-depth analysis of various demographic, clinical, and treatment-related variables on the total of 104 patients with OSCC and on the subset of specific histopathological analysis of 42 patients randomly chosen within the OSCC group for further IHC evaluation (Table 1). Differences in the baseline characteristics of the patients belonging to the larger cohort and the smaller subgroup did not show any significance.

The median age at the initiation of treatment for the entire OSCC cohort was 67 years (95% CI: 19-96 years). Further narrowing the focus to the subgroup of 42 patients revealed a median age of 64 years (95% CI: 22-90 years).

Gender distribution in the OSCC cohort was relatively balanced, with 51 males (49%) and 53 females (51%). This pattern persisted in the subgroup, comprising 22 males (52.4%) and 20 females (47.6%). Smoking habits and alcohol consumption, known risk factors for OSCC, were reported by a significant portion of the patients. Smoking was prevalent in 39.4% of the entire cohort and 40.5% of the subgroup. Similarly, alcohol consumption was noted in 29.8% of the total OSCC population and 31.0% of the subgroup.

The Eastern Cooperative Oncology Group Performance Status (ECOG PS) was utilized to assess the patients' overall health and functional status. The majority of patients in both the overall OSCC cohort and the subgroup exhibited favorable ECOG PS scores, predominantly falling into categories 0 and 1.

According to the pathological staging based on the 8th edition of the TNM, the cohort was distributed as follows: Stage I Oral Squamous Cell Carcinoma (OSCC), representing an early and localized form of the disease, was observed in 28.8% of the overall cohort and slightly less, at 26.2%, in the subgroup. Stage II OSCC, characterized by a larger tumor size or slight spread to nearby structures, was identified in 17.3% of the total OSCC population and 19.0% in the subgroup. This suggests that a notable proportion of patients

were diagnosed at an early stage, potentially facilitating more favorable treatment outcomes.⁶⁷

Stage III, representing further progression with increased tumor size and potential lymph node involvement, was documented in 9.6% of the overall cohort and 19.0% of the subgroup. A significant portion of the patients presented with Stage IVa disease, constituting 34.6% of the entire OSCC cohort. Within this stage, 26.2% belonged to the subgroup of 42 patients, suggesting an advanced and extensive disease manifestation in both the overall population and the more focused subset.

The less common stages, IVb and IVc, were observed in a smaller proportion of patients. Stage IVb, indicating extensive local invasion, was documented in 1.9% of the overall cohort and 4.8% in the subgroup. Similarly, Stage IVc, indicating metastatic spread, was noted in 2.9% of the overall cohort. This staging information provides a comprehensive overview of the distribution of pathological stages in the studied OSCC cohort, highlighting the varied presentations and stages of disease severity within this population (Fig.14).

Treatment modalities ranged from transoral local excision to compartmental or total resection, with or without the need for surgical reconstruction. Patients underwent sentinel lymph node biopsy (SLNB), elective neck dissection, or therapeutic neck dissection based on the affected oral cavity subsite and the preoperative clinical N stage in 10%, 30%, and 38% of cases, respectively. Additionally, 22% of the population did not undergo any neck dissection.

Adjuvant treatments, such as radiotherapy and chemotherapy, were administered to 21.2% and 25% of patients, respectively, according to the pathological TNM assessed postoperatively and in consideration of any previous radiation therapy which may contraindicate reirradiation of the site of interest or presence of comorbidities which contraindicated adjuvant systemic chemotherapeutic treatment.

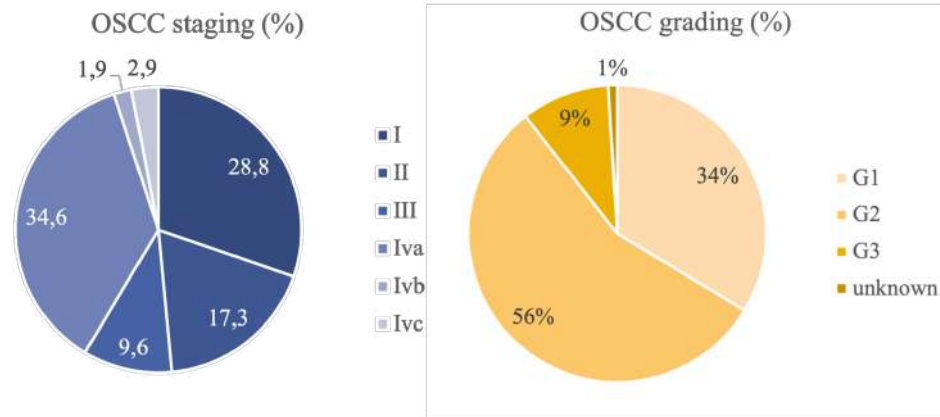


Figure 14: Pie charts representing the distribution of the oncological stage and pathological grade in our OSCC population.

Variable	OSCC population (n = 104)	sample (n = 42)	OSCC Subgroup (n = 42)	P value
Age start treatment (median, range)	67 (19-96)		64 (22-90)	ns
Male/female (n, %)	51/53 (49%-51%)		22/20 (52.4%-47.6%)	ns
Smoke	41 (39.4%)		17 (40.5%)	ns
Alcohol consumption	31 (29.8%)		13 (31.0%)	ns
ECOG PS				ns
0	57 (54.8%)		25 (59.5%)	
1	18 (17.3%)		10 (23.8%)	
2	6 (5.8%)		1 (2.4%)	
3	5 (4.8%)		2 (4.8%)	
4	3 (2.9%)		1 (2.4%)	
Pathological stage				ns
• I	30 (28.8%)		11 (26.2%)	
• II	18 (17.3%)		8 (19.0%)	
• III	10 (9.6%)		8 (19.0%)	
• IVA	36 (34.6%)		11(26.2%)	
• IVB	2 (1.9%)		2 (4.8%)	
• IVC	3 (2.9%)			
Treatment				ns
• Transoral local excision (TLE)	50 (48.1%)		19 (45.3%)	
• Compartmental resection w/wo reconstruction	50 (48.1%)		20 (47.6%)	
• Total resection w reconstruction	4 (3.8%)		3 (7.2%)	
Neck dissection				ns
• None	23 (22.1%)		6 (14.4%)	
• Elective nd	31 (29.8%)		12 (28.8%)	
• Sentinel lymph node biopsy (SLNB)	10 (23.8%)		10 (23.8%)	
• Therapeutic nd	40 (38.5%)		14 (33.3%)	
Adjuvant treatment				ns
• Radiotherapy	22 (21.2%)		14 (33.3%)	
• Chemotherapy	26 (25.0%)		8 (19.0%)	

Table 1: Clinical characteristics of OSCC population

Evaluation of the disease-free survival and overall survival in OSCC

The study uncovered a median overall survival (OS) of 96.0 months (95% CI: 50.3-141.6) and a median disease-free survival (DFS) of 26.5 months (95% CI: 9.7-43.3) among patients with Oral Squamous Cell Carcinoma (OSCC).

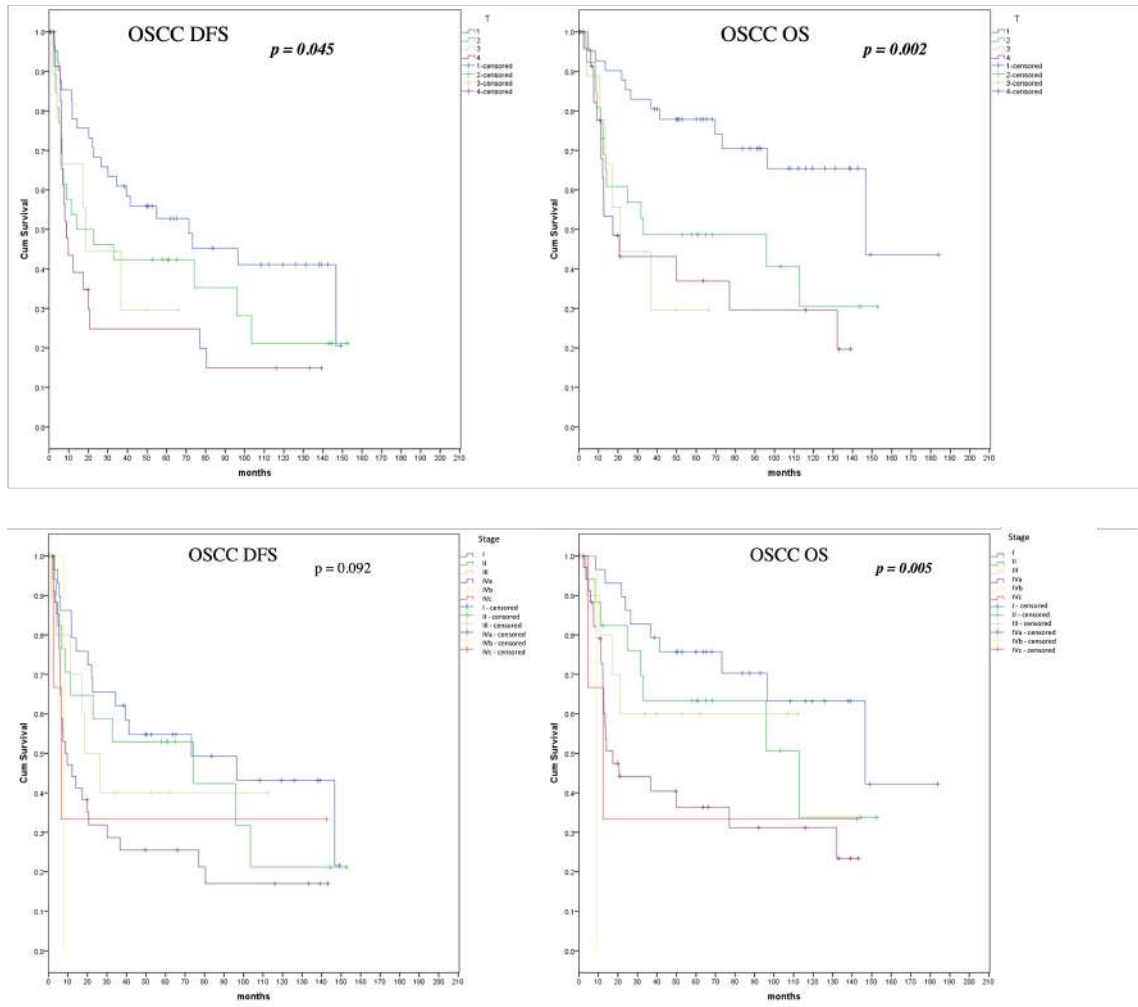


Figure 15: Top left: Kaplan-Meier curve illustrating DFS in Oral Squamous Cell Carcinoma (OSCC) patients according to the known pathological prognostic marker T, classified according to the 8th edition of TNM. The difference in DFS between the groups is statistically significant ($p = 0.045$). Top right: Kaplan-Meier curve depicting OS in OSCC patients according to the T stage. The difference in OS between the groups is statistically significant ($p = 0.002$). Bottom left: Kaplan-Meier curve demonstrating DFS in OSCC patients stratified according to the stage. The difference in DFS between the groups is not statistically significant ($p = 0.092$). Bottom right: Kaplan-Meier curve illustrating OS in OSCC patients stratified according to the stage. The difference in OS between the groups is statistically significant ($p = 0.005$).

Consistent with expectations, there is a correlation between an elevated T classification and a more unfavorable prognosis in both DFS and OS (Fig. 15), supported by significant p-values of 0.045 and 0.002, respectively (Fig.15).

According to nodal involvement, there is a noticeable disparity in OS between patients classified as N0 and N1 compared to those with higher nodal involvement. However, despite the apparent difference, the statistical analysis indicates that these distinctions are not significant, neither in terms of OS nor DFS. No significance was found in OS and DFS according to pathological Grade in our population.

Our results also suggest a notable correlation between *age* and OS in patients with OSCC (Fig.16). Specifically, the mean OS for individuals aged 67 years old or younger is significantly higher at 117.6 months, with a standard deviation of 12.2. In contrast, for individuals aged over 67 years old, the mean OS is notably lower at 70.3 months (± 8.8 SD). The statistical analysis, with a calculated p-value of 0.048, demonstrates the significance of the difference, implying that age plays a pivotal role in influencing overall survival outcomes for individuals affected by OSCC. It is deemed essential to note that this correlation impacts the long-term survivors (>24 months). No significant correlation is observed between age and Disease-Free Survival (DFS).

Moreover, a significant impact of ECOG-Performance status on both Disease-Free Survival (DFS) and Overall Survival (OS) was observed among patients with OSCC. When examining DFS, the data reveals distinct differences across ECOG-PS categories. Patients with an ECOG-PS of 0 demonstrated a notably longer DFS of 41.4 months [0 - 91.9], indicating a more extended period without disease recurrence. In contrast, patients with higher ECOG-PS scores experienced shorter DFS durations, with a noticeable decrease in months: 14.2 [3.8 - 24.6] months for ECOG-PS 1, 6.2 [4.7 - 7.7] months for ECOG-PS 2, 18.7 [0 - 51.8] ECOG-PS 3, and 8.8 [0 - 17.7] ECOG-PS 4. The overall statistical analysis, denoted by the p-value of 0.036, underscores the significance of ECOG-PS in influencing DFS outcomes. Similar trends are observed in the context of Overall Survival (OS). Patients with ECOG-PS 0 exhibit an impressive median OS of 146.7 months, indicating an extended survival period. Conversely, higher ECOG-PS scores are associated with decreased median OS values: 32.9 months [0 - 74.6] for ECOG-PS 1, 25.0 months [4.0 - 46.0] for ECOG-PS 2), 21.1 [5.1 - 37.1] for ECOG-PS 3, and

11.3 [0 - 24.2] ECOG-PS 4. The overall analysis yields a p-value of 0.002, emphasizing the significant impact of ECOG-PS on OS (Table 2). These findings suggest that ECOG-PS, as a measure of overall health and functional status, is a crucial determinant leading to the importance of considering patients' performance status in treatment planning and prognostic assessments, as it emerges as a key factor influencing their outcomes.

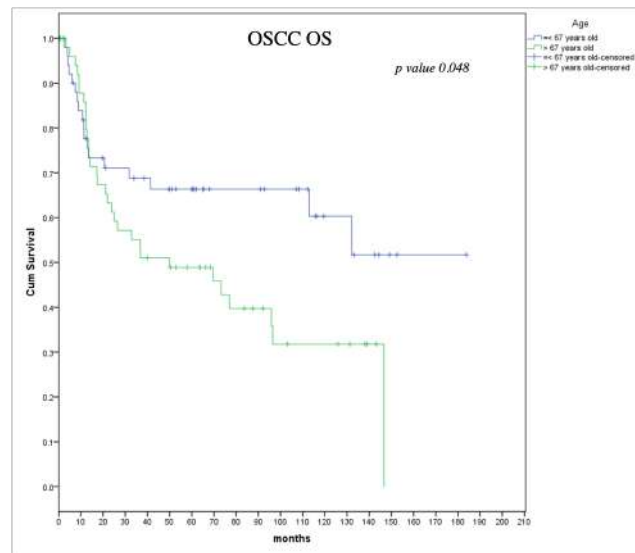


Figure 16: Kaplan-Meier curve illustrating OS in Oral Squamous Cell Carcinoma (OSCC) patients stratified by age (cutoff 67 years old). The difference in OS between the groups is statistically significant ($p = 0.048$)

ECOG PS	0	1	2	3	4	Tot	p value
DFS (months)	41.4 [0 - 91.9]	14.2 [3.8 - 24.6]	6.2 [4.7 - 7.7]	18.7 [0 - 51.8]	8.8 [0 - 17.7]	26.5 [10.1 - 42.8]	0.036
OS (months)	146.7	32.9 [0 - 74.6]	25.0 [4.0 - 46.0]	21.1 [5.1 - 37.1]	11.3 [0 - 24.2]	96.0 [42.4 - 149.5]	0.002

Table 2: Data on DFS and OS according to the ECOG Performance status of the patients (median [IQR])

We further analysed how subsite of disease may impact on the OS and DFS. Specifically, we found no difference in OS, however, the analysis of DFS based on different sites of disease within the oral cavity reveals distinctive median values. Notably, for cases involving the Lips and vestibule of the mouth, the median DFS is calculated at 6.9 months [0 – 15.0]. Similarly, the retromolar area, alveolar crest and palate subsites demonstrate a median DFS value of 6.1 months [1.1 - 11.1]. In contrast, cases associated with the Floor of mouth and tongue exhibit a substantially higher median DFS value of 34.4

months [0 – 80.1]. However, the statistical analysis, denoted by the p-value of 0.52, indicates that these observed differences in DFS among the different sites of disease are not statistically significant. Of note, grouping together subsites with worst prognosis compared to floor of mouth and tongue subgroup reveals interesting results. In the univariate analysis for OS, patients with the disease located in the floor of the mouth or tongue still exhibited a Hazard Ratio (HR) of 1.507 (95% CI: 0.834-2.725), indicating a non-significant trend towards increased risk compared to other sites ($p = 0.175$). However, for DFS, the HR increased to 1.784 (95% CI: 1.071-2.971), and the difference was statistically significant with a p-value of 0.026 (data shown in Table 4).

Interestingly, pathological assessment of extracapsular spread (ECS) significantly correlates with worst prognosis in terms of both DFS and OS, with a p value of 0.034 and 0.014 respectively (Fig. 17) This finding aligns with the recognition that ECS serves as one of the prognostic variables, alongside dimensional characteristics, acknowledged in the 8th edition of the TNM staging system for Oral malignancies. Notably, ECS is regarded as a factor necessitating progression to the subsequent prognostic nodal stage, even when the lymph node size remains constant (For instance, the engagement of a single lymph node, located on the same side as the primary disease and measuring less than 3 cm in dimension, is classified as N1. However, the presence of extracapsular spread (ECS) elevates the staging to N2a).

The data reveals a significant contrast in DFS based on the status of surgical margins ($p = 0.044$) (Fig.17). Specifically, when surgical resection results in a clear margin (R0), the median DFS reaches a substantial 39.5 [0 - 84.0] months. In contrast, cases where the surgical margin is not microscopically clear (R1) show a significantly lower median DFS of 8.8 [2.4 - 15.2] months. This discrepancy underscores the crucial role of achieving a clear margin in surgical interventions for patients with OSCC. A clear margin, indicating the complete removal of cancerous tissue, appears to be associated with a markedly prolonged period of disease-free survival compared to situations where the margin status is not definitively clear. These findings emphasize the importance of meticulous surgical procedures and thorough margin assessments in optimizing the long-term outcomes for individuals undergoing resection for OSCC.

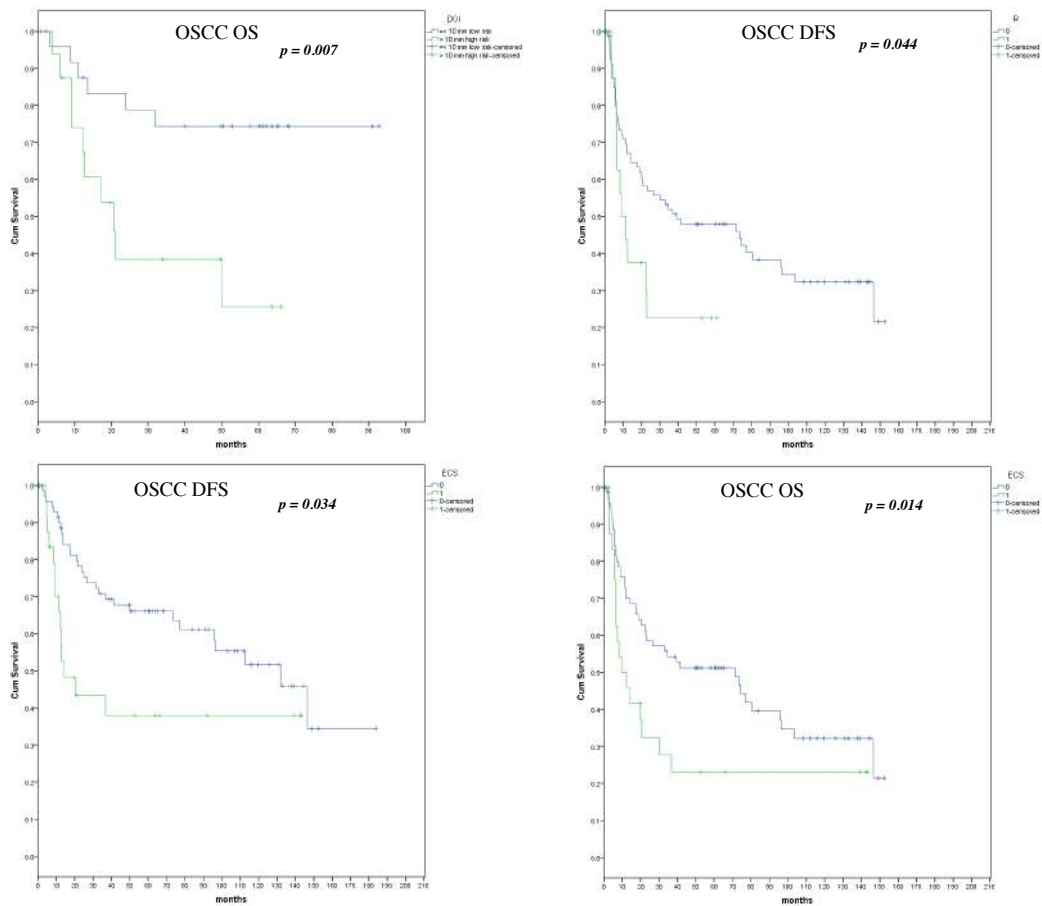


Figure 17: Top left: Kaplan-Meier curve illustrating Overall Survival (OS) in Oral Squamous Cell Carcinoma (OSCC) patients according to the known pathological prognostic marker “Depth of invasion” (DOI) <math>< 10</math> mm or >10 mm. The difference in OS between the groups is statistically significant ($p = 0.007$). Top right: Kaplan-Meier curve depicting DFS in OSCC patients with R0 (clear) and R1 (positive) surgical margins. The difference in DFS between the groups is statistically significant ($p = 0.044$). Bottom left: Kaplan-Meier curve demonstrating DFS in OSCC patients stratified by the absence (ECS 0) or presence (ECS 1) of extracapsular spread. The difference in DFS between the two groups is statistically significant ($p = 0.034$). Bottom right: Kaplan-Meier curve illustrating OS in OSCC patients based on the presence or absence of extracapsular spread. The difference in OS between the two groups is statistically significant ($p = 0.014$).

In the subgroup of 42 patients we further investigated the prognostic significance of Depth of Invasion (DOI), utilizing a dichotomized variable to categorize cases as either low risk (≤ 10 mm) or high risk (> 10 mm). Notably, the findings revealed a statistically significant impact on OS ($p=0.007$), where low-risk cases exhibited a substantially longer

mean OS of 73.0 [59.2 - 86.8] months compared to 31.3 [18.5 – 44.0] months for high-risk cases. However, when considering DFS, the difference between low and high-risk cases was not statistically significant. The mean DFS was 41.8 [29.2 - 54.4] months for low-risk cases and 23.1 [10.9 - 35.4] months for high-risk cases, with a p-value of 0.065 suggesting a trend but not reaching statistical significance (Fig.17). As mentioned earlier in the context of ECS, DOI has been integrated into the TNM classification, supplementing the dimension variable. Our findings underscore the significance of DOI as a prognostic factor, particularly in forecasting OS for patients with Oral OSCC. While our data align with the recognized prognostic value linked to DOI, it is important to note that DOI alone may not fully address the comprehensive histopathological risk assessment post-surgery.

LUSCC patients' clinical characteristics

In our study focusing on Lung Squamous Cell Carcinoma (LUSCC), we examined various demographic and clinical variables within the overall sample population of 138 patients, with a closer IHC analysis of a subgroup consisting of 31 individuals. The median age at the start of treatment was 72 years for the entire cohort, ranging from 33 to 87, with no significant difference observed in the subgroup (74 years, range 33-87). The male-to-female ratio was 81% to 19% in the total sample and 77% to 23% in the subgroup, showing no statistically significant variation.

Regarding smoking habits, the distribution among the categories of 'Never,' 'Past,' and 'Current' smokers demonstrated no significant differences between the overall population and the subgroup. However, among the total sample of 138 LUSCC patients, only 5.1% were no-smokers. The great majority of the patients had a history of smoking, with 43.5% falling into the 'Past' smoker category, indicating those who had quit smoking at least 6 months before surgery. Current smokers, constituting 34.1% of the total sample, were individuals who were actively smoking at the time of the study. These percentages shed light on the prevalence of smoking within the LUSCC patient population, underscoring the known significance of smoking as a potential risk factor for the development of lung squamous cell carcinoma.

In terms of comorbidities, there was no notable distinction between the two groups in the prevalence of various conditions such as arterial disease, cardiac surgery history, hypertension treatment, arrhythmia treatment, and cardiac failure treatment.

In the overall LUSCC cohort, the distribution of cases across pathological stages was as follows: 26.7% in Stage I, 23.9% in Stage II, 24.6% in Stage III, and an additional 24.6% in Stage IV. This reveals a relatively balanced representation of cases across different pathological stages, allowing for a comprehensive analysis of the disease spectrum (Fig. 18).

When examining the surgical procedures performed, a diverse array of interventions was observed. Notably, the majority underwent lobectomy (34.8%), while other procedures such as bilobectomy (4.3%), pneumonectomy (12.3%), segmentectomy (6.5%), and wedge resection (5.1%) were also conducted. A considerable percentage (37.0%) fell under the category of "Others," indicating various bioptical approaches tailored to individual cases. The patterns of lymph node dissection varied within this cohort. A substantial proportion underwent radical lymph node dissection (50.0%), reflecting a comprehensive approach to address regional lymph nodes (Table 3).

Upon evaluating the pathological stage in our study, a statistically significant difference was identified ($p = 0.017$), revealing a higher proportion of Stage I cases within the subgroup (38.7%) compared to the overall population (26.7%). Our group acknowledges and explains this observation, attributing it to the intentional selection of a smaller cohort consisting of patients who underwent curative surgical treatment. This choice was made to facilitate multiple histopathological analyses in the subgroup, feasible only with surgical specimens due to the limited tissue obtained during biopsy, especially in cases of more advanced tumors where surgical resection is not pursued, and histological assessment is performed solely on biopsy samples.

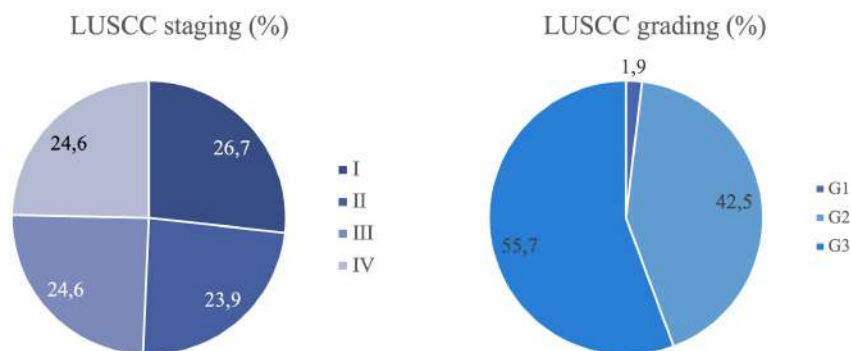


Figure 18: Pie charts representing the distribution of the oncological stage and pathological grade in our Lung SCC population.

Variable	LUSCC sample population (n = 138)	LUSCC Subgroup (n = 31)	P value
Age start treatment (median, range)	72 (33-87)	74 (33-87)	ns
Male/female (n, %)	112/26 (81%-19%)	24/7 (77%-23%)	ns
Smoke			ns
• Never	7 (5.1%)	1 (3.2%)	
• Past	60 (43.5%)	12 (38.7%)	
• Current	47 (34.1%)	15 (48.4%)	
Comorbidity			ns
• None	22 (16%)	8 (26%)	
• Comorbidity artery disease	25 (18%)	8 (26)	
• Previous cardiac surgery	5 (4%)	1 (3%)	
• Current treatment hypertension	49 (36%)	14 (45%)	
• Current treatment arrhythmia	8 (6%)	1 (3%)	
• Current treatment cardiac failure	2 (1%)	1 (3%)	
Pathological stage			0.0170*
• I	37 (26.7%)	12 (38.7%)	
• II	33 (23.9%)	11 (35.5%)	
• III	34 (24.6%)	8 (25.8%)	
• IV	34 (24.6%)		
Surgical procedure			0.0015**
• Bilobectomy	6 (4.3%)	3 (2.4%)	
• Lobectomy	48 (34.8%)	17 (54.8%)	
• Pneumonectomy	17 (12.3%)	4 (12.9%)	
• Segmentectomy	9 (6.5%)	6 (19.4%)	
• Wedge	7 (5.1%)	0	
• Others	51 (37.0%)	1 (3.2%)	
Lymph node dissection			0.0025**
• None	62 (44.9%)	4 (12.9%)	
• Radical	69 (50.0%)	26 (83.9%)	
• Sampling	7 (5.1%)	1 (3.2%)	
• Other	0	0	

Table 3: Clinical characteristics of Lung Squamous Cell Carcinoma population.

A similar difference between the total population and the subgroup was observed in terms of treatment modality and lymph node dissection. A more in-depth analysis of surgical procedures revealed significant differences ($p = 0.0015$) in the distribution of interventions. Notably, the smaller subgroup exhibited a higher percentage of lobectomy (54.8%) compared to the total sample (34.8%). Various other procedures, such as bilobectomy, pneumonectomy, segmentectomy, and wedge resection, also displayed differences between the overall population and the subgroup. The examination of lymph node dissection patterns underscored additional distinctions between the two groups ($p = 0.0025$). The subgroup demonstrated a higher prevalence of radical lymph node dissection (83.9%) compared to the overall population (50%), suggesting a propensity for more extensive surgical approaches within this specific subset. All these data align with the research group's intended approach, where the smaller subgroup was deliberately chosen from patients who underwent major resective surgery rather than simple biopsy. This selection aimed to provide an ample tissue sample for subsequent immunohistochemistry analysis.

Evaluation of the disease-free survival and overall survival in LUSCC

In our study focused on Lung squamous cell carcinoma population, the analysis of overall survival (OS) revealed a median duration of 61.2 months, with a 95% confidence interval (CI) ranging from 19.9 to 102.5 months. This suggests a considerable variability in the survival times within the studied population, emphasizing the need for personalized and nuanced treatment strategies.

Similarly, when exploring DFS, the median duration was found to be 31.7 months, with a 95% confidence interval spanning from 24.1 to 39.3 months. These findings shed light on the potential challenges faced by patients in maintaining a disease-free state over time.

These results underscore the heterogeneity within the squamous cell carcinoma of the lung population, emphasizing the importance of considering individual patient characteristics and tailoring treatment plans to achieve optimal outcomes in terms of both overall and disease-free survival. The wide confidence intervals also highlight the inherent variability in these outcomes and the necessity for a comprehensive approach to managing this particular subtype of lung cancer.

As expected, the staging parameters demonstrate a substantial prognostic significance. Notably, for patients in the early stage, the median DFS stands at 44.8 months, with a 95% confidence interval (CI) ranging from 26.5 to 63.1. In stark contrast, the advanced-stage patients experience a considerably shorter DFS of 7.1 months, with a narrower CI of 5.0 to 9.2. This stark difference is statistically significant, as indicated by a p-value of less than 0.001 (Fig.19).

Similarly, in terms of OS, the disparity between early and advanced stages is evident. The median OS for patients in the early stage is 61.2 months, with a broader CI spanning from 20.0 to 102.4. On the other hand, patients in the advanced stage have a markedly reduced median OS of 9.6 months, and a more limited CI of 5.1 to 14.2. Once again, this divergence reaches statistical significance, emphasizing the robust prognostic value associated with the staging of Lung SCC ($p < 0.001$) (Fig.19).

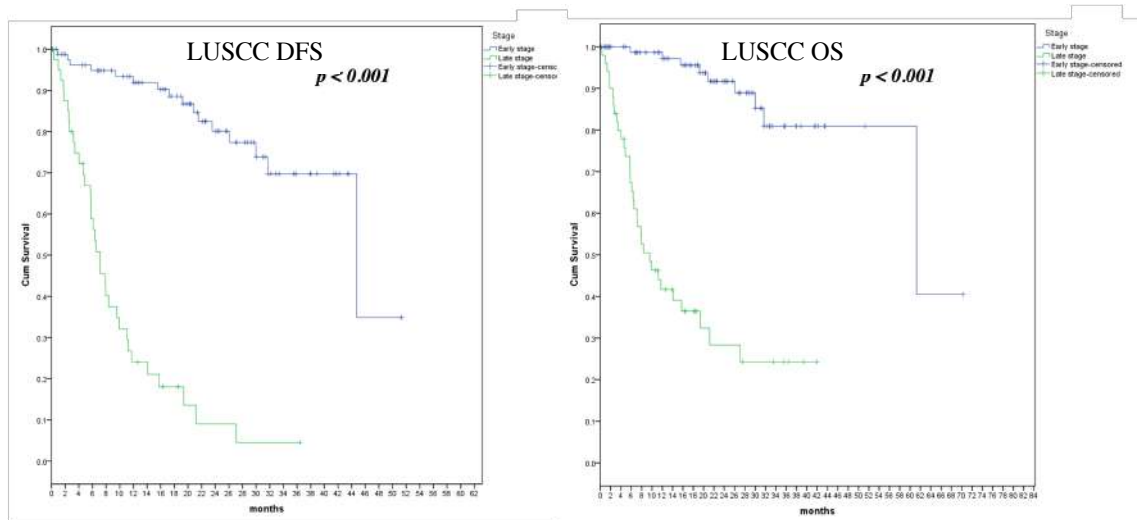


Figure 19: Left: Kaplan-Meier curve demonstrating DFS in Lung SCC patients stratified according to the stage. The difference in DFS between the groups is statistically significant ($p < 0.001$). Right: Kaplan-Meier curve illustrating OS in LUSCC patients stratified according to the stage. The difference in OS between the groups is statistically significant ($p < 0.001$).

The analysis of grading in our study has revealed that there is no statistically significant difference in terms of DFS and OS. This implies that the various histological grades, when considered independently, do not exhibit a notable impact on the prognosis of the patients with Lung SCC. Whether categorized as low or high grade, the outcomes in terms of DFS and OS do not display a discernible divergence, indicating that the histological grading

alone may not be a decisive factor in predicting the survival outcomes for individuals with Lung SCC in our study cohort.

Our analysis regarding smoking habits in individuals with Lung SCC has demonstrated that there is no statistically significant association with OS and DFS. Regardless of whether patients identified as never smokers, past smokers, or current smokers, the differences in OS and DFS did not reach statistical significance. This suggests that, in our study cohort, smoking status alone does not appear to be a decisive factor influencing the prognosis of individuals with Lung SCC. Other variables or factors may play a more prominent role in determining survival outcomes in this population.

Evaluation of the systemic Immune response: Tumor Macroenvironment

We investigated the role of systemic inflammation and host response in patients with Oral Squamous Cell Carcinoma and SCC of the Lung through established hematological parameters proposed in the literature as potential markers of the inflammatory response to cancer.

Initially, we examined the Neutrophil-to-Lymphocyte Ratio (NLR), Platelet-to-Lymphocyte Ratio (PLR), and Monocyte-to-Lymphocyte Ratio (MLR) in the two study populations.

First of all, we noticed interesting correlations between these parameters. In fact, the Spearman correlation analysis revealed significant relationships among NLR, MLR, and PLR in our dataset (Fig. 20).

Particularly, there is a strong positive correlation between NLR and MLR in both OSCC and LUSCC, with a coefficient of 0.720 and 0.741 respectively, and a highly significant p-value (<0.001). This indicates that an increase in NLR is associated with a proportional increase in MLR. Similarly, a robust positive correlation was observed between NLR and PLR, with a correlation coefficient of 0.672 and 0.728 and a highly significant p-value of less than 0.001, in OSCC and LUSCC respectively. This suggests that variations in NLR coincide with corresponding variations in PLR. Additionally, a significant positive correlation exists between MLR and PLR, though slightly less pronounced compared to the NLR-MLR and NLR-PLR associations. The correlation coefficient for MLR and PLR

is 0.483 in OSCC and 0.575 in LUSCC, with a p-value less than 0.001, indicating that changes in MLR are positively associated with changes in PLR.

These findings collectively imply a cohesive relationship between these immune-related ratios, signifying shared underlying mechanisms or common systemic influences of these inflammatory markers. The results provide valuable insights into the interconnected dynamics of these ratios within the immune and inflammatory contexts in the studied population.

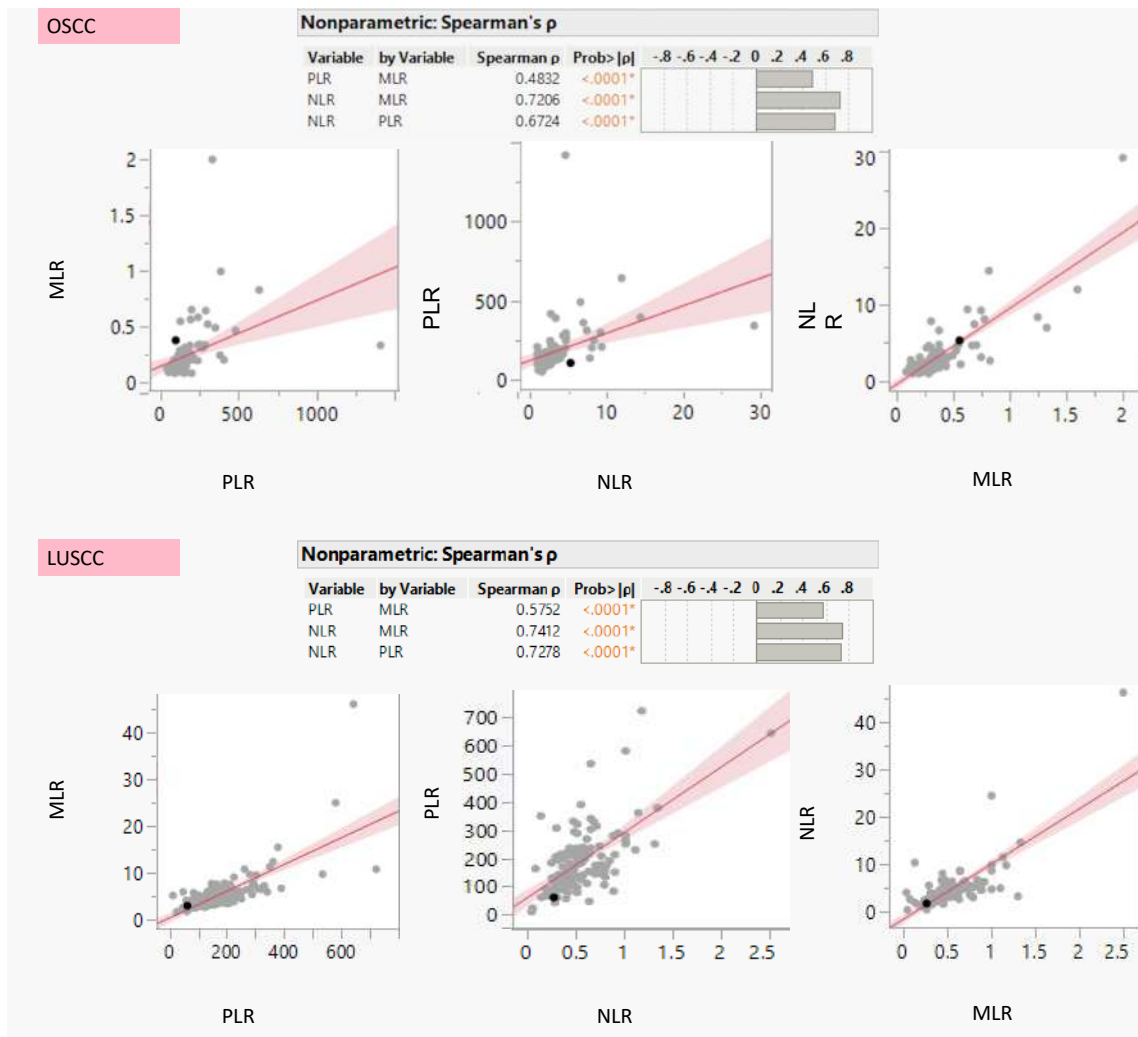


Figure 20: Spearman's correlation between Systemic Inflammatory Markers Neutrophil-to-Lymphocyte Ratio (NLR), Monocyte-to-Lymphocyte Ratio (MLR), and Platelet-to-Lymphocyte Ratio (PLR) in Oral Squamous Cell Carcinoma (OSCC) and Lung Squamous Cell Carcinoma (LUSCC).

Furthermore, we noted that all inflammatory markers were higher in patients with advanced-stage OSCC compared to those in early stages (Fig. 21).

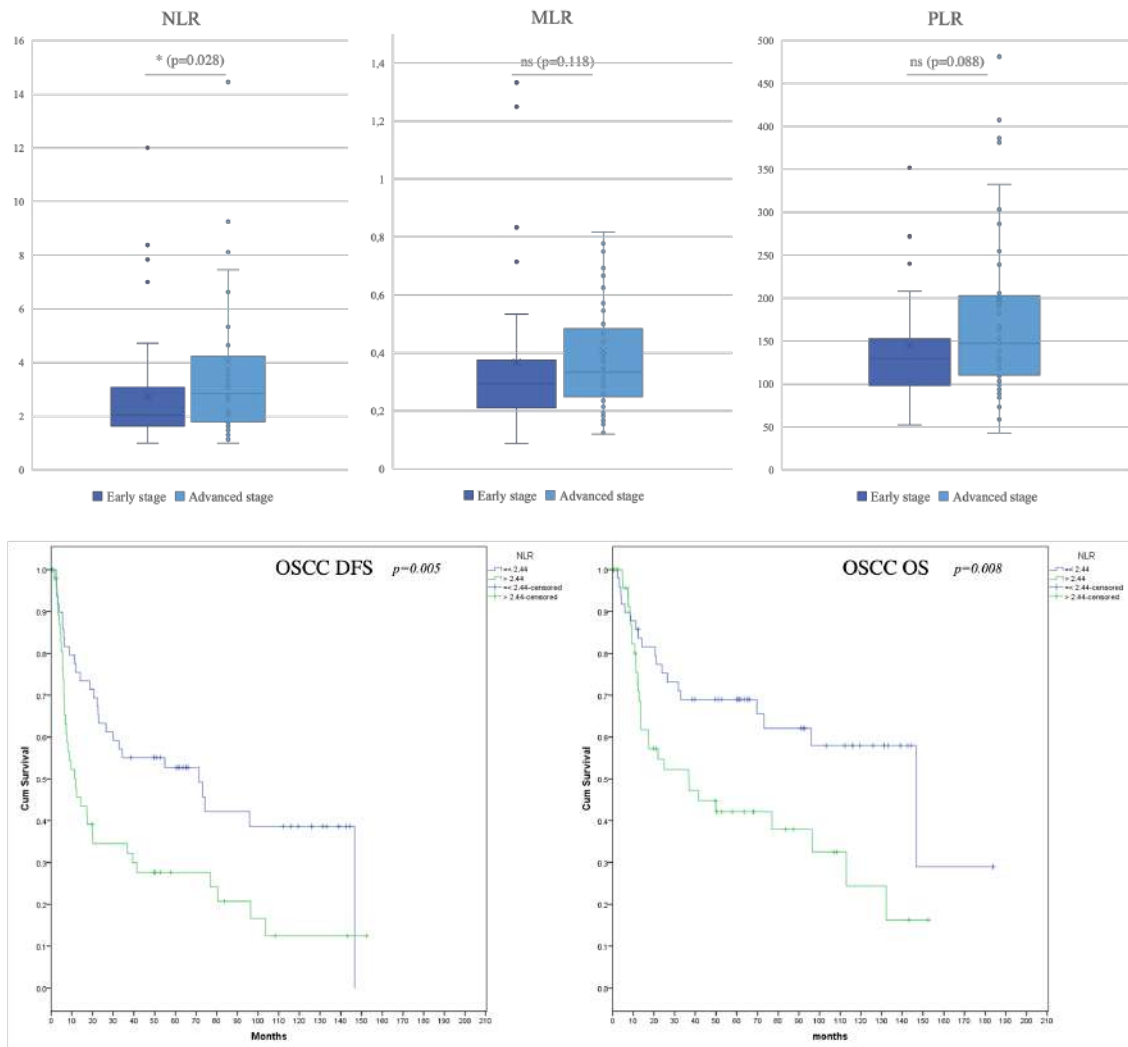


Figure 21: At the top: Boxplots illustrating the distribution of NLR, MLR, and PLR values between early and advanced stages of Oral Squamous Cell Carcinoma (OSCC) patients. At the bottom: Kaplan-Meier survival curves depicting Disease-Free Survival (DFS) and Overall Survival (OS) in OSCC based on NLR levels (< 2.44 and > 2.44), with corresponding p-values (DFS: $p = 0.005$, OS: $p = 0.008$).

Same trend was observed in the patients affected by LUSCC (Fig. 22).

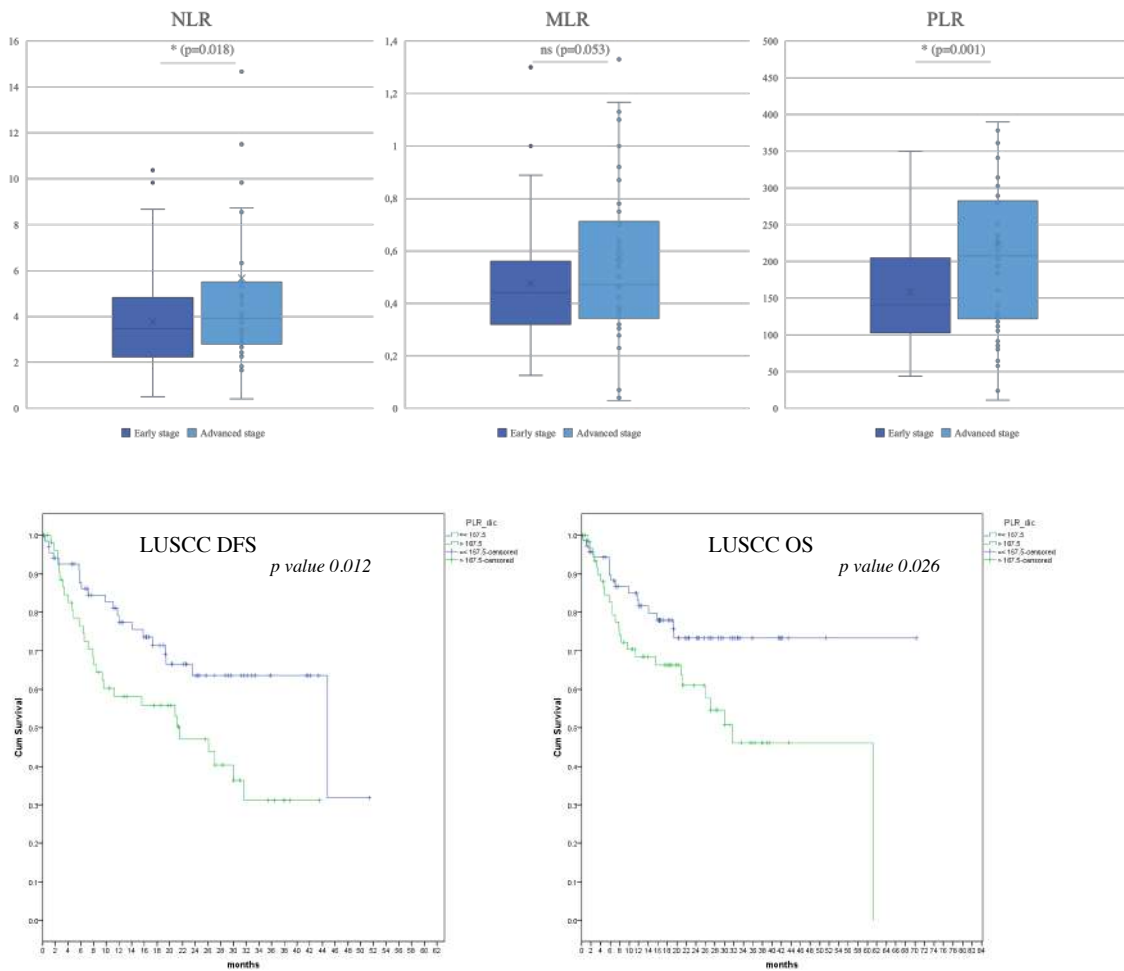


Figure 22: At the top: Boxplots illustrating the distribution of NLR, MLR, and PLR values between early and advanced stages of Lung Squamous Cell Carcinoma (LUSCC) patients. At the bottom: Kaplan-Meier survival curves depicting Disease-Free Survival (DFS) and Overall Survival (OS) in LUSCC based on PLR levels (cut-off 167.5), with corresponding p-values (DFS: $p = 0.012$, OS: $p = 0.026$).

However, only NLR exhibited a significant difference, with a mean of 2.76 ± 2.07 in early stages compared to 4.04 ± 4.47 in advanced stages ($p=0.028$) in OSCC (Fig.21). In the LUSCC population, we identified a statistically significant difference in both NLR and PLR parameters (Fig.22). Specifically, the mean values for early and advanced stages were 3.76 ± 1.95 and 5.67 ± 6.99 , respectively ($p=0.018$) for NLR, indicating a substantial variation. Similarly, for PLR, the means were 158.34 ± 70.73 and 224.22 ± 148.30 ($p=0.001$), emphasizing a significant difference in platelet-to-lymphocyte dynamics between early and advanced stages.

It's noteworthy that, upon consideration of histological grading, there were no observed differences in NLR, MLR, and PLR variables. This indicates that the immune-related ratios did not vary significantly based on the corresponding histological grading in our sample.

Subsequently, a cumulative analysis considering only the NLR values for every stage of the disease in OSCC revealed a significant association between NLR values and prognosis. Specifically, lower NLR values were associated with a worse prognosis. Patients with $NLR < 2.44$ (our defined cutoff) demonstrated a longer DFS of 71.4 [26.1 - 116.7] months compared to those with NLR above the cutoff value (11.7 [4.9 - 18.6] months) with a *p-value* of 0.005. A similar trend was observed in OS, with a median of 146.7 months [75.0 - 218.3] in patients with a lower NLR compared to 36.7 months [7.9 - 65.5] (*p-value* = 0.008).

In the context of LUSCC, the PLR serves as a significant parameter for predicting prognosis. In fact, putting a cutoff value of $PLR < 167.5$ a better prognosis was found in patients with lower PLR values in both DFS (*p* = 0.012) and OS (*p* = 0.026).

For individuals with a $PLR < 167.5$, the median DFS is notably prolonged, measuring at 44.8 months [15.0 to 74.5]. Conversely, for those with a PLR exceeding 167.5, the median DFS significantly decreases to 21.5 months [8.6 - 34.5].

In summary, these results suggest a potential prognostic value of PLR in LUSCC. A PLR of 167.5 or lower appears associated with a more favorable DFS, while values exceeding this threshold are linked to a shorter median DFS. These findings contribute valuable insights for risk stratification and prognostic assessments in Lung SCC patients.

Tumor-autonomous factors

P53 positivity express worst prognosis in OSCC

P53 is widely acknowledged for its significant prognostic value across various tumors, and it is identified as a promising prognostic factor in the 8th edition of TNM. Consequently, we embarked on a thorough evaluation of its presence in our sample population, encompassing both OSCC and LUSCC.

The assessment involved quantifying p53 immunostaining positivity by evaluating the percentage of cells expressing p53 in the tumor.

In our study, we found no statistically significant variations in p53 positivity between the two cohorts comprising patients with Oral Squamous Cell Carcinoma (OSCC) and Lung Squamous Cell Carcinoma (LUSCC), regardless of tumor stage or pathological grade. Nevertheless, our results did reveal an interesting pattern of p53 expression, which aligns with our expectations. We observed a distinctive bimodal distribution across all stages and within both cancer types (Fig.23).

This bimodal distribution of p53 expression can be attributed to the underlying genetic mutations within the TP53 gene. Specifically, we noticed that p53 positivity tends to manifest either as a high percentage of positivity or a complete absence thereof. These two distinct patterns of expression correspond to the various types of mutations that can occur within the TP53 gene.

When p53 is entirely absent in immunohistochemistry (IHC), it is indicative of disruptive mutations in the TP53 gene. These disruptive mutations encompass truncations, frameshifts, splice site mutations, and deep deletions. On the other hand, a high presence of p53 positivity in tumoral cells suggests the presence of an in-frame mutation, particularly within the DNA-binding domain of the TP53 gene. This type of mutation ultimately leads to elevated protein expression and its accumulation within the cells.¹³⁹

Of note, in transforming the variable into a dichotomy ($\leq 10\%$ positivity HPF was considered absence, and $> 10\%$ positivity HPF was considered presence), the analysis reveals a distinct prognostic difference in OSCC patients' DFS based on the expression level.

Individuals exhibiting no p53 expression present a notably improved prognosis with a statistically significant difference ($p=0.029$). The mean Disease-Free Survival (DFS) for this subgroup is substantially higher, reaching 44.4 months (confidence interval: 32.5 - 56.2), in contrast to 27.4 months (confidence interval: 15.0 - 39.8) for those with higher expression levels (Fig. 24).

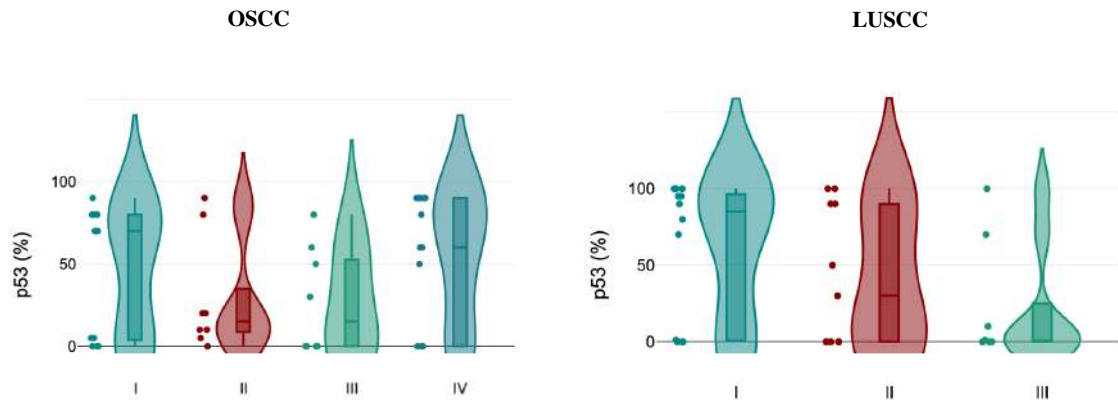


Figure 23: Violin plots for the distribution of p53 positivity (%) according to the stage of disease in Oral SCC and Lung SCC (ns).

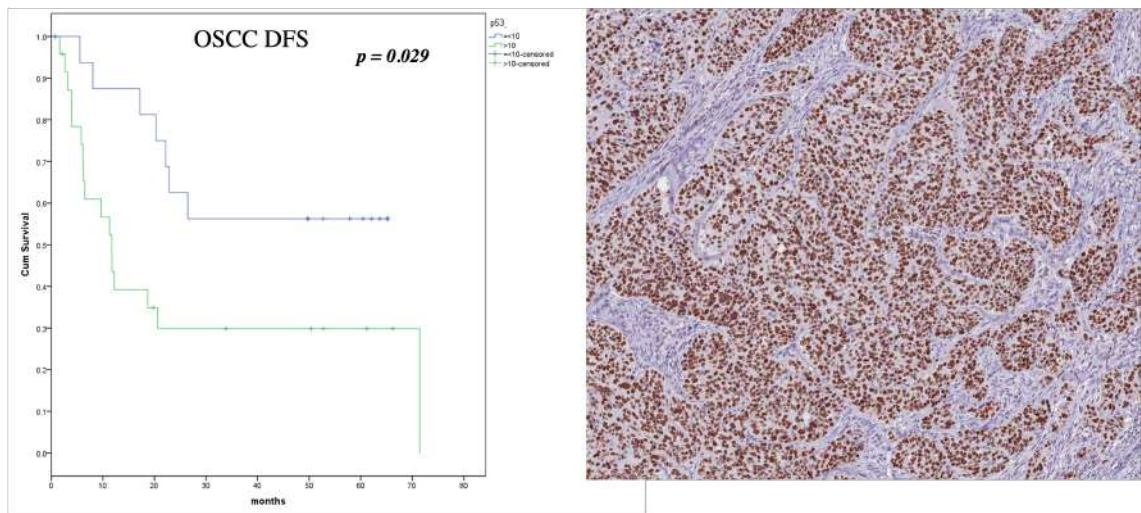


Figure 24 On the left Kaplan-Meier curves depicting Disease-Free Survival (DFS) in Oral Squamous Cell Carcinoma (OSCC) patients stratified by p53 expression levels (<10% and >10%). Statistical significance ($p = 0.029$) is observed. On the right, an illustrative case displays p53 immunostaining in OSCC.

Nevertheless, it is crucial to emphasize that the observed trend did not translate into statistically significant findings for Lung SCC patients. Neither OS nor DFS reached statistical significance in this cohort. This discrepancy could be attributed to the relatively small sample size or the shorter follow-up period in Lung SCC compared to Oral SCC.

Indeed, interpreting the data requires caution because both the complete absence and high levels of p53 are indicative of pathological states driven by somatic mutations in tumor

cells. This dual pattern of p53 expression underscores the complexity of the underlying genetic alterations within the TP53 gene and their implications in the context of cancer (Fig.25).

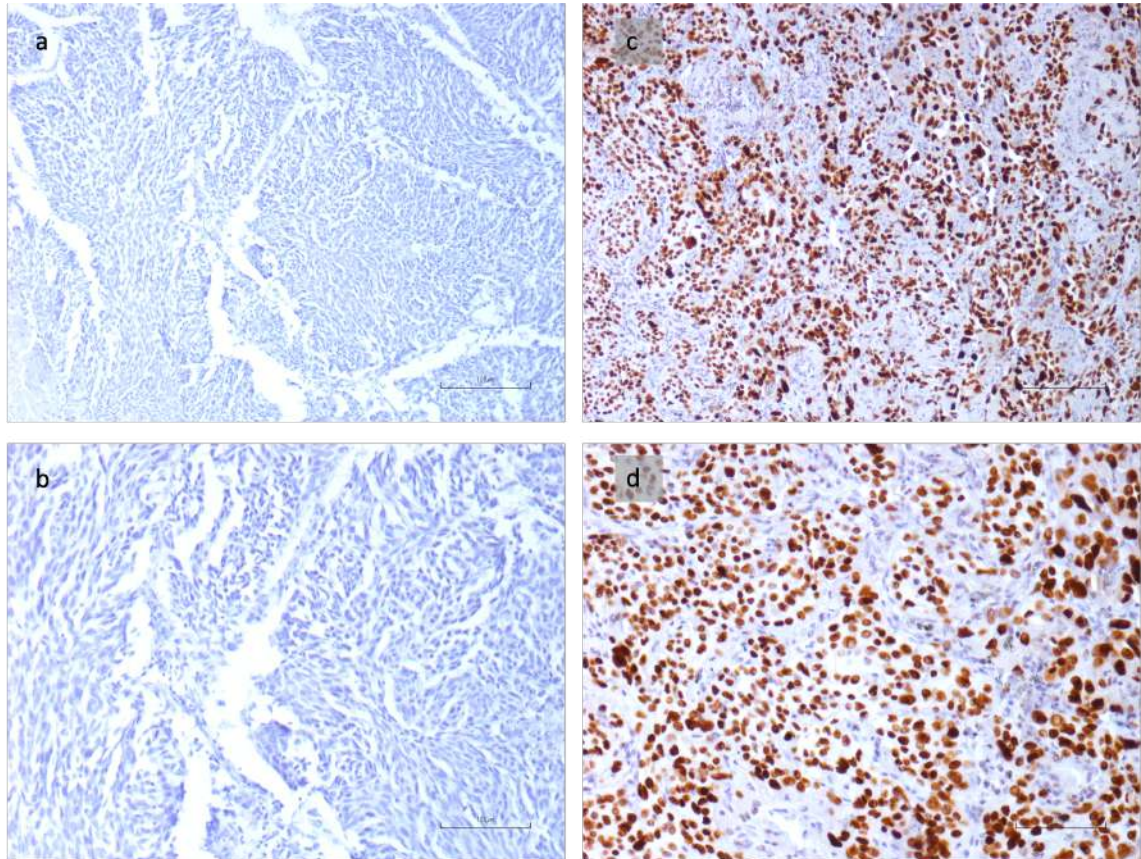


Figure 25: Representative histological sections for p53 IHC evaluation in the tumor cells, Lung SCC: a) 10x and b) 20x, p53+ immunohistochemistry (IHC) showing complete absence of P53 staining (0%); c) 10x and d) 20x, p53+ immunohistochemistry (IHC) with a high presence of P53 staining (100%).

PDL1

We further explored potential correlations between PDL1 expression in LUSCC and other variables under investigation. In the context of LUSCC, our analysis revealed the absence of any correlation between the expression of PDL1 and the immune-related parameters NLR, MLR, and PLR.

Furthermore, the significance of PDL1 as a predictor of patient outcomes was not established. Specifically, PDL1 expression did not demonstrate statistical significance in predicting OS or DFS in individuals with LUSCC.

It's noteworthy that in the analysis of LUSCC samples, a Spearman correlation was conducted to explore the relationship between p53 and PDL1 expression. The correlation coefficient between PDL1 percentage and p53 percentage was 0.523, indicating a positive correlation. Although the p-value was 0.067, not reaching conventional significance, the relatively small sample size might have influenced the statistical outcome.

Of note, no correlation was observed between PDL1 expression and the presence of lymphocytic infiltrates in the tumor stroma, as indicated by both TILs and CD8+ lymphocytes.

P62/SQSTM1

The investigation focused on examining the role of p62 as a surrogate marker for autophagic levels in tumor cells. To comprehensively assess this, various variables in Immunohistochemistry (IHC) for p62 were initially considered:

1. Percentage of Positivity: Evaluation of the percentage of cells expressing p62 in normal peritumoral tissue/dysplastic/reactive epithelium, the tumor stroma, and at the tumor's advancing front.
2. Pattern of Cytosolic and Nuclear Positivity: Examination of the cytosolic and nuclear patterns of p62 positivity within the tumor cells.

This comprehensive approach aimed to capture nuanced information about p62 expression, providing insights into its potential role as a reliable indicator of autophagic activity in tumor cells. The investigation delves into various aspects of p62 immunostaining, shedding light on its diverse patterns and distributions within the tumor microenvironment.

In the comparison between LUSCC and OSCC, the median percentage of p62-positive tumor cells was found to be 90% for LUSCC and 75% for OSCC. For LUSCC, the IQR spans from 75% to 95%. In OSCC, the IQR ranges from 60% to 90%. Despite the observed differences in means and IQRs, the statistical comparison using a p-value of 0.1057 did not reach significance. This suggests that there is no significant distinction in the percentage of p62-positive tumor cells between Lung SCC and Oral SCC (Fig. 26). However, it's essential to interpret these results with caution, considering the potential

impact of individual patient variations and the inherent heterogeneity within each tumor type.

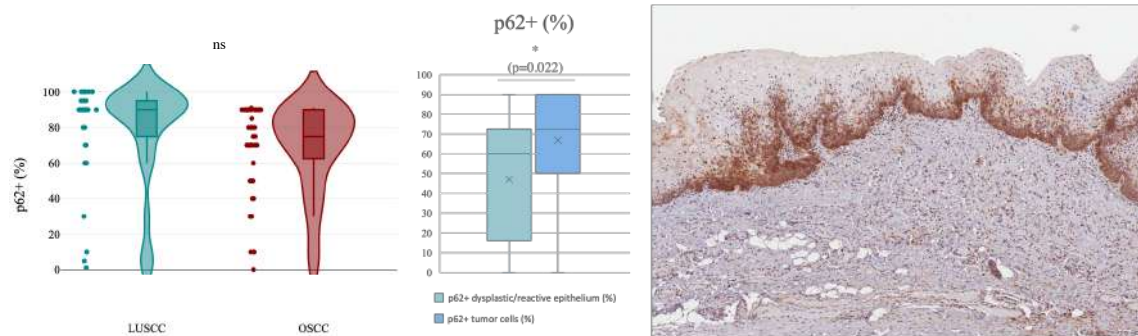


Figure 26: On the left: Violin plots for the distribution of p62 positivity (%) in Oral SCC and Lung SCC (ns); the great majority of samples have high expression of p62. In the middle, a graphical representation using box plots depicting the differential expression of p62 positivity in tumor cells and dysplastic/reactive epithelium (%). On the right, an illustrative case of p62 IHC staining in dysplastic/reactive epithelium adjacent to tumoral tissue.

Additionally, we conducted an analysis to compare the percentage of p62-positive tumor cells with the percentage of p62-positive dysplastic/reactive epithelium in OSCC. However, it's important to note that a similar analysis was not feasible in the case of lung SCC due to the limited presence of dysplastic-non neoplastic bronchial epithelium in close proximity (Fig.26).

The results revealed that median percentage of p62-positive tumor cells was significantly higher (75%, IQR 60% -90%), while for p62-positive dysplastic/reactive epithelium, it was 60% [IQR 25% - 75%], with a p-value of 0.0224 (Fig.26). These findings provide valuable insights into the differential expression of p62 in neoplastic and non-neoplastic cells, with possible interpretation on this differential expression.

The percentage of p62 positivity did not reveal any noteworthy correlation with parameters such as TNM staging, oncological stage, or the presence of tumor-infiltrating lymphocytes (TILs) and CD8+ lymphocytes in the tumor stroma or at the tumor margin. Nevertheless, it is crucial to acknowledge that the lack of significant correlations could potentially be attributed to the relatively limited number of samples processed in our study.

We must emphasize the comprehensive nature of our analysis, which considered the diverse p62 expression patterns observed in the samples. To the best of our knowledge, our immunohistochemistry (IHC) report stands as the inaugural documentation of these unique p62⁺ staining patterns in OSCC and LUSCC. These patterns encompass cytoplasmic (as illustrated in Fig. 27), nuclear (as demonstrated in Fig. 28), and nucleo-cytoplasmic distribution (depicted in Fig. 29) within the context of OSCC and LUSCC.

The results indicate that when looking at the three identified p62⁺ staining patterns, there are differences in their prevalence between the tumoral core and the tumor invasive margin. In the tumoral core, the cytoplasmic pattern was observed in 37.5% of the samples, while the nuclear pattern was seen in 31.25% of the samples. Interestingly, the nucleo-cytoplasmic pattern was also present in 31.25% of the samples in the tumoral core. Conversely, at the tumor invasive margin, the distribution of these patterns varied. The cytoplasmic pattern was observed in 20.9% of the samples, the nuclear pattern in 16.4%, and the nucleo-cytoplasmic pattern was notably more prevalent, appearing in 62.7% of the samples (Fig. 30, pie charts).

These findings suggest that the distribution of p62⁺ staining patterns differs between the central tumoral core and the surrounding tumor invasive margin, highlighting potential spatial variations in p62 expression within the tissue samples.

Moreover, we found very interesting data about the percentage of samples (OSCC and LUSCC combined) that demonstrated different p62 patterns of expression according to tumor grade in both the tumor core and tumor invasive margin (Fig. 30).

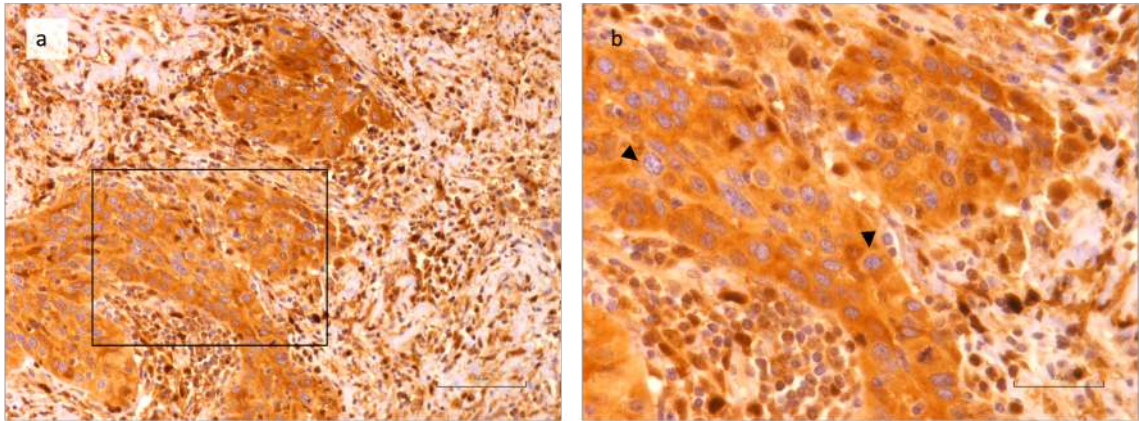


Figure 27: Representative histological sections for p62+ evaluation, cytoplasmic pattern in LUSCC: p62+ immunohistochemistry (IHC) a) 20x, b) 40x of the same section. Notably, p62 staining is diffuse in the cytoplasm, but nuclei are unstained (arrowheads).

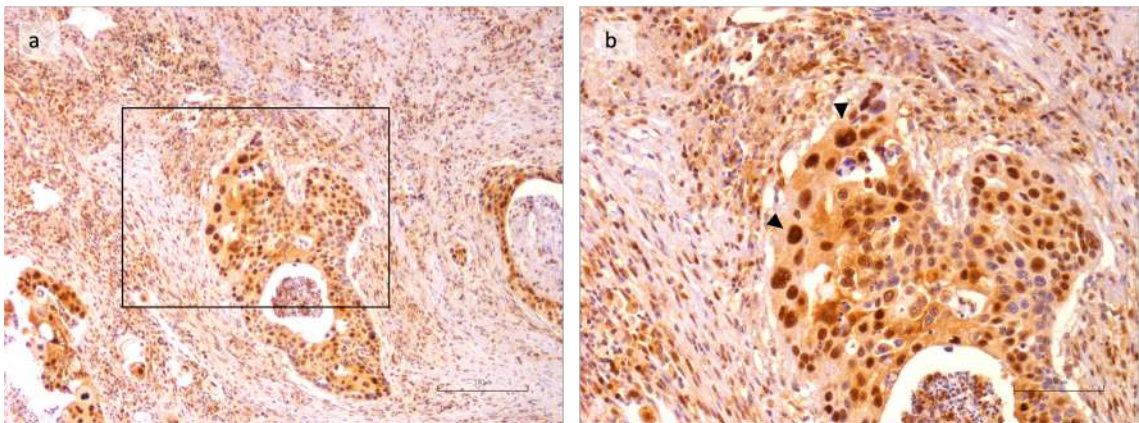


Figure 28: Representative histological sections for p62+ evaluation, nuclear pattern in LUSCC: p62+ immunohistochemistry (IHC) a) 10x, b) 20x of the same section. Notably, p62 staining is concentrated in the nuclei (arrowheads).

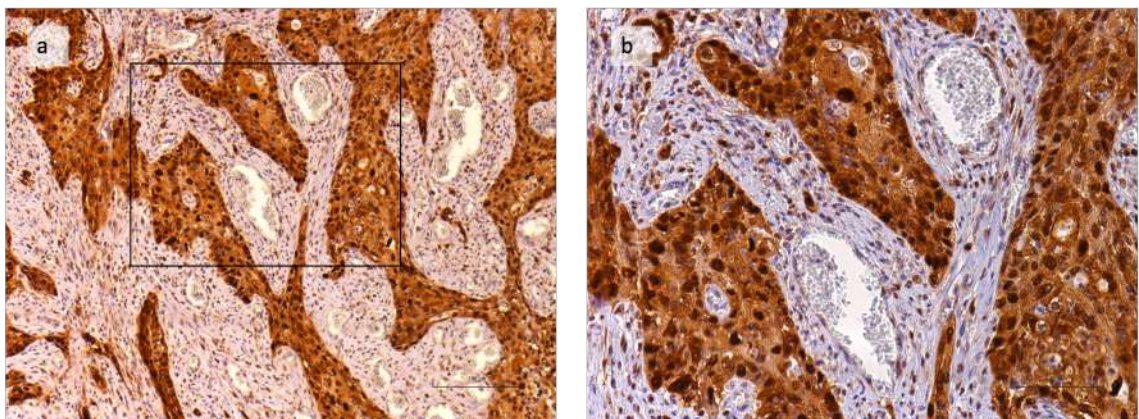


Figure 29: Representative histological sections for p62+ evaluation, nucleo-cytosolic pattern in LUSCC: p62+ immunohistochemistry (IHC) a) 10x, b) 20x of the same section. Notably, p62 staining is present in both the nuclei and cytoplasm, and this pattern is consistent at the tumor invasive margin and the core.

In the tumor core, our analysis revealed intriguing insights into how p62 expression patterns vary with different tumor grades. For well-differentiated tumors (G1), a considerable proportion of samples showed a nuclear pattern, accounting for 53.8%. This suggests that in the early stages of tumor development, p62 may have a tendency to accumulate within the cell nucleus. Conversely, only 7.7% of G1 samples displayed a cytoplasmic pattern, indicating a relatively lower presence of p62 in the cytoplasm. A moderate number of samples (38.5%) exhibited a nucleo-cytoplasmic pattern, highlighting some degree of cellular heterogeneity.

Moving on to moderately differentiated tumors (G2), a shift in p62 patterns became apparent. Here, the cytoplasmic pattern became more prevalent at 29.7%, while the nuclear pattern remained substantial at 32.4%. Interestingly, a notable portion of samples (37.8%) displayed a nucleo-cytoplasmic pattern, indicating that as tumors progress toward moderate differentiation, p62 might be distributed across both the nucleus and cytoplasm.

In less-differentiated tumors (G3), the most striking change occurred. The cytoplasmic pattern dominated, with 66.7% of samples exhibiting this pattern. The nuclear and nucleo-cytoplasmic patterns decreased considerably to 11.1% and 22.2%, respectively. This suggests that as tumors become less differentiated, p62 appears to accumulate primarily in the cytoplasm, possibly indicating a shift in its cellular functions.

When we examined the tumor invasive margin, a similar trend emerged, but with some noteworthy variations. In well-differentiated tumors (G1), we observed 15.4% of samples with a cytoplasmic pattern and 38.5% with a nuclear pattern, somewhat mirroring the pattern observed in the tumor core. However, the nucleo-cytoplasmic pattern was more prominent at the invasive margin, accounting for 46.2% of samples.

For moderately differentiated tumors (G2), the distribution shifted. The cytoplasmic pattern decreased to 8.1%, while the nuclear pattern was observed in 16.2% of samples.

Remarkably, the nucleo-cytoplasmic pattern became the most prevalent at the margin, with 75.7% of samples displaying this pattern.

Although statistical significance is not reached ($p = 0.054$ for DFS and $p = 0.062$ for OS), this trend, while suggestive, may reveal a higher prognostic value when assessed on a larger sample size.

As p53 has been identified to modulate autophagic expression in cancer, our study aimed to explore the potential correlation between p53 expression and p62 expression, measured as a percentage in tumor cells. However, no significant correlation was observed within our combined sample of Oral SCC and Lung SCC. These findings should be interpreted considering the limited sample size in our study and its retrospective nature.

Similarly, no correlation was identified between the autophagic marker p62 and key determinants of the tumor immune microenvironment, such as PDL1 expression, TILs, and CD8⁺ lymphocytes. It is important to note that while these results suggest an absence of correlation, the potential for such associations cannot be entirely ruled out, considering the limitations imposed by our sample size.

In less-differentiated tumors (G3) at the invasive margin, the cytoplasmic pattern increased substantially to 50%, while the nuclear pattern reduced to 5.6%. The nucleo-cytoplasmic pattern remained substantial at 44.4%. These findings suggest that, particularly at the tumor invasive margin, p62 may play a role in less-differentiated tumors by accumulating predominantly in the cytoplasm, which could be indicative of altered cellular processes and tumor aggressiveness (Fig.30).

Overall, these observations highlight the dynamic relationship between p62 expression patterns and tumor grade, with notable differences between the tumor core and invasive margin. These variations could potentially offer insights into the underlying molecular mechanisms driving tumor progression and may have implications for therapeutic strategies targeting p62 in different stages of cancer development. Further research is warranted to fully understand the functional significance of these patterns in cancer biology (Fig.31).

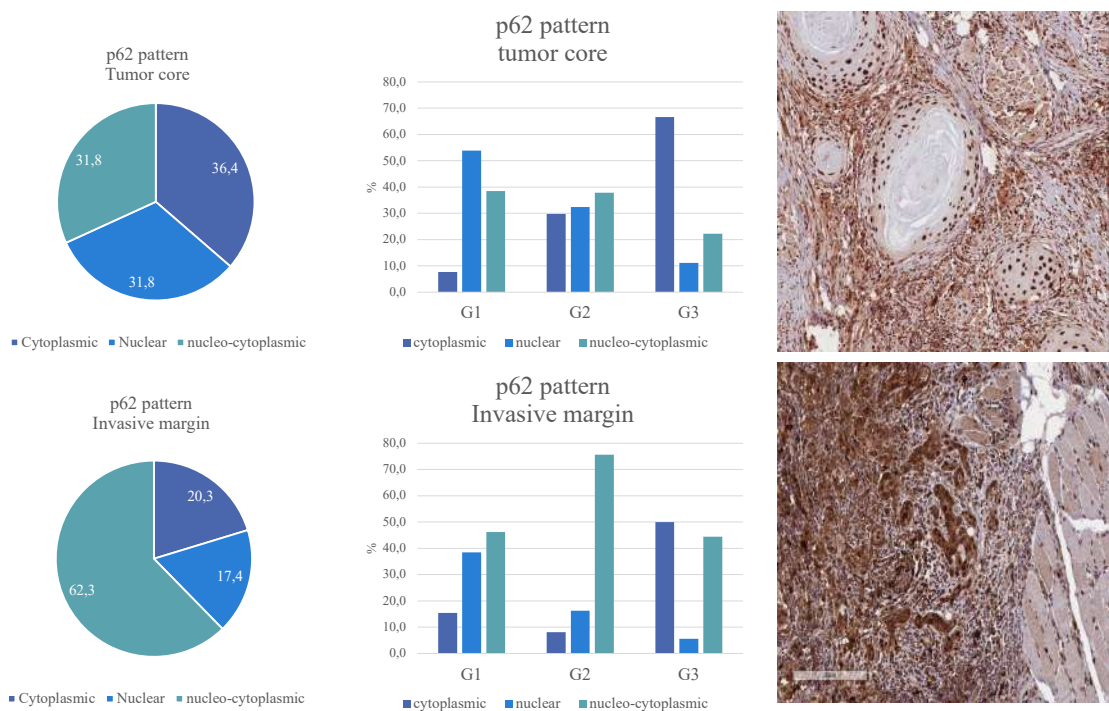


Figure 30: On the left, pie charts depict the distribution of the three patterns (cytoplasmic, nuclear, and nucleo-cytoplasmic) in the tumor core and at the invasive tumor margin. In the middle, the same three patterns are presented based on the tumor cell differentiation grade, both in the tumoral core and at the tumor invasive margin. On the right, two representative histological sections illustrate p62+ evaluation in OSCC. The image above displays the nuclear pattern in a well-differentiated tumor area, while the image below shows a combined nuclear and cytoplasmic pattern in a less differentiated tumor area at the invasive front of the tumor.

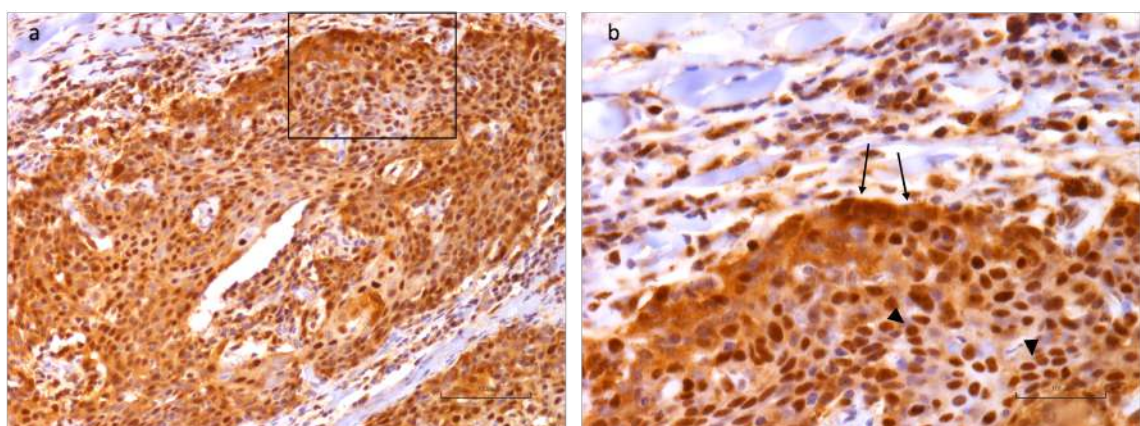


Figure 31: Representative histological sections for p62+ evaluation in the tumor core and at the invasive margin, in LUSCC: p62+ immunohistochemistry (IHC) a) 20x, b) 40x of the same section. Arrows highlight the tumor infiltrative margin where a nucleo-cytoplasmic pattern is identified. Of note, in the tumor core, a prevalent nuclear pattern is depicted (arrowheads).

Interestingly, in patients affected by OSCC, the expression of p62 exhibits a noteworthy trend. This expression, considered as a cumulative variable that takes into account both high percentages of p62 positivity (> 80%) and the cytoplasmic or nucleo-cytoplasmic pattern of expression, demonstrates an inclination towards a worse prognosis in both OS and DFS when compared to lower levels of p62 positivity or nuclear expression (Fig.32).

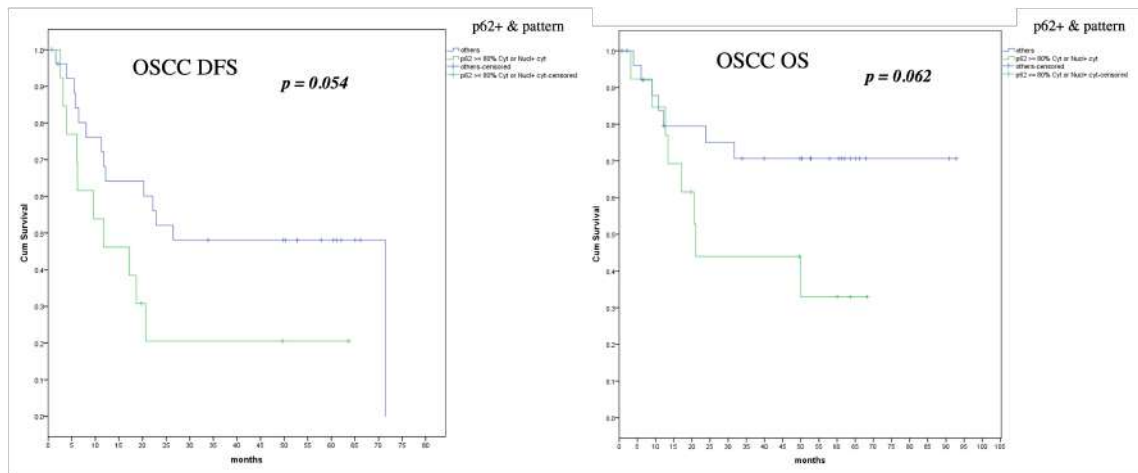


Figure 32: Kaplan-Meier curves illustrating DFS (left) and OS (right) in the OSCC population. The curves represent the subgroups of patients categorized based on p62 levels >80% and cytoplasmic or nucleo-cytoplasmic staining at IHC.

Role of tumor microenvironment in Lung SCC and Oral SCC

We then focused our attention on the Tumor immune microenvironment.

The spearman correlation results reveal a statistically significant correlation ($r=0.441$, $p=0.013$) between Tumor-Infiltrating Lymphocytes (TILs) and CD8 expression. This suggests a positive relationship between the presence of TILs and the expression of CD8. Being CD8 part of the TILs this is in line with what we have expected, but help interpreting the following results.

Tumor-Infiltrating Lymphocytes as Potential Prognostic Indicators

Importantly we noted that the presence of Tumor-Infiltrating Lymphocytes (TILs) emerges as a significant predictor for OS, considering the two populations combined (Fig. 33). In particular in the combined population of OSCC and LUSCC, the prognostic role

of TILs in OS is highlighted ($p= 0.013$). For individuals with TILs constituting less than or equal to 15% of the tumor stroma, the median OS stands at 43.1 months, with a confidence interval spanning from 32.7 to 53.5 months. Contrastingly, patients with TILs exceeding 15% experience a substantially prolonged median OS of 80.4 months, with a confidence interval ranging from 70.4 to 90.5 months. This indicates a more precise estimate of potential OS durations within the specified confidence level.

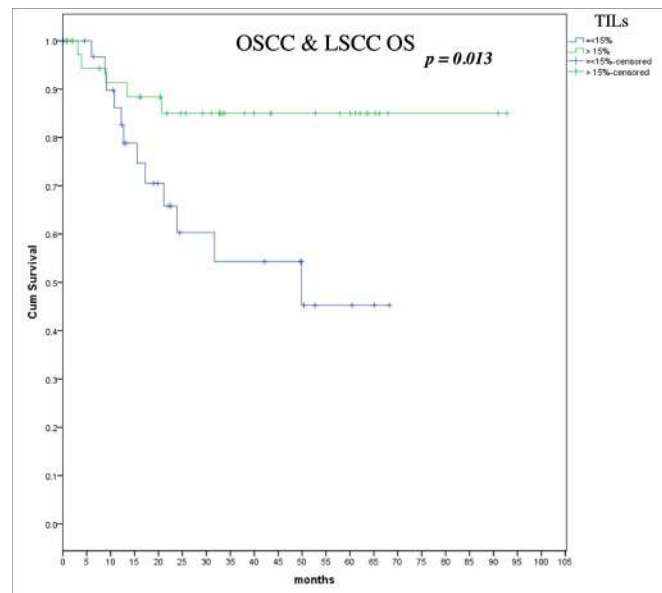
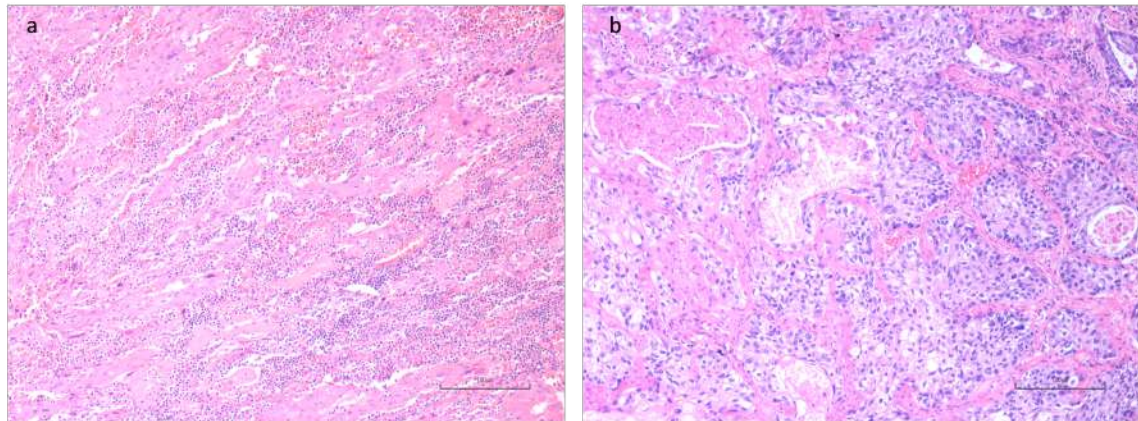


Figure 33: Top: Representative histological sections for TILs evaluation in LUSCC: a) High presence of TILs (60%) compared to b) Low presence of TILs (5%), Hematoxylin and eosin staining, 10x. Bottom: Kaplan-Meier curves illustrating Overall Survival (OS) in the combined Oral Squamous Cell Carcinoma (OSCC) and Lung Squamous Cell Carcinoma (LUSCC) cohort. The curves represent the subgroups of patients categorized based on Tumor-Infiltrating Lymphocytes (TILs) levels within the tumor stroma, specifically TILs <15% and TILs >15%.

These results collectively suggest a significant association between higher TILs levels and prolonged OS in the combined population of OSCC and Lung SCC. However, this trend was still significant only in the OSCC subgroup. In fact, patients with TILs < 15% of the tumor stroma exhibit a median OS of 37.0 months [26.3 - 47.7]. In contrast, individuals with TILs > 15% experience a markedly extended median OS of 80.9 months [65.5 to 96.3]. The observed p-value of 0.010 indicates a statistically significant difference in OS between the two groups. This underscores the prognostic relevance of TILs in OSCC, with higher TILs levels associated with a significantly prolonged OS compared to lower TILs levels. In our analysis of Lung SCC patients, counting Tumor-Infiltrating Lymphocytes (TILs) in H&E staining did not reveal any prognostic value for either DFS or Overall Survival OS. The presence or quantity of TILs in this specific context did not exhibit a statistically significant correlation with the observed outcomes, suggesting that, in this population, TILs in H&E staining may not serve as a reliable prognostic indicator for the evaluated survival metrics.

The observed trend in the prognostic role of TILs in Overall Survival OS was not replicated when assessing DFS. This lack of consistency was evident in both the OSCC population, the Lung SCC population, and the combined cohort.

In terms of DFS, TILs failed to demonstrate a significant association with survival outcomes in these populations. This discrepancy highlights the nuanced nature of immune responses and their impact on different aspects of cancer progression.

These results emphasize the heterogeneity of tumor microenvironments and the complex interplay between the immune response and cancer progression, underscoring the need for a nuanced understanding of the specific tumor type and its unique characteristics in the quest for reliable prognostic markers.

CD8+ cells

We further evaluate CD8+ lymphocytes at the *leading edge of tumor invasion*, categorizing them into four grades based on the number of positive cells observed on average across five High Power Fields (HPF), as showed in Fig. 34

- Grade 1: Less than 10 positive cells per HPF.
- Grade 2: 10 to 30 positive cells per HPF.

- Grade 3: 31 to 100 positive cells per HPF.
- Grade 4: More than 101 positive cells per HPF.

This grading system provides a quantitative assessment of the CD8+ lymphocyte *infiltration at the tumor front*, allowing for a nuanced characterization of the immune response in the microenvironment. Each grade represents a distinct level of CD8+ lymphocyte presence, offering a valuable tool for evaluating the immune landscape and its potential implications for the tumor's interaction with the host immune system.

Notably, in Lung Squamous Cell Carcinoma (SCC), the presence of CD8 positivity in the tumor immunomicroenvironment emerges as a significant prognostic factor for DFS.

The median DFS for patients with low CD8+ expression (grade 1-2, less than 30 cells/HPF) is notably shorter, measuring at 2.8 months. This is accompanied by a relatively narrow confidence interval, ranging from 0.2 to 5.3 months, indicating a more precise estimate. In contrast, for individuals with CD8+ expression exceeding this cutoff (grade 3-4, >30 cells/HPF), the median DFS significantly extends to 40.6 months. The corresponding confidence interval, spanning from 36.7 to 44.5 months, suggests a relatively tight range, reinforcing the robustness of the estimate. The observed p-value, being < 0.001, indicates a highly statistically significant difference in DFS between the two groups. This underscores the prognostic relevance of CD8 positivity in Lung SCC, with higher CD8 expression levels associated with a significantly prolonged DFS compared to lower expression levels. These findings provide valuable insights for risk stratification and may have implications for treatment planning in Lung Squamous Cell Carcinoma patients (Fig.35).

It's noteworthy that the same trend observed in Lung SCC, where CD8 positivity served as a prognostic factor for DFS, was not replicated in the population with OSCC. The absence of a similar trend in the OSCC group may suggest either that the prognostic significance of CD8 positivity may vary across different types of squamous cell carcinomas or the possible limited sample in our OSCC study. This highlights the importance of considering tumor-specific factors and characteristics that contribute to the heterogeneous nature of cancer and underscores the need for distinct prognostic markers in different cancer types.

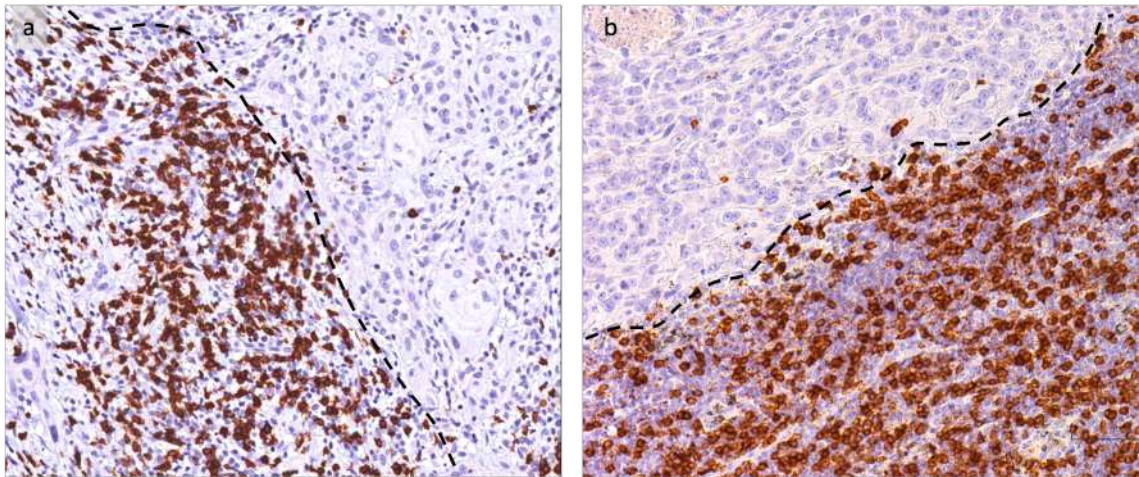


Figure 34: Representative histological sections for CD8+ lymphocytes evaluation at the invasive tumoral margin (dotted line) in OSCC (a) and LUSCC (b), CD8+ immunohistochemistry (IHC), 20x

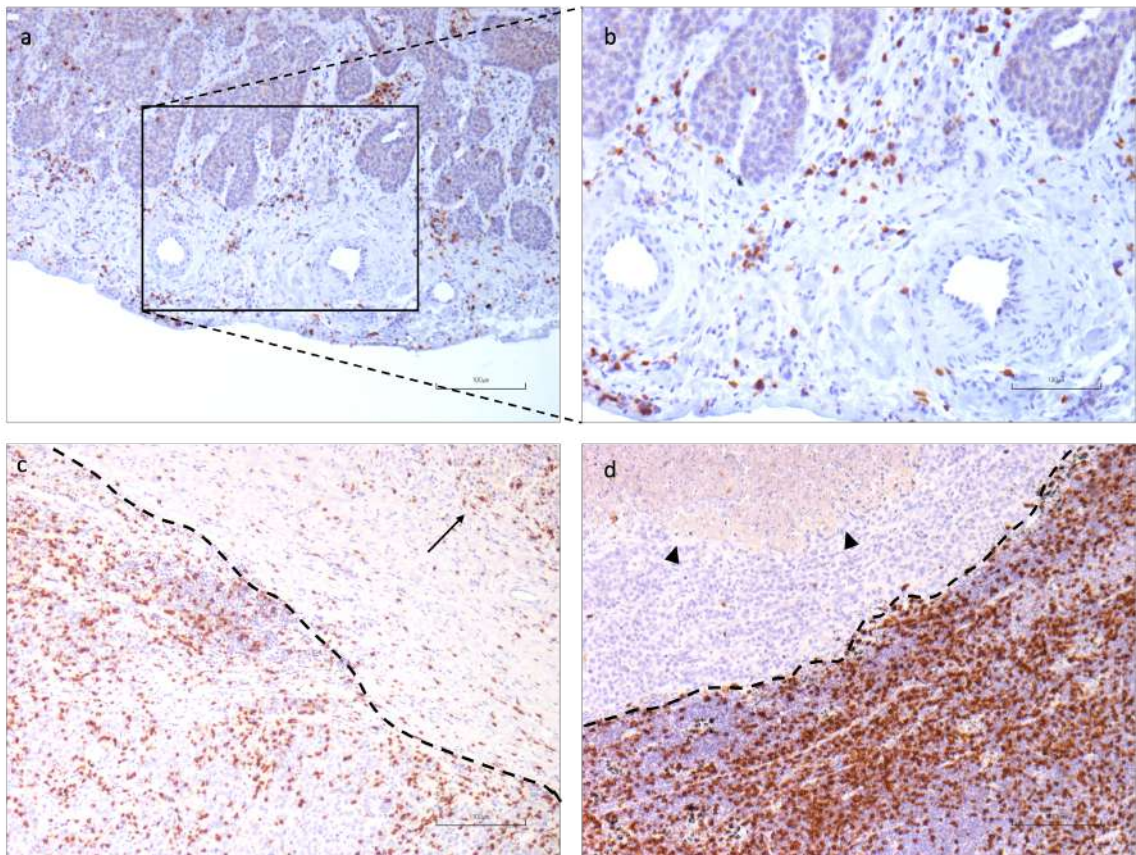


Figure 35: Representative histological sections for CD8+ lymphocytes evaluation at the invasive tumoral margin in LUSCC: CD8+ immunohistochemistry (IHC) a) Grade 2 CD8 positivity, 10x; b) same section, 20x, very few CD8+ lymphocytes at the tumor margin; c) Grade 3 CD8 positivity at the invasive tumor margin (dotted line); arrow highlights nests of lung squamous cell

carcinoma. Notably, mononuclear cells at the invasive tumoral margin consist mostly of CD8+ lymphocytes; b) Grade 4 CD8+ cells at the tumor margin (dotted line), with an area of necrosis in the left superior corner (arrowheads).

A particular observation was made upon the positivity of CD8+ expressed in the setting of TILs. This last parameter was not evaluated as a single variable, since we focus our attention at the tumor infiltrating margin for evaluation of CD8+ lymphocytes. However, some descriptive observation highlights the great variance of CD8 positivity in the context of TILs, meaning that the other different subpopulations may influence the TIME. As a representative example we show in Fig. 36 the relatively low positivity of CD8 in the contest of TILs in a LUSCC sample.

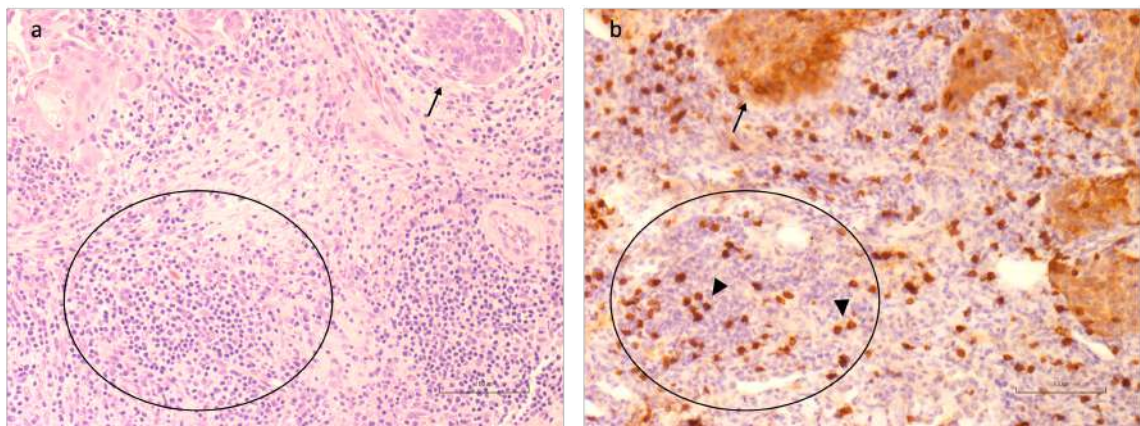


Figure 36: Representative histological sections for CD8+ lymphocytes evaluation at the invasive tumoral margin in LUSCC: a) Hematoxylin and eosin staining, 20x, b) CD8+ immunohistochemistry (IHC), 20x. Arrows highlight nests of lung squamous cell carcinoma, while circles indicate one of the regions of the infiltrative tumoral margin rich in lymphocytes. Notably, consecutive sections of the same sample stained with CD8 Ab reveal that these mononucleate cells are only in part CD8+ lymphocytes (arrowhead).

Prognostic assessment of tumor burden and host response

We proceeded from univariate analysis to multivariate analysis, including only the variables that demonstrated significance as predictors of oncological outcomes. Table 4 presents a summary of the univariate analysis for OS and DFS in OSCC patients.

Variable	OS			DFS		
	HR	95% C.I.	P value	HR	95% C.I.	P value

Age: ≤67years	0.559	0.312-1.002	0.051	0.732	0.450-1.192	0.210
> 67 ref	1			1		
NLR: ≤ 2.44	0.461	0.257-0.826	0.009 *	0.495	0.302-0.813	0.005 *
> 2.44				1		
Sex: male	0.721	0.407-1.276	0.261	0.835	0.514-1.356	0.465
Female	1			1		
Smoking: no	0.575	0.326-1.016	0.057	0.742	0.454-1.213	0.742
Yes	1			1		
Alcohol consumption: yes	1.149	0.622-2.125	0.657	1.487	0.860-2.572	0.156
No	1			1		
Ecog-ps: 0	0.315	0.170-0.581	≤0.001 **	0.445	0.265-0.749	0.002 *
Others	1			1		
Site of disease: others	1.507	0.834-2.725	0.175	1.784	1.071-2.971	0.026
Floor of mouth or tongue	1			1		
Treatment: TLE	0.557	0.305-1.019	0.058	0.519	0.311-0.867	0.012
Compartmental surgery	1			1		
Adjuvant: no	0.326	0.179-0.595	≤0.001 **	0.437	0.265-0.723	0.001 **
Yes	1			1		
Stage I and II	0.367	0.201-0.671	0.001 **	0.473	0.286-0.784	0.003 *
III and IV	1			1		
Grading: 1	0.578	0.313-1.066	0.079	0.662	0.392-1.117	0.112
2 and 3	1			1		
ECS: no	0.455	0.239-0.866	0.017 *	0.551	0.316-0.962	0.036 *
Yes	1			1		
Doi: ≤ 10 mm	0.265	0.095-0.741	0.011 *	0.471	0.208-1.065	0.070
> 10 mm	1			1		
WPOI: 1 and 2	1.627	0.588-4.497	0.348	1.143	0.488-2.675	0.758
3 and 4	1			1		
P53: ≤10%	0.405	0.128-1.276	0.123	0.380	0.155-0.933	0.035 *
> 10%	1			1		
TILs: ≤15%	5.758	1.296-25.588	0.021 *	1.890	0.788-4.589	0.160
> 15%	1			1		
P62: others	0.389	0.140-1.083	0.071	0.447	0.193-1.035	0.060
≥80% cyto/n+cyto pattern	1			1		

Table 4: Summary of Univariate Analysis for Overall Survival (OS) and Disease-Free Survival (DFS) in Oral Squamous Cell Carcinoma (OSCC) Patients, showcasing variables demonstrating significance as predictors of oncological outcomes.

Variable	OS			DFS		
	HR	95% C.I.	P value	HR	95% C.I.	P value
Age: ≤67	1.424	0.424-4.311	0.532	1.110	0.490-2.514	0.802
> 67 ref	1			1		
NLR: ≤ 2.44	0.986	0.313-3.100	0.980	1.079	0.455-2.563	0.863
> 2.44				1		
Sex: male	0.375	0.129-1.094	0.073	0.582	0.265-1.283	0.180
Female	1			1		
Stage I and II	0.182	0.057-0.582	0.004 *	0.329	0.144-0.755	0.009
III and IV	1			1		
CD8 1&2	0.926	0.221-3.875	0.916	2.309	0.696-7.656	0.171
CD8 3&4	1			1		
P53: ≤10%	0.409	0.114-1.474	0.172	0.377	0.146-0.975	0.044
> 10%	1			1		
TILs: ≤15%	2.487	0.691-8.943	0.163	1.216	0.468-3.158	0.688
> 15%	1			1		
P62: others	0.833	0.272-2.543	0.743	1.068	0.465-2.451	0.877
≥80% cyto/n+cyto pattern	1			1		

Table 5: Summary of Multivariate Analysis for Overall Survival (OS) and Disease-Free Survival (DFS) in the Combined Cohort of Oral Squamous Cell Carcinoma (OSCC) and Lung Squamous Cell Carcinoma (LUSCC) Patients, including only variables with potential significance as predictors of oncological outcomes.

The multivariate analysis conducted in this study aimed to assess the impact of the different variables on OS and DFS outcomes. Each variable's hazard ratio (HR), 95% confidence interval (C.I.), and p-value were calculated to determine its significance in predicting these outcomes.

Age was one of the variables analyzed, with a cutoff at 67 years. Patients aged over 67 years had a higher HR for both OS and DFS compared to those aged 67 or younger, though the difference was not statistically significant. This suggests that age may not be a strong predictor of survival outcomes in this context.

NLR (Neutrophil-to-Lymphocyte Ratio) was assessed with a cutoff at 2.44. There was no significant difference in HR for patients with NLR above 2.44 compared to those with NLR below 2.44, indicating that NLR may not be a significant predictor of OS or DFS in this study.

Sex was another variable examined, with male patients serving as the reference group. Female patients had a lower HR for both OS and DFS, though the difference was only marginally significant (p-value close to the significance threshold of 0.05). This suggests that gender may play a role in predicting survival outcomes, with females having a potentially better prognosis.

Tumor stage was assessed with a dichotomy between stages I and II versus stages III and IV. Patients with stages III and IV had a significantly higher HR for both OS and DFS, indicating that advanced tumor stages are associated with worse survival outcomes.

CD8 (Cluster of Differentiation 8) was categorized into CD8 1&2 and CD8 3&4 groups, respectively <30 cells/HPF and >30 at the tumor infiltrating margin. There was no significant difference in HR between these two groups for OS. However, for DFS, patients in the CD8 3&4 group had a substantially higher HR, though the difference did not reach statistical significance, suggesting that CD8 levels may have some impact on DFS.

P53 expression levels were dichotomized into $\leq 10\%$ and $>10\%$. Patients with P53 expression $>10\%$ had a significantly higher HR for OS, indicating that higher P53 expression is associated with worse OS outcomes. Similarly, for DFS, patients with P53 expression $>10\%$ had a significantly higher HR, indicating a negative impact on DFS.

TILs (Tumor-Infiltrating Lymphocytes) were categorized into $\leq 15\%$ and $>15\%$ groups. Patients with TILs $>15\%$ had a higher HR for OS, though the difference was not statistically significant. Similarly, for DFS, there was no significant difference in HR between the two groups, suggesting that TILs may not be a strong predictor of survival outcomes in this study.

P62 expression patterns were classified as $>80\%$ positivity with a cytoplasmic/nucleo-cytoplasmic pattern Vs all the other percentages and patterns. There was no significant difference in HR for OS between these two groups. However, for DFS, patients with $>80\%$ positivity with a cytoplasmic/nucleo-cytoplasmic pattern had a higher HR, although the difference was not statistically significant. This implies that P62 expression patterns may not strongly predict OS or DFS in this context.

In summary, this multivariate analysis provides insights into the potential predictors of OS and DFS in the studied population. While some variables, such as tumor stage and P53 expression, demonstrated significant associations with survival outcomes, others did not reach statistical significance, highlighting the complexity of predicting cancer survival based on these factors.

DISCUSSION

Unraveling the Enigmatic World of p62 Patterns: Insights from Tumor Microenvironments

The role of autophagy in cancer biology remains a complex and incompletely understood phenomenon. Despite significant research efforts in both preclinical and clinical settings over the past decades, a comprehensive understanding of its intricacies remains elusive.

Autophagy, a cellular process often described as a double-edged sword,¹²⁹ plays a critical role in normal cells' homeostasis and response to physiological stress and in guiding apoptotic events when stress levels become excessive. Notably, autophagy has been shown to exert a profound influence on tumor cells too, demonstrating both early anti-tumoral activity and late pro-tumoral effects. Malignant cells can employ this versatile mechanism primarily to cope with proteotoxic and oxidative stresses, ultimately influencing various cellular pathways.

Furthermore, autophagy is emerging as a prominent player in the realm of the immune system, where it regulates the host's anti-tumor response. Its role is highly context-dependent and time-dependent, adding to the complexity of its involvement in cancer.

In our study, we aimed to investigate whether autophagic activity within tumor cells could alter the tumor immune microenvironment. Surprisingly, we did not find significant correlations with TILs and CD8 populations. However, our research shed light on a novel aspect of the autophagic pathway. In addition to identifying a higher percentage of p62 positivity in tumor cells compared to adjacent dysplastic epithelium in OSCC, we also uncovered different patterns of accumulation, including cytoplasmic, nuclear, and nucleocytoplasmic.

To the best of our knowledge, our study is the first to describe these distinct patterns in OSCC and LUSCC. Existing knowledge indicates that p62 is widely distributed within the cell, with its nucleocytoplasmic shuttling being mediated by signals still not completely understood. Noguchi et al in 2018 established that the redox-sensing function of p62 is essential for the nuclear accumulation of p62-based Aggresome-like induced

structures (ALIS), consequently leading to the initiation of parthanatos, a non-apoptotic programmed cell death.

In fact, as demonstrated by Pankiv et al., p62 possesses two nuclear localization signals (NLS1 and NLS2) and one nuclear export signal (NES). Thanks to these domains, it exhibits a swift shuttling between the cytosol and the nucleus.¹¹⁸ Although it is well-recognized for its cytosolic functions, p62 occasionally forms nuclear bodies, a phenomenon that researchers have increasingly observed in recent years. Nonetheless, the significance of nuclear p62 remains enigmatic, particularly considering that autophagy primarily occurs in the cytoplasm. This dynamic behavior adds another layer of complexity to our observations.

Interestingly, we identified a specific trend related to overall survival (OS) and disease-free survival (DFS) in patients expressing p62⁺ at levels exceeding 80%, particularly when the pattern was cytoplasmic or nucleocytoplasmic. Nevertheless, a comprehensive biological understanding is essential to interpret these findings, and further analyses are imperative.

In line with our findings, previous studies have highlighted the importance of p62's subcellular localization in cancer. For instance, Shi's work in 2018 demonstrated a shift from nuclear to cytoplasmic p62 expression in esophageal squamous cell carcinoma (ESCC), suggesting that nucleocytoplasmic translocation of p62 might be an early event in ESCC development.¹⁵² Subsequent research from the same group in 2024 revealed that cytoplasmic p62 enhanced ESCC cell migration, invasion, tumor metastasis, and tumor growth compared to nuclear localization.

In their research, Fu and colleagues have illuminated a new distinct role of p62 within the cellular context. Along with its role in the cytosol, where it participates in the autophagic machinery, p62 may be crucial in the nucleus, where it takes on a role in proteasomal degradation. Their groundbreaking findings, published in 2021, revealed that nuclear p62 undergoes a unique process mediated by LLPS (Liquid-Liquid Phase Separation), resulting in the formation of condensates. These condensates function as active proteolytic centers by effectively capturing the 26S proteasome, ubiquitinated substrates, and the associated conjugation machinery. Within these nuclear proteolytic p62 foci, they demonstrated a notable enhancement in the degradation of nuclear proteins, such as c-

Myc. Interestingly, it is conceivable that different signals and adaptors, including various ubiquitin chains, may orchestrate these distinct cellular processes. Notably, many transcriptional regulators, which are tightly regulated and have relatively short lifespans, primarily reside within the nucleus. Therefore, it is suggested by this group of researchers that it is plausible that the specialized p62 foci that employ the highly specific ubiquitin system have predominantly evolved to function in this cellular compartment. In contrast, autophagy, which primarily responds to stress and is characterized by a less specific targeting mechanism, has evolved to operate predominantly in the cytosol.

In summary, our study adds new dimensions to the intricate interplay between autophagy, p62, and cancer biology, shedding light on previously unexplored patterns of p62 expression and their potential implications for patient outcomes. Further investigations are crucial to fully unravel the underlying biological mechanisms and clinical relevance of these findings.

Future Perspectives and Therapeutic Potential

Understanding the multifaceted role of p62 within tumor cells holds significant promise. It may not only serve as a source of prognostic markers, given its varying expressions observed in the tumor invasive margin and dedifferentiated tumors (G3), but it could also unveil potential therapeutic targets within the autophagic pathway for cancer treatment. This deeper comprehension of p62's functions within cancer cells may pave the way for more tailored and effective therapeutic strategies.

Looking ahead, we contemplate the potential clinical implications of modulating autophagy in the context of Head and Neck cancer and Non-Small Cell Lung Cancer (NSCLC). One intriguing avenue involves the use of Hydroxychloroquine (HCQ), an autophagic inhibitor with promising attributes. HCQ has demonstrated its effectiveness not only through direct actions on tumor cells but also by modulating the antitumoral immune response. Furthermore, HCQ has exhibited a favorable safety profile in clinical contexts.

Significantly, HCQ has exhibited antitumor activity in preclinical studies across various cancer types, impacting crucial mechanisms such as tumor cell cycle regulation,

apoptosis, proliferation, and autophagy. Additionally, HCQ has shown promise in overcoming chemoresistance, enhancing radiosensitivity, and targeting cancer stem cells. This versatile potential of HCQ makes it a compelling candidate for adjuvant therapy in conjunction with standard treatments like chemotherapy and radiotherapy.

Through a comprehensive systematic review of the literature, we found 87 clinical trials related to the use of Hydroxychloroquine in cancer treatment. Among these trials, seven studies have highlighted its potential role in NSCLC, and three have investigated its neoadjuvant administration in various solid tumors. Based on the evidence from phase I-II studies, we are launching a prospective interventional pharmacological phase II clinical trial involving the preoperative use of Hydroxychloroquine in patients with Laryngeal and Oral Squamous Cell Carcinoma (SCC) and NSCLC. This trial aims to elucidate the molecular and biological changes induced by HCQ within the autophagic machinery of Head and Neck cancer and NSCLC, as well as to assess the tumor microenvironment's response to autophagic inhibition mediated by HCQ.

Deciphering the Host Immune system in oncological patients: A Prognostic Paradigm

One of the main interests in dissecting cancer biology is finding prognostic variables which help clinician to select a more aggressive treatment in high-risk patients.

Numerous efforts to enhance cancer categorization have been suggested, encompassing the integration of parameters derived from immunohistochemistry for tumor biomarkers, flow cytometry for subcellular populations, molecular signatures, deep proteomics, or genetic features. These approaches mainly emphasize tumor-cell characteristics and rely on 'omics' and bulk strategies, which may obscure intratumor heterogeneity and disregard the influences of the tumor microenvironment (TME) and immune elements.¹⁵³

In the contest of HN cancers, numerous studies have suggested various clinical assessments for biomarkers.¹⁵⁴ Regarding pathological H&E or IHC biomarkers, the only one that has been incorporated into the TNM classification is p16 IHC. This marker is considered indicative of HPV infection when carefully examined in the appropriate anatomical subsite and in accordance with the recognized characteristic HPV-typical

morphology of tumor cells. The well-demonstrated favorable prognostic impact of HPV positivity has translated into tailored, less aggressive treatment approaches for OPSCC displaying HPV positivity.⁶

Of note our study has investigated the role of possible promising histopathological and blood biomarkers. In addition to our investigation into the autophagic pathway, in fact, our study has reaffirmed the prognostic significance of the immune tumor macroenvironment. Specifically, we have validated the importance of parameters such as Neutrophil-to-Lymphocyte Ratio (NLR), Monocyte-to-Lymphocyte Ratio (MLR), and Platelet-to-Lymphocyte Ratio (PLR) in predicting patient outcomes. These markers hold great promise due to their simplicity in data collection, derived from routine blood samples, and their cost-effectiveness.

Furthermore, our research has validated the prognostic significance of both Tumor-Infiltrating Lymphocytes (TILs) and CD8⁺ lymphocytes, underlining the importance of characterizing the immune population within the tumor microenvironment (TME). While flow cytometry is a widely employed method for profiling immune cells, offering various advantages such as the characterization of immune cell subsets through multiple markers, quantitative data acquisition, broad accessibility, and the capability to analyze specific subpopulations of interest, it does come with limitations. Notably, the technique can be relatively expensive, necessitates fresh tissue samples, and lacks details regarding the spatial distribution or organization of the immune infiltrate, as well as its relationship to other microenvironmental structures.

In this context, immunohistochemistry (IHC) emerges as a cost-effective alternative, feasible with formalin-fixed specimens, and reproducible through standard antibody acquisition and result interpretation methods, all within a spatial configuration. Importantly, IHC enables the analysis of tumor-infiltrating lymphocyte (TIL) subpopulations, which has shown significant promise as a prognostic biomarker. Furthermore, TIL analysis can be simplified using a plain H&E-stained section, which is both affordable and accessible, without the need for further characterization of lymphocytic subpopulations. Despite this potential, the integration of TIL analysis into routine clinical practice has not been realized thus far. Indeed, despite encouraging outcomes, challenges may hinder the integration of TNM-Immune (TNM-I) staging into

clinical practice. Distinct methodologies might be necessary for various malignancies, and this diversity may even exist within each cancer type. Nonetheless, a standardized approach across different cancers would be beneficial. Even though over a decade has passed since the proposal of the Immunoscore for various tumor types, its integration into clinical practice remains challenging due to the absence of comprehensive pathological guidelines and the need to establish its clinical prognostic value in tumor boards. This highlights the necessity for a comprehensive understanding of the multifaceted interactions between the immune system and cancer progression across distinct tumor types.

In our sample, there is no clear discrimination between the prognostic roles of TILs or CD8+ lymphocytes. It appears that TILs may serve as a good surrogate for the tumor immune microenvironment (TIME) and an effective prognostic factor for OSCC. However, this outcome was not replicated in the lung subpopulation. In contrast, CD8+ lymphocytes assume a prognostic role in lung SCC. It's essential to note that TILs do not precisely coincide with CD8+ lymphocytes, as illustrated previously in Figure 36.

This underscores the potential for adopting a TNM-immune staging approach, akin to the proposal made by Galon et al. in colorectal cancer, although this concept has not yet gained widespread acceptance in clinical oncology disciplines.

However, it is vital to acknowledge that our study, along with others investigating the pathological assessment of the tumor immune microenvironment, has highlighted the challenge of varied methodologies used to assess TILs or their subpopulations. To ensure meaningful and comparable results, the adoption of a standardized methodology is imperative for clinical implementation. While TILs hold promise due to their straightforward assessment within H&E staining, CD8+ lymphocytes provide a more precise evaluation of their antitumoral cytotoxic activity. Although this precision was not explicitly demonstrated in our sample, it underscores the potential significance of CD8+ lymphocytes in predicting clinical outcomes.

A more comprehensive understanding of the tumor immune microenvironment holds the promise of advancing therapeutic strategies, particularly with the recent incorporation of immunotherapy. It is noteworthy that immunotherapies have predominantly been tested and administered in clinical trials to patients with advanced-stage cancers. This

concentration on advanced disease has created gaps in our comprehension of how immunotherapies may perform in less advanced cases. To move towards universally effective immunotherapeutic approaches, gaining a deeper understanding of the intricate immunological interactions occurring between tumors and their host organisms throughout the entire body is imperative. This broader knowledge will not only aid in optimizing treatment outcomes for advanced-stage cancer patients but also shed light on the potential benefits and limitations of immunotherapy in earlier stages of the disease. It is through this comprehensive understanding that we can pave the way for more effective and personalized cancer treatments.

Study limitations

While our study has provided valuable insights into the clinical aspects of p62 expression and its implications in tumor microenvironments, it is essential to acknowledge its limitations.

Firstly, our study primarily focused on clinical data and did not encompass the translational preclinical aspects, which could have provided a more comprehensive understanding of the underlying mechanisms. Secondly, the retrospective nature of our study poses inherent limitations, including potential bias and the reliance on available historical data. Moreover, the number of samples analyzed, although substantial, may not have reached statistical significance for certain parameters, which calls for cautious interpretation of some findings. Despite these limitations, our study offers a significant foundation for future research in this domain and underscores the need for larger-scale prospective investigations to validate and expand upon our findings.

Conclusion

In summary, our research not only delves into the complex biology of p62 and its prognostic and therapeutic implications in cancer but also reaffirms the prognostic role of immune tumor macroenvironment markers and advocates for the standardization of methodologies to assess TILs and their subpopulations, ultimately advancing our understanding and clinical management of cancer.

To think big, we need to transcend the boundaries of our current clinical practice, moving beyond guidelines that often compartmentalize various components. Shifting from a concept of tumor cell-autonomous processes to one of systemic host-tumor relationships in malignant diseases requires a broader perspective.

Thinking big also involves surpassing our current analytical capabilities. Integrating various data elements, including pathological tumor data, tumor immune microenvironment information, systemic immune system responses, and genetic mutational data specific to tumor subtypes that can guide subtype-specific biological therapies, can be complex. To handle this vast amount of data, machine learning and AI studies become essential. However, to train neural networks and make them efficient, a substantial number of cases and patients are required, emphasizing the need for multicenter studies.

The advent of liquid biopsy has brought about a revolution in cancer patient management. Liquid biopsy-based testing is particularly advantageous for identifying actionable cancer markers, especially in cases where solid tissue biopsies are inadequate or unattainable. Beyond its predictive role, liquid biopsy proves useful for comprehensive tumor genotyping, detecting emergent resistance mechanisms, monitoring minimal residual disease, early detection, and cancer interception. The application of next-generation sequencing to liquid biopsy represents a "quantum leap" in predictive molecular pathology.^{155,156} In this perspective, a breakthrough in the screening system, tumor diagnostics, follow-up with evidence of disease recurrence, and tailored therapy may be achieved. This could involve a simple blood which can be integrated with systemic immunological data, playing a prognostic role and predicting outcomes. This integration can guide patients toward more or less aggressive treatments or narrower or more extended follow-ups. The impact extends to early diagnosis, treatment, and healthcare expenditure, directing resources where the risk is higher and optimizing healthcare spending.

In fact, the economic impact of a more precise prediction of patient outcomes is multifaceted and holds the potential for substantial benefits across various facets of healthcare: Targeted Interventions, Reduced Unnecessary Tests and Procedures, Healthcare Spending Efficiency, Tailored Therapies, Avoidance of Complications,

Financial Relief for Patients, Societal and Economic Productivity, Reduced Long-term Costs.

In conclusion, a more precise prediction of patient outcomes has the potential to bring about a paradigm shift in our curative capabilities but also in healthcare economics. By focusing on early diagnosis, treatment optimization, targeted resource allocation, and overall spending efficiency, healthcare systems can achieve better patient outcomes while simultaneously promoting financial sustainability. This approach not only benefits individual patients but also contributes to the broader goals of cost-effective and patient-centered healthcare.

MATERIALS AND METHODS

Genomic analysis

Genomic data for Head and Neck Cancers and Lung Cancers were retrieved from the CBioPortal platform, a comprehensive cancer genomics database that integrates diverse genomic datasets.^{149–151}

Our investigation focused on specific genes associated with key cellular pathways relevant to cancer development and progression. The selected gene panels include:

- **P53 Pathway:** TP53, MDM2, MDM4, CDKN2A, CDKN2B, TP53BP1
- **Autophagic pathway:** SQSTM1, MAP1LC3A, ATG5, ATG3, ATG7, ATG12, ATG13, ATG14, ULK1, ULK2, ATG101, ATG10, RB1CC1, AMBRA1, BECN1, ATG4A, ATG4B
- **Immune Dysregulation:** FAS, CTLA4, LRBA, JAK3, JAK1, JAK2, TYK2, STAT1, STAT3, STAT5B, IKZF1, GATA2, CYLD, NFKB1, NFKB2, REL, RELA, RELB

We navigated to the CBioPortal website (<https://www.cbioportal.org/>), selected the specific cancer types (Head and Neck Cancers and NSCLC) for analysis and utilized the portal's advanced query options to input the selected genes for each pathway. Genomic alterations, mutations, and expression data were analyzed along with the retrieved genomic data, including mutation profiles, copy number alterations, and mRNA expression levels for the selected genes.

CBioPortal's visualization tools were utilized to generate interactive plots for visualizing alterations in the selected genes. Data were interpreted to identify patterns and correlations. Survival curves were analyzed in specific subgroups of patients according to their mutational status in the mentioned genes. Significant findings and trends were reported.

Neutrophils to lymphocytes ratio, Platelets to lymphocytes ratio, Monocytes to lymphocytes ratio

Data related to NLR, MLR, and PLR were collected from the electronic health records (EHR) of the participants. The following variables were extracted:

Neutrophil-to-Lymphocyte Ratio (NLR): NLR was calculated by dividing the absolute neutrophil count by the absolute lymphocyte count obtained from complete blood count (CBC) results.

Monocyte-to-Lymphocyte Ratio (MLR): MLR was calculated by dividing the absolute monocyte count by the absolute lymphocyte count obtained from CBC results.

Platelet-to-Lymphocyte Ratio (PLR): PLR was calculated by dividing the absolute platelet count by the absolute lymphocyte count obtained from CBC results

Tumor Infiltrating Lymphocytes

To assess Tumor-Infiltrating Lymphocytes (TILs), we employed the method established by the International Immuno-Oncology Biomarkers Working Group to standardize the evaluation of TILs in routine Hematoxylin and Eosin (H&E)-stained sections.²⁹ In summary, the entire slide was initially scanned at low magnification using a $\times 5$ or $\times 10$ objective lens, followed by a higher magnification with a $\times 20$ objective lens. Stromal TILs were quantified as the percentage of the stromal area occupied by infiltrating lymphocytes. The average number of TILs was evaluated in multiple stromal regions, with scoring limited to mononuclear immune cells while excluding polymorphonuclear leukocytes. Additionally, areas of necrosis and stromal areas not directly adjacent to the tumor were excluded from the analysis.

Immunohistochemistry staining and evaluation of the samples

All the specimens were evaluated by two independent expert pathologists.

Following morphological review of the specimens, a representative section of the neoplasm was selected for each case.

Tissue samples were fixed in buffered formalin and routinely processed to paraffin wax. Five-micrometer-thick sections were routinely stained with hematoxylin and eosin (H&E). Immunohistochemical (IHC) reactions were performed on additional 3- μ m-thick sections using prediluted ready-to-use vials of the antibodies listed in Table 6 with an automated immunostainer (BenchMark Ultra, Ventana Roche Diagnostics) and standardized protocols (Ventana OptiView DAB IHC Detection Kit).

Antibody	Clone	Dilution	Vendor
p62	D5L7G	1:200	Cell Signaling
CD8	SP57	RTU	Ventana
p53	DO7	RTU	Ventana

Table 6: Antibodies used in Immunohistochemistry for p62, CD8 and p53 staining.

Based on previous studies, p53 expression was assessed by defining the percentage of cells with nuclear positivity; the expression of p53 in more than 10% of tumor cells was defined as positive expression.

CD8+ lymphocytes at the front of tumor invasion were assessed defining 4 grades based on the number of cells positive on an average of five High Power Field (HPF), as described by Sakakura et al.¹⁵⁷:

- Grade 1: <10 positive cells/HPF;
- Grade 2: 10-30 cells/HPF;
- Grade 3: 31-100 cells/HPF;
- Grade 4: >101 cells/HPF

p62/SQSTM1 Immunohistochemistry

Staining for p62 was evaluated separately in the reactive and/or dysplastic epithelium and in the neoplasm, respectively in the tumor core and at the advancing tumor margin. For each of the components, the percentage of positive cells was estimated, and three patterns of antibody expression (nuclear, cytoplasmic, or nuclear and cytoplasmic) were evaluated.

Tumor slides were divided between superficial portion and invasion front, for each of these two groups the antibody expression pattern was evaluated.

PDL-1 Immunohistochemistry

For the definition of PD-L1 positivity, previous pathological reports were consulted.

Ethic declaration

This study adhered to the principles outlined in the 1975 Declaration of Helsinki and received approval from the Local Ethics Committee.

Statistical and data analysis

The distribution of continuous data was assessed using the Shapiro-Wilk test. Non-normally distributed variables were presented as median and interquartile range, while categorical variables were reported as absolute numbers and percentages.

Mann-Whitney U test was employed for comparing continuous variables, and Chi-square test was used for categorical variables. OS and DFS were assessed through the unadjusted Kaplan-Meier method, and group survivals were compared using the log-rank test (Cox-Mantel test). Cox proportional hazards regression analysis was employed to identify significant predictors of endpoints.

Variables with a univariate statistical significance of <0.05 were chosen for inclusion in the multivariable model. Multivariate analysis, utilizing stepwise forward selection, was ultimately conducted to analyze the association of baseline characteristics with study endpoints, expressed as hazard ratio (HR) with 95% confidence interval (CI) and p values.

All statistical tests were two-sided, and p values <0.05 were deemed statistically significant. The statistical analyses were performed using SPSS software version 25.0.0 (SPSS Inc., Chicago, IL) and GraphPad Prism software version 6 (GraphPad, Inc., San Diego, CA).

REFERENCES

1. Bray, F., Laversanne, M., Weiderpass, E. & Soerjomataram, I. The ever-increasing importance of cancer as a leading cause of premature death worldwide. *Cancer* **127**, 3029–3030 (2021).
2. Sung, H. *et al.* Global Cancer Statistics 2020: GLOBOCAN Estimates of Incidence and Mortality Worldwide for 36 Cancers in 185 Countries. *CA. Cancer J. Clin.* **71**, 209–249 (2021).
3. Barsouk, A., Aluru, J. S., Rawla, P., Saginala, K. & Barsouk, A. Epidemiology, Risk Factors, and Prevention of Head and Neck Squamous Cell Carcinoma. *Med. Sci.* **11**, 42 (2023).
4. Mehanna, H., Paleri, V., West, C. M. L. & Nutting, C. Head and neck cancer--Part 1: Epidemiology, presentation, and prevention. *Bmj* **341**, c4684–c4684 (2010).
5. De Meulenaere, A. *et al.* TILs in Head and Neck Cancer: Ready for Clinical Implementation and Why (Not)? *Head Neck Pathol.* **11**, 354–363 (2017).
6. National Comprehensive Cancer Network. NCCN Guidelines Head and Neck Cancers. *December 08, 2023*
https://www.nccn.org/professionals/physician_gls/pdf/head-and-neck.pdf (2023).
7. National Comprehensive Cancer Network. NCCN Guidelines Non Small Cell Lung Cancer. *December 21, 2023*
https://www.nccn.org/professionals/physician_gls/pdf/nscl.pdf (2023).
8. Kam, D. *et al.* Incidence of Suicide in Patients With Head and Neck Cancer. *JAMA Otolaryngol. Head Neck Surg.* **141**, 1075–1081 (2015).
9. Chakoma, T., Megwalu, U. & Holsinger, F. C. Suicide in head and neck oncology. *Eur. Ann. Otorhinolaryngol. Head Neck Dis.* (2023)
doi:10.1016/J.ANORL.2023.06.007.
10. Hoffman, H. T. *et al.* Laryngeal cancer in the United States: changes in demographics, patterns of care, and survival. *Laryngoscope* **116**, 1–13 (2006).

11. Brierley J.D., Gospodarowicz M.K. & Wittekind C. *TNM Classification of Malignant Tumours, 8 th edition December 2016. Union for International Cancer Control* (Wiley-Blackwell, 2017).
12. Brandwein-Gensler, M. *et al.* Oral squamous cell carcinoma: histologic risk assessment, but not margin status, is strongly predictive of local disease-free and overall survival. *Am. J. Surg. Pathol.* **29**, 167–178 (2005).
13. National Institutes of Health (NIH). SEER Cancer Statistics Review, 1975-2012. https://seer.cancer.gov/archive/csr/1975_2012/.
14. Program, S. R. N. C. I. SEER*Explorer: An interactive website for SEER cancer statistics [Internet]. 2023 Apr 19 https://seer.cancer.gov/statistics-network/explorer/application.html?site=1&data_type=4&graph_type=2&compareBy=relative_survival_interval&chk_relative_survival_interval_5=5&sex=1&race=1&age_range=1&hdn_stage=101&advopt_precision=1&advopt_show_ci=on&hdn_vi.
15. Gonzalez, H., Hagerling, C. & Werb, Z. Roles of the immune system in cancer: from tumor initiation to metastatic progression. *Genes Dev.* **32**, 1267 (2018).
16. Hiam-Galvez, K. J., Allen, B. M. & Spitzer, M. H. Systemic immunity in cancer. *Nat. Rev. Cancer* **21**, 345–359 (2021).
17. Hegde, P. S. & Chen, D. S. Top 10 Challenges in Cancer Immunotherapy. *Immunity* **52**, 17–35 (2020).
18. Mantovani, A., Sozzani, S., Locati, M., Allavena, P. & Sica, A. Macrophage polarization: Tumor-associated macrophages as a paradigm for polarized M2 mononuclear phagocytes. *Trends Immunol.* **23**, 549–555 (2002).
19. Mantovani, A., Marchesi, F., Malesci, A., Laghi, L. & Allavena, P. Tumour-associated macrophages as treatment targets in oncology. *Nat. Rev. Clin. Oncol.* **14**, 399–416 (2017).
20. Donskov, F. Immunomonitoring and prognostic relevance of neutrophils in clinical trials. *Semin. Cancer Biol.* **23**, 200–207 (2013).

21. Que, H., Fu, Q., Lan, T., Tian, X. & Wei, X. Tumor-associated neutrophils and neutrophil-targeted cancer therapies. *Biochim. Biophys. Acta. Rev. cancer* **1877**, (2022).
22. Cerwenka, A. & Lanier, L. L. Natural killer cell memory in infection, inflammation and cancer. *Nat. Rev. Immunol.* **16**, 112–123 (2016).
23. PM, S. & LH, B. Dendritic Cell-Based Cancer Vaccines. *J. Immunol.* **200**, 71–74 (2018).
24. Stanton, S. E. & Disis, M. L. Clinical significance of tumor-infiltrating lymphocytes in breast cancer. *J. Immunother. cancer* **4**, (2016).
25. Bai, Z. *et al.* Tumor-Infiltrating Lymphocytes in Colorectal Cancer: The Fundamental Indication and Application on Immunotherapy. *Front. Immunol.* **12**, (2022).
26. Maibach, F., Sadozai, H., Seyed Jafari, S. M., Hunger, R. E. & Schenk, M. Tumor-Infiltrating Lymphocytes and Their Prognostic Value in Cutaneous Melanoma. *Front. Immunol.* **11**, (2020).
27. Warner, A. B., Corrie, P. G. & Hamid, O. Tumor-Infiltrating Lymphocyte Therapy in Melanoma: Facts to the Future. *Clin. Cancer Res.* **29**, 1835–1854 (2023).
28. Fridman, W. H., Pagès, F., Sauts-Fridman, C. & Galon, J. The immune contexture in human tumours: impact on clinical outcome. *Nat. Rev. Cancer* **12**, 298–306 (2012).
29. Hendry, S. *et al.* Assessing Tumor-infiltrating Lymphocytes in Solid Tumors: A Practical Review for Pathologists and Proposal for a Standardized Method From the International Immunooncology Biomarkers Working Group: Part 1: Assessing the Host Immune Response, TILs in Invasive Breast Carcinoma and Ductal Carcinoma In Situ, Metastatic Tumor Deposits and Areas for Further Research. *Adv. Anat. Pathol.* **24**, 235–251 (2017).
30. Galon, J. *et al.* Towards the introduction of the ‘Immunoscore’ in the classification of malignant tumours. *J. Pathol.* **232**, 199–209 (2014).

31. Galon, J. *et al.* Cancer classification using the Immunoscore: a worldwide task force. *J. Transl. Med.* **10**, (2012).
32. Galon, J. *et al.* Type, density, and location of immune cells within human colorectal tumors predict clinical outcome. *Science* **313**, 1960–1964 (2006).
33. Galon, J. & Lanzi, A. Immunoscore and its introduction in clinical practice. *Q. J. Nucl. Med. Mol. Imaging* **64**, 152–161 (2020).
34. Salgado, R. *et al.* The evaluation of tumor-infiltrating lymphocytes (TILs) in breast cancer: recommendations by an International TILs Working Group 2014. *Ann. Oncol. Off. J. Eur. Soc. Med. Oncol.* **26**, 259–271 (2015).
35. Network, N. C. C. NCCN Guidelines Breast Cancer. *December 5, 2023* https://www.nccn.org/professionals/physician_gls/pdf/breast.pdf (2023).
36. Loi, S. *et al.* Tumor infiltrating lymphocyte stratification of prognostic staging of early-stage triple negative breast cancer. *NPJ breast cancer* **8**, (2022).
37. Hendry, S. *et al.* Assessing Tumor-Infiltrating Lymphocytes in Solid Tumors: A Practical Review for Pathologists and Proposal for a Standardized Method from the International Immuno-Oncology Biomarkers Working Group: Part 2: TILs in Melanoma, Gastrointestinal Tract Carcinomas, Non-Small Cell Lung Carcinoma and Mesothelioma, Endometrial and Ovarian Carcinomas, Squamous Cell Carcinoma of the Head and Neck, Genitourinary Carcinomas, and Primary Brain Tumors. *Adv. Anat. Pathol.* **24**, 311–335 (2017).
38. National Comprehensive Cancer Network. NCCN Guidelines Melanoma: Cutaneous. *October 27, 2023* (2023).
39. Zhang, D. *et al.* Scoring system for tumor-infiltrating lymphocytes and its prognostic value for gastric cancer. *Front. Immunol.* **10**, 71 (2019).
40. Donnem, T. *et al.* Stromal CD8+ T-cell Density—A Promising Supplement to TNM Staging in Non-Small Cell Lung Cancer. *Clin. Cancer Res.* **21**, 2635–2643 (2015).
41. Donnem, T. *et al.* Strategies for clinical implementation of TNM-Immunoscore in

- resected nonsmall-cell lung cancer. *Ann. Oncol. Off. J. Eur. Soc. Med. Oncol.* **27**, 225–232 (2016).
42. Pan, X. *et al.* Computerized tumor-infiltrating lymphocytes density score predicts survival of patients with resectable lung adenocarcinoma. *iScience* **25**, 105605 (2022).
 43. de Ruiter, E. J., Ooft, M. L., Devriese, L. A. & Willems, S. M. The prognostic role of tumor infiltrating T-lymphocytes in squamous cell carcinoma of the head and neck: A systematic review and meta-analysis. *Oncoimmunology* **6**, (2017).
 44. Almagush, A. *et al.* Improving Risk Stratification of Early Oral Tongue Cancer with TNM-Immune (TNM-I) Staging System. *Cancers (Basel)*. **13**, (2021).
 45. Almagush, A. *et al.* Tumour-infiltrating lymphocytes in oropharyngeal cancer: a validation study according to the criteria of the International Immuno-Oncology Biomarker Working Group. *Br. J. Cancer* **126**, 1589–1594 (2022).
 46. Almagush, A. *et al.* Clinical significance of overall assessment of tumor-infiltrating lymphocytes in oropharyngeal cancer: A meta-analysis. *Pathol. Res. Pract.* **243**, (2023).
 47. Pokrývková, B. *et al.* PD1+CD8+ Cells Are an Independent Prognostic Marker in Patients with Head and Neck Cancer. *Biomedicines* **10**, (2022).
 48. Borsetto, D. *et al.* Prognostic Significance of CD4+ and CD8+ Tumor-Infiltrating Lymphocytes in Head and Neck Squamous Cell Carcinoma: A Meta-Analysis. *Cancers (Basel)*. **13**, 1–15 (2021).
 49. Saltz, J. *et al.* Spatial Organization and Molecular Correlation of Tumor-Infiltrating Lymphocytes Using Deep Learning on Pathology Images. *Cell Rep.* **23**, 181-193.e7 (2018).
 50. Wu, W. C. *et al.* Circulating hematopoietic stem and progenitor cells are myeloid-biased in cancer patients. *Proc. Natl. Acad. Sci. U. S. A.* **111**, 4221–4226 (2014).
 51. Mastelic-Gavillet, B. *et al.* Quantitative and qualitative impairments in dendritic cell subsets of patients with ovarian or prostate cancer. *Eur. J. Cancer* **135**, 173–

182 (2020).

52. Della Bella, S. *et al.* Altered maturation of peripheral blood dendritic cells in patients with breast cancer. *Br. J. Cancer* **89**, 1463–1472 (2003).
53. Tabarkiewicz, J., Rybojad, P., Jablonka, A. & Rolinski, J. CD1c⁺ and CD303⁺ dendritic cells in peripheral blood, lymph nodes and tumor tissue of patients with non-small cell lung cancer. *Oncol. Rep.* **19**, 237–243 (2008).
54. Van Crujisen, H. *et al.* Sunitinib-induced myeloid lineage redistribution in renal cell cancer patients: CD1c⁺ dendritic cell frequency predicts progression-free survival. *Clin. Cancer Res.* **14**, 5884–5892 (2008).
55. Almand, B. *et al.* Clinical significance of defective dendritic cell differentiation in cancer. *Clin. Cancer Res.* **6**, 1755–1766 (2000).
56. Failli, A., Legitimo, A., Orsini, G., Romanini, A. & Consolini, R. Numerical defect of circulating dendritic cell subsets and defective dendritic cell generation from monocytes of patients with advanced melanoma. *Cancer Lett.* **337**, 184–192 (2013).
57. Tumeh, P. C. *et al.* PD-1 blockade induces responses by inhibiting adaptive immune resistance. *Nature* **515**, 568–571 (2014).
58. Verronèse, E. *et al.* Immune cell dysfunctions in breast cancer patients detected through whole blood multi-parametric flow cytometry assay. *Oncoimmunology* **5**, (2015).
59. Togashi, Y., Shitara, K. & Nishikawa, H. Regulatory T cells in cancer immunosuppression - implications for anticancer therapy. *Nat. Rev. Clin. Oncol.* **16**, 356–371 (2019).
60. Ahmadzadeh, M. *et al.* Tumor-infiltrating human CD4⁺ regulatory T cells display a distinct TCR repertoire and exhibit tumor and neoantigen reactivity. *Sci. Immunol.* **4**, (2019).
61. Zhou, J. *et al.* Enhanced frequency and potential mechanism of B regulatory cells in patients with lung cancer. *J. Transl. Med.* **12**, (2014).

62. Murakami, Y. *et al.* Increased regulatory B cells are involved in immune evasion in patients with gastric cancer. *Sci. Rep.* **9**, (2019).
63. Noman, M. Z. *et al.* Blocking hypoxia-induced autophagy in tumors restores cytotoxic T-cell activity and promotes regression. *Cancer Res.* **71**, 5976–5986 (2011).
64. Charrier, M. *et al.* Circulating innate immune markers and outcomes in treatment-naïve advanced non-small cell lung cancer patients. *Eur. J. Cancer* **108**, 88–96 (2019).
65. Guthrie, G. J. K. *et al.* The systemic inflammation-based neutrophil-lymphocyte ratio: Experience in patients with cancer. *Crit. Rev. Oncol. Hematol.* **88**, 218–230 (2013).
66. Templeton, A. J. *et al.* Prognostic role of neutrophil-to-lymphocyte ratio in solid tumors: a systematic review and meta-analysis. *J. Natl. Cancer Inst.* **106**, (2014).
67. Brierley, J. D., Gospodarowicz, M. K. & Wittekind, C. *TNM classification of malignant tumours - 8th edition.* Union for International Cancer Control (Wiley-Blackwell, 2017). doi:10.1002/ejoc.201200111.
68. National Comprehensive Cancer Network. NCCN Guidelines Pancreatic Adenocarcinoma. *December 13, 2023* (2023).
69. National Comprehensive Cancer Network. NCCN Hepatocellular carcinoma. *September 14, 2023* https://www.nccn.org/professionals/physician_gls/pdf/hcc.pdf (2023).
70. Kourilovitch, M. & Galarza–Maldonado, C. Could a simple biomarker as neutrophil-to-lymphocyte ratio reflect complex processes orchestrated by neutrophils? *J. Transl. Autoimmun.* **6**, 100159 (2023).
71. Zahorec, R. Neutrophil-to-lymphocyte ratio, past, present and future perspectives. *Bratisl. Lek. Listy* **122**, 474–488 (2021).
72. Kourilovitch, M. & Galarza–Maldonado, C. Could a simple biomarker as neutrophil-to-lymphocyte ratio reflect complex processes orchestrated by

- neutrophils? *J. Transl. Autoimmun.* **6**, (2022).
73. Mariani, P. *et al.* Pre-treatment neutrophil-to-lymphocyte ratio is an independent prognostic factor in head and neck squamous cell carcinoma: Meta-analysis and trial sequential analysis. *J. Oral Pathol. Med.* **51**, 39–51 (2022).
 74. Takenaka, Y. *et al.* Prognostic role of neutrophil-to-lymphocyte ratio in head and neck cancer: A meta-analysis. *Head Neck* **40**, 647–655 (2018).
 75. Kang, D. *et al.* A systematic review and meta-analysis of prognostic indicators in patients with head and neck malignancy treated with immune checkpoint inhibitors. *J. Cancer Res. Clin. Oncol.* **149**, 18215–18240 (2023).
 76. Li, B. *et al.* Platelet-to-lymphocyte ratio in advanced Cancer: Review and meta-analysis. *Clin. Chim. Acta.* **483**, 48–56 (2018).
 77. Yin, Y. *et al.* Prognostic value of the neutrophil to lymphocyte ratio in lung cancer: A meta-analysis. *Clinics (Sao Paulo)*. **70**, 524–530 (2015).
 78. Platini, H. *et al.* Neutrophil-to-Lymphocyte Ratio and Platelet-to-Lymphocyte Ratio as Prognostic Markers for Advanced Non-Small-Cell Lung Cancer Treated with Immunotherapy: A Systematic Review and Meta-Analysis. *Medicina (Kaunas)*. **58**, (2022).
 79. Tham, T., Olson, C., Khaymovich, J., Herman, S. W. & Costantino, P. D. The lymphocyte-to-monocyte ratio as a prognostic indicator in head and neck cancer: a systematic review and meta-analysis. *Eur. Arch. Otorhinolaryngol.* **275**, 1663–1670 (2018).
 80. Jin, J., Yang, L., Liu, D. & Li, W. M. Prognostic Value of Pretreatment Lymphocyte-to-Monocyte Ratio in Lung Cancer: A Systematic Review and Meta-Analysis. *Technol. Cancer Res. Treat.* **20**, (2021).
 81. Gong, J. *et al.* Prognostic value of lymphocyte-to-monocyte ratio in ovarian cancer: a meta-analysis. *J. Ovarian Res.* **12**, (2019).
 82. Xu, Z. *et al.* Predictive value of the monocyte-to-lymphocyte ratio in the diagnosis of prostate cancer. *Medicine (Baltimore)*. **100**, (2021).

83. Hu, R. jin, Ma, J. ying & Hu, G. Lymphocyte-to-monocyte ratio in pancreatic cancer: Prognostic significance and meta-analysis. *Clin. Chim. Acta.* **481**, 142–146 (2018).
84. Tan, D., Fu, Y., Tong, W. & Li, F. Prognostic significance of lymphocyte to monocyte ratio in colorectal cancer: A meta-analysis. *Int. J. Surg.* **55**, 128–138 (2018).
85. Napolitano, L. *et al.* Preoperative monocyte-to-lymphocyte ratio as a potential predictor of bladder cancer. *J. Basic Clin. Physiol. Pharmacol.* **33**, 751–757 (2022).
86. Ma, J. ying & Liu, Q. Clinicopathological and prognostic significance of lymphocyte to monocyte ratio in patients with gastric cancer: A meta-analysis. *Int. J. Surg.* **50**, 67–71 (2018).
87. Hanahan, D. & Weinberg, R. a. The Hallmarks of Cancer Review University of California at San Francisco. *Cell Press* **100**, 57–70 (2000).
88. Hanahan, D. & Weinberg, R. A. Hallmarks of cancer: The next generation. *Cell* vol. 144 646–674 (2011).
89. Luo, J., Solimini, N. L. & Elledge, S. J. Principles of Cancer Therapy: Oncogene and Non-oncogene Addiction. *Cell* **136**, 823–837 (2009).
90. Mizushima, N. & Komatsu, M. Autophagy: Renovation of cells and tissues. *Cell* **147**, 728–741 (2011).
91. Choi, A. M. K., Ryter, S. W. & Levine, B. Autophagy in Human Health and Disease. *Nejm* **368**, 651–662 (2013).
92. Jung, C. H., Ro, S. H., Cao, J., Otto, N. M. & Kim Do-Hyung, D. H. MTOR regulation of autophagy. *FEBS Lett.* **584**, 1287–1295 (2010).
93. Kim, J., Kundu, M., Viollet, B. & Guan, K.-L. AMPK and mTOR regulate autophagy through direct phosphorylation of Ulk1. *Nat. Cell Biol.* **13**, 132–41 (2011).
94. Geng, J. & Klionsky, D. J. The Atg8 and Atg12 ubiquitin-like conjugation systems

- in macroautophagy. ‘Protein modifications: beyond the usual suspects’ review series. *EMBO Rep.* **9**, 859–64 (2008).
95. Fan, W., Nassiri, A. & Zhong, Q. Autophagosome targeting and membrane curvature sensing by Barkor/Atg14(L). *Proc. Natl. Acad. Sci. U. S. A.* **108**, 7769–7774 (2011).
 96. Ladoire, S. *et al.* Immunohistochemical detection of cytoplasmic LC3 puncta in human cancer specimens. *Autophagy* **8**, 1175–1184 (2012).
 97. Johansen, T. & Lamark, T. Selective autophagy mediated by autophagic adapter proteins. *Autophagy* **7**, 279–296 (2011).
 98. Bjørkøy, G. *et al.* p62/SQSTM1 forms protein aggregates degraded by autophagy and has a protective effect on huntingtin-induced cell death. *J. Cell Biol.* **171**, 603–614 (2005).
 99. Pankiv, S. *et al.* p62/SQSTM1 binds directly to Atg8/LC3 to facilitate degradation of ubiquitinated protein aggregates by autophagy*[S]. *J. Biol. Chem.* **282**, 24131–24145 (2007).
 100. Geetha, T. & Wooten, M. W. Structure and functional properties of the ubiquitin binding protein p62. *FEBS Lett.* **512**, 19–24 (2002).
 101. Emanuele, S. *et al.* p62: Friend or Foe? Evidences for OncoJanus and NeuroJanus Roles. *Int. J. Mol. Sci.* 2020, Vol. 21, Page 5029 **21**, 5029 (2020).
 102. Wirth, M. *et al.* Molecular determinants regulating selective binding of autophagy adapters and receptors to ATG8 proteins. *Nat. Commun.* **10**, (2019).
 103. Duran, A. *et al.* P62 Is a Key Regulator of Nutrient Sensing in the mTORC1 Pathway. *Mol. Cell* **44**, 134–146 (2011).
 104. Linares, J. F. *et al.* K63 polyubiquitination and activation of mTOR by the p62-TRAF6 complex in nutrient-activated cells. *Mol. Cell* **51**, 283–296 (2013).
 105. Raasi, S., Varadan, R., Fushman, D. & Pickart, C. M. Diverse polyubiquitin interaction properties of ubiquitin-associated domains. *Nat. Struct. Mol. Biol.* **12**, 708–714 (2005).

106. Ichimura, Y. *et al.* Structural basis for sorting mechanism of p62 in selective autophagy. *J. Biol. Chem.* **283**, 22847–22857 (2008).
107. Lamark, T. *et al.* Interaction Codes within the Family of Mammalian Phox and Bem1p Domain-containing Proteins. *J. Biol. Chem.* **278**, 34568–34581 (2003).
108. Wooten, M. W. *et al.* The p62 scaffold regulates nerve growth factor-induced NF- κ B activation by influencing TRAF6 polyubiquitination. *J. Biol. Chem.* **280**, 35625–35629 (2005).
109. Jin, Z. *et al.* Cullin3-Based Polyubiquitination and p62-Dependent Aggregation of Caspase-8 Mediate Extrinsic Apoptosis Signaling. *Cell* **137**, 721–735 (2009).
110. Rodriguez A, Durán A, Selloum M, Champy MF, Diez-Guerra FJ, Flores JM, Serrano M, Auwerx J, Diaz-Meco MT, M. J. Mature-onset obesity and insulin resistance in mice deficient in the signaling adapter p62. *Cell Metab.* **3**, 211–222 (2006).
111. Goode, A. & Layfield, R. Recent advances in understanding the molecular basis of Paget disease of bone. *J. Clin. Pathol.* **63**, 199–203 (2010).
112. Liu, Y. *et al.* A genomic screen for activators of the antioxidant response element. *Proc. Natl. Acad. Sci. U. S. A.* **104**, 5205–5210 (2007).
113. Komatsu, M. *et al.* The selective autophagy substrate p62 activates the stress responsive transcription factor Nrf2 through inactivation of Keap1. *Nat. Cell Biol.* **12**, 213–223 (2010).
114. Jiang, T. *et al.* p62 links autophagy and Nrf2 signaling. *Free Radic. Biol. Med.* **88**, 199–204 (2015).
115. Lau, A. *et al.* A noncanonical mechanism of Nrf2 activation by autophagy deficiency: direct interaction between Keap1 and p62. *Mol. Cell. Biol.* **30**, 3275–3285 (2010).
116. Copple, I. M. *et al.* Physical and functional interaction of sequestosome 1 with Keap1 regulates the Keap1-Nrf2 cell defense pathway. *J. Biol. Chem.* **285**, 16782–16788 (2010).

117. Pikkarainen, M., Hartikainen, P., Soininen, H. & Alafuzoff, I. Distribution and pattern of pathology in subjects with familial or sporadic late-onset cerebellar ataxia as assessed by p62/sequestosome immunohistochemistry. *Cerebellum* **10**, 720–731 (2011).
118. Pankiv, S. *et al.* Nucleocytoplasmic Shuttling of p62/SQSTM1 and Its Role in Recruitment of Nuclear Polyubiquitinated Proteins to Promyelocytic Leukemia Bodies. *J. Biol. Chem.* **285**, 5941 (2010).
119. Levine, B. & Kroemer, G. Autophagy in the Pathogenesis of Disease. *Cell* **132**, 27–42 (2008).
120. White, E. the role for autophagy in cancer (White, 2015).pdf. **125**, 42–46 (2015).
121. Komatsu, M. *et al.* Homeostatic Levels of p62 Control Cytoplasmic Inclusion Body Formation in Autophagy-Deficient Mice. *Cell* **131**, 1149–1163 (2007).
122. Liang, X. H. *et al.* Induction of autophagy and inhibition of tumorigenesis by beclin 1. *Nature* **402**, 672–676 (1999).
123. Takamura, A. *et al.* Autophagy-deficient mice develop multiple liver tumors. *Genes ...* **5**, 795–800 (2011).
124. Rosenfeldt, M. T. *et al.* P53 Status Determines the Role of Autophagy in Pancreatic Tumour Development. *Nature* **504**, 296–300 (2013).
125. Debnath, J., Gammoh, N. & Ryan, K. M. Autophagy and autophagy-related pathways in cancer. *Nat. Rev. Mol. Cell Biol.* **24**, 560–575 (2023).
126. Guo, J. Y. *et al.* Activated Ras requires autophagy to maintain oxidative metabolism and tumorigenesis. *Genes Dev.* **25**, 460–470 (2011).
127. Degenhardt, K. *et al.* Autophagy promotes tumor cell survival and restricts necrosis, inflammation, and tumorigenesis. *Cancer Cell* **10**, 51–64 (2006).
128. Yang, Z. J., Chee, C. E., Huang, S. & Sinicrope, F. A. The role of autophagy in cancer: therapeutic implications. *Mol. Cancer Ther.* **10**, 1533–41 (2011).
129. White, E. & DiPaola, R. S. The double-edged sword of autophagy modulation in cancer. *Clin. Cancer Res.* **15**, 5308–5316 (2009).

130. Kitamura, H. *et al.* Cytosolic overexpression of p62 sequestosome 1 in neoplastic prostate tissue. *Histopathology* **48**, 157–161 (2006).
131. Thompson, H. G. R., Harris, J. W., Wold, B. J., Lin, F. & Brody, J. P. p62 overexpression in breast tumors and regulation by prostate-derived Ets factor in breast cancer cells. *Oncogene* **22**, 2322–2333 (2003).
132. Rolland, P. *et al.* The ubiquitin-binding protein p62 is expressed in breast cancers showing features of aggressive disease. *Endocr. Relat. Cancer* **14**, 73–80 (2007).
133. Battista, R. A. *et al.* Autophagy mediates epithelial cancer chemoresistance by reducing p62 / SQSTM1 accumulation. 1–18 (2018).
134. Karsli-Uzunbas, G. *et al.* Autophagy is required for glucose homeostasis and lung tumor maintenance. *Cancer Discov.* **4**, 915–927 (2014).
135. New, J. *et al.* Secretory Autophagy in Cancer-Associated Fibroblasts Promotes Head and Neck Cancer Progression and Offers a Novel Therapeutic Target. *Cancer Res.* **77**, 6679–6691 (2017).
136. Carlsen, L. *et al.* The role of p53 in anti-tumor immunity and response to immunotherapy. *Front. Mol. Biosci.* **10**, (2023).
137. Amaravadi, R. K. *et al.* Autophagy inhibition enhances therapy-induced apoptosis in a Myc-induced model of lymphoma. *J. Clin. Invest.* **117**, 326–336 (2007).
138. Tasdemir, E. *et al.* Regulation of autophagy by cytoplasmic p53. *Nat. Cell Biol.* **10**, 676–687 (2008).
139. Sung, Y. N., Kim, D. & Kim, J. p53 immunostaining pattern is a useful surrogate marker for TP53 gene mutations. *Diagn. Pathol.* **17**, 1–9 (2022).
140. Yang, S. *et al.* Pancreatic cancers require autophagy for tumor growth. *Genes Dev.* **25**, 717–729 (2011).
141. Yamamoto, K. *et al.* Autophagy promotes immune evasion of pancreatic cancer by degrading MHC-I. *Nature* **581**, 100–105 (2020).
142. Eng, C. H. *et al.* Macroautophagy is dispensable for growth of KRAS mutant tumors and chloroquine efficacy. *Proc. Natl. Acad. Sci. U. S. A.* **113**, 182–187

- (2016).
143. Loi, M. *et al.* Macroautophagy Proteins Control MHC Class I Levels on Dendritic Cells and Shape Anti-viral CD8(+) T Cell Responses. *Cell Rep.* **15**, 1076–1087 (2016).
 144. Yamamoto, K. *et al.* Autophagy promotes immune evasion of pancreatic cancer by degrading MHC-I. *Nature* (2020) doi:10.1038/s41586-020-2229-5.
 145. Xia, H., Green, D. R. & Zou, W. Autophagy in tumour immunity and therapy. *Nat. Rev. Cancer* **21**, 281–297 (2021).
 146. Wang, X. *et al.* Autophagy inhibition enhances PD-L1 expression in gastric cancer. *J. Exp. Clin. Cancer Res.* **38**, (2019).
 147. Guo, Y., Feng, Y., Cui, X., Wang, Q. & Pan, X. Autophagy inhibition induces the repolarisation of tumour-associated macrophages and enhances chemosensitivity of laryngeal cancer cells to cisplatin in mice. *Cancer Immunol. Immunother.* **68**, 1909–1920 (2019).
 148. Li, Y. *et al.* Hydroxychloroquine induced lung cancer suppression by enhancing chemo-sensitization and promoting the transition of M2-TAMs to M1-like macrophages. *J. Exp. Clin. Cancer Res.* **37**, 1–16 (2018).
 149. Cerami, E. *et al.* The cBio cancer genomics portal: an open platform for exploring multidimensional cancer genomics data. *Cancer Discov.* **2**, 401–404 (2012).
 150. de Bruijn, I. *et al.* Analysis and Visualization of Longitudinal Genomic and Clinical Data from the AACR Project GENIE Biopharma Collaborative in cBioPortal. *Cancer Res.* **83**, 3861–3867 (2023).
 151. Gao, J. *et al.* Integrative analysis of complex cancer genomics and clinical profiles using the cBioPortal. *Sci. Signal.* **6**, (2013).
 152. Shi, C. *et al.* Sequestosome 1 protects esophageal squamous carcinoma cells from apoptosis via stabilizing SKP2 under serum starvation condition. *Oncogene* **37**, 3260–3274 (2018).
 153. Bruni, D., Angell, H. K. & Galon, J. The immune contexture and Immunoscore in

- cancer prognosis and therapeutic efficacy. *Nat. Rev. Cancer* **20**, 662–680 (2020).
154. Mäkitie, A. A., Agaimy, A. & Almangush, A. Insight into Classification and Risk Stratification of Head and Neck Squamous Cell Carcinoma in Era of Emerging Biomarkers with Focus on Histopathologic Parameters. *Cancers (Basel)*. **14**, (2022).
 155. Malapelle, U. *et al.* The evolving role of liquid biopsy in lung cancer. *Lung Cancer* **172**, 53–64 (2022).
 156. Rolfo, C. *et al.* Liquid Biopsy for Advanced NSCLC: A Consensus Statement From the International Association for the Study of Lung Cancer. *J. Thorac. Oncol.* **16**, 1647–1662 (2021).
 157. Sakakura, K. *et al.* Immunological significance of the accumulation of autophagy components in oral squamous cell carcinoma. *Cancer Sci.* **106**, 1–8 (2015).



ACKNOWLEDGMENTS

I express my deepest gratitude to my Director of Study, Prof. Giulia Veronesi, for welcoming me during a pivotal transition period of my PhD project under her wing. Your trust and belief in my potential have been monumental, and your guidance has illuminated my path every step of the way. You inspired me about the woman, surgeon, and researcher I want to be.

My sincere thanks also go to my past Director of Study, Dr. Vanesa Gregorc, for opening the doors to this incredible journey. Your willingness to foster a close collaboration with the research community, especially when I was eager to expand my horizons beyond clinical knowledge as a resident, has left an indelible mark on my professional development.

To my director, Prof. Mario Bussi, my professional father and a significant point of reference, your unwavering support for my ambitious projects and your inspirational presence have always been invaluable. Your insights on clinical, professional, and life matters have greatly enriched my perspective. I know that the otorhinolaryngologist I am today is thanks to you.

A heartfelt thank you to my Second Supervisor, Dr. Umberto Malapelle, for embracing this role and always being open for discussion.

To my PhD tutor, Prof. Federica Pedica, your experience and positive energy have instilled in me a steadfast belief in my success.

I am deeply indebted to the Department of Pathological Anatomy, without whom this project would not have been possible. Special thanks to Prof Doglioni, Prof Ponzoni, Dr. Arrigoni, Dr.ssa Filipello, and Dr. Pini (to me, Giacomo! Our friendship since university days is very precious to me). Your collaborative spirit, work, and inspiring insights have been crucial to the completion of this project.

I also wish to extend my appreciation to the entire Thoracic Surgery Department team and Oncologic department for fostering a strong collaborative bond between our units. Your support and teamwork have been foundational.

A great thank you to Dr. Giorgia Foggetti. Meeting you has been an inspiration for me. Your immense skills, passion, strength, and ambition have always impressed me, and you have been of fundamental help to me. Thanks also to the entire laboratory team that welcomed me to the lab meetings with always very translational discussions among us!

I'm deeply grateful to Dr. Matteo Paccagnella for his invaluable and prompt statistical support.

A big thank you to all my ENT colleagues, with whom I share the majority of my professional life. Special thanks to Dr. Aurora Mirabile for our close collaboration. My appreciation also goes to Filippo, Alex, and Marco, who contributed to the realization of this thesis with dedicated work, as well as smiles and laughter. Thanks to Sandra, always my point of reference in the daily work chaos, always ready with advice, help, or a hug. You know how important you are to me.

To my medical friends, Marialuisa, Claudio, Michele, Gianluca, and Andrea. I've always known that discussing with you was valuable, because you've been able to support me as friends but understand me in a way that only colleagues can.

And to my lifelong friends, Ida, Diletta, Rossella, Giovanna, Gemma, Pask, Andre, and Paul (a new but precious addition), you have been unwavering pillars in my life, always there to support me.

Finally...to my invaluable family. Nonna Rosa, Mamma, Papà, and Federica, my person. What more can I say? Another milestone has been achieved (maybe not yet the one Nonna Rosa is hoping for =P), and I am filled with joy. This happiness is all because of you, thanks to the person I've become with your guidance and your boundless love.

Grazie!